Scuola Internazionale Superiore Studi Avanzati

(SISSA)

Neuroinflammation and inhibitory synaptic control of cultured premotor circuits

Candidate

Vincenzo Giacco

Supervisor

Prof. Laura Ballerini

A thesis submitted for the degree of *Doctor of Philosophy*
in Neurobiology
June 12th 2018

Table of contests

ABSTRACT **5**

INTRODUCTION **7**

1. Neuroinflammation and neurodegeneration **7**

1.1 The immune response in the CNS 8

2.1 Neuroglia 10

- Microglia 10
- Astrocytes 13
- Oligodendrocytes 14
- Schwann cells 15

1.3 Microglia and astrocytes in neuroinflammation and diseases 16

1.4 Cytokines network in neuroinflammation 19

- Interferons 19
- Colony-Stimulating Factors 20
- Transforming Growth Factor-β Family 21
- Tumor Necrosis Factor Family 21
- Interleukin Family 21

1.5 Inflammation in neurodegenerative and neuroimmunological disorders 22

- Multiple sclerosis 23

1.6 Neuroinflammation and neuronal activity 25

2. Spinal cord networks **27**

2.1 Structure and function of spinal cord 27

- The somatosensory system 28
- The motor system 29

2.2 Molecular and cellular development of the spinal cord 30

- Heterogeneous classes of interneurons during spinal cord development 31
- GABAergic and glycinergic changes in the developing spinal networks 33

2.3 Synaptic activity and cytokines effect on the spinal networks 35

3. Organotypic spinal cord cultures 37

3.1 Ex-vivo spinal cord model from mouse embryos 37

4. Fast inhibitory synaptic network: the GABAergic transmission 39

4.1 $GABA_A$ receptors: structural composition and function 40

4.2 $GABA_A$Rs post-synaptic organization and plasticity 42

4.3 The dynamic of intracellular chloride regulation 43

4.4 Chloride regulation in CNS disorders 45

AIM OF THE THESIS 48

MATERIALS, METHODS AND RESULTS 49

1. Paper 1: Bridging pro-inflammatory signals, synaptic transmission and protection in spinal explants in vitro .....

2. Paper 2: Neuroinflammation by Cytokines but not by LPS shapes GABAergic currents in mouse spinal cord explants culture (*MS in preparation*) 63

CONCLUSION 89

REFERENCES 91

Abstract

My PhD project is focused on the impact of neuroinflammation processes in the mouse spinal cord, with particular attention to cytokines and their functional role. In particular, I have used as model the organotypic spinal cultures, which allowed me to investigate: i. spinal network activity changes induced by pro-inflammatory cytokines; ii. resident microglia and astrocytes response to inflammatory stress; iii. mechanisms by which pro-inflammatory cytokines modulate the inhibitory transmission. The principal aim of my work was to understand the crosstalk between neuroinflammation and the spinal pre-motor network. For this purpose, I combined electrophysiological and immunofluorescence methods to assess the interneurons synaptic activity especially localized in the ventral organotypic cultures from embryonic mouse spinal cord.

I investigated a specific cytokines cocktail (TNF-α, IL-1β, and GM-CSF; CKs) and their effects on spontaneous and inhibitory postsynaptic currents (sPSCs and IPSCs). In cultured spinal networks, I have observed a progressive increase in the frequency of PSCs and IPSCs accompanied by a fastening of GABAergic currents, due to a reduction in the decay time constant (τ). This difference in the GABAergic PSCs kinetic properties is maintained in miniature PSCs (mPSCs) recorded after CKs treatments, suggesting mechanisms strictly associated with post-synaptic modification. The specific CKs modulation of GABAergic currents is strengthened by the absence of such a regulation by another danger signal as LPS.

In this work, I evaluated and compared resident neuroglial cells response to CKs and LPS. Microglia and astrocytes show a different activation in the spinal slices. In particular, CKs induce an increase of microglia proliferation and astrogliosis followed by decreasing of microglia ramification. On the other hand, LPS increases only microglia ramification maintaining unaffected the other properties. Regardless the cell morphology, the activation of an inflammatory status was confirmed by the presence of cytokines and chemokines release in the supernatants in both conditions.

I investigated the mechanisms by which cytokines speeded up the $GABA_AR$-mediated currents, and pharmacologically based electrophysiological experiments strongly indicated the presence of a modulation of $GABA_AR$ subunit, in particular of α-subunit.

In conclusion, my work highlighted the effect of cytokines in compromising the pre-motor circuits that may contribute to induce spinal network increased excitability ultimately leading to neurodegeneration.

Introduction

1. Neuroinflammation and neurodegeneration

The Central Nervous System (CNS) is characterized by a high structural and functional complexity enabling the control of different tasks. CNS high specialization and complexity hardly recover upon damage in the adult, thus leading to permanent functional deficits. In many cases, CNS dysfunctions are associated with neuroinflammation.

Neuroinflammation is an important protective mechanism adopted by the organism to repair, regenerate and remove damaged cells or pathogens (Kulkarni *et al*., 2016). Several immune and inflammatory cells are involved in reacting to the damaged CNS (Fig. 1). In the CNS, neuroinflammation is primarily mediated by microglia, astrocytes, and neurons to be followed by T-cells, neutrophils, mast cells, and involves inflammatory mediators such as cytokines and chemokines (Shabab *et al*., 2017). The development of chronic inflammation results in progressive neuronal death (Chen *et al*., 2016). In fact, chronic neuroinflammation plays an important role in the onset and progression of several neurodegenerative diseases, as in the case of Alzheimer's disease (AD) and Parkinson's disease (PD), or Amyotrophic Lateral Sclerosis (ALS) and Multiple Sclerosis (MS).

Neurodegeneration is a pathological condition in which neuronal structure and functions are altered, leading to neuronal death and loss of cognitive and motor functions. Despite the progression in understanding the mechanisms involved in the neurodegenerative diseases, the causes of these disorders are essentially unknown.

Different factors are implicated in the onset and development of many disorders. Some neurodegenerative diseases are associated with a genetic basis (<5%) as in the specific case of SOD1 gene mutation related with ALS, α-synuclein with PD, and amyloid precursor protein (APP) in AD. These mutations once inherited could contribute partly to the disease symptoms. On the other hand, environmental factors are particularly involved in the progression of the neurological disorder, as for instance in the MS in which reactive immune response towards myelin fibres promote degradation and axonal loss (Ransohoff, 2016; Schwartz and Deczkowska, 2016).

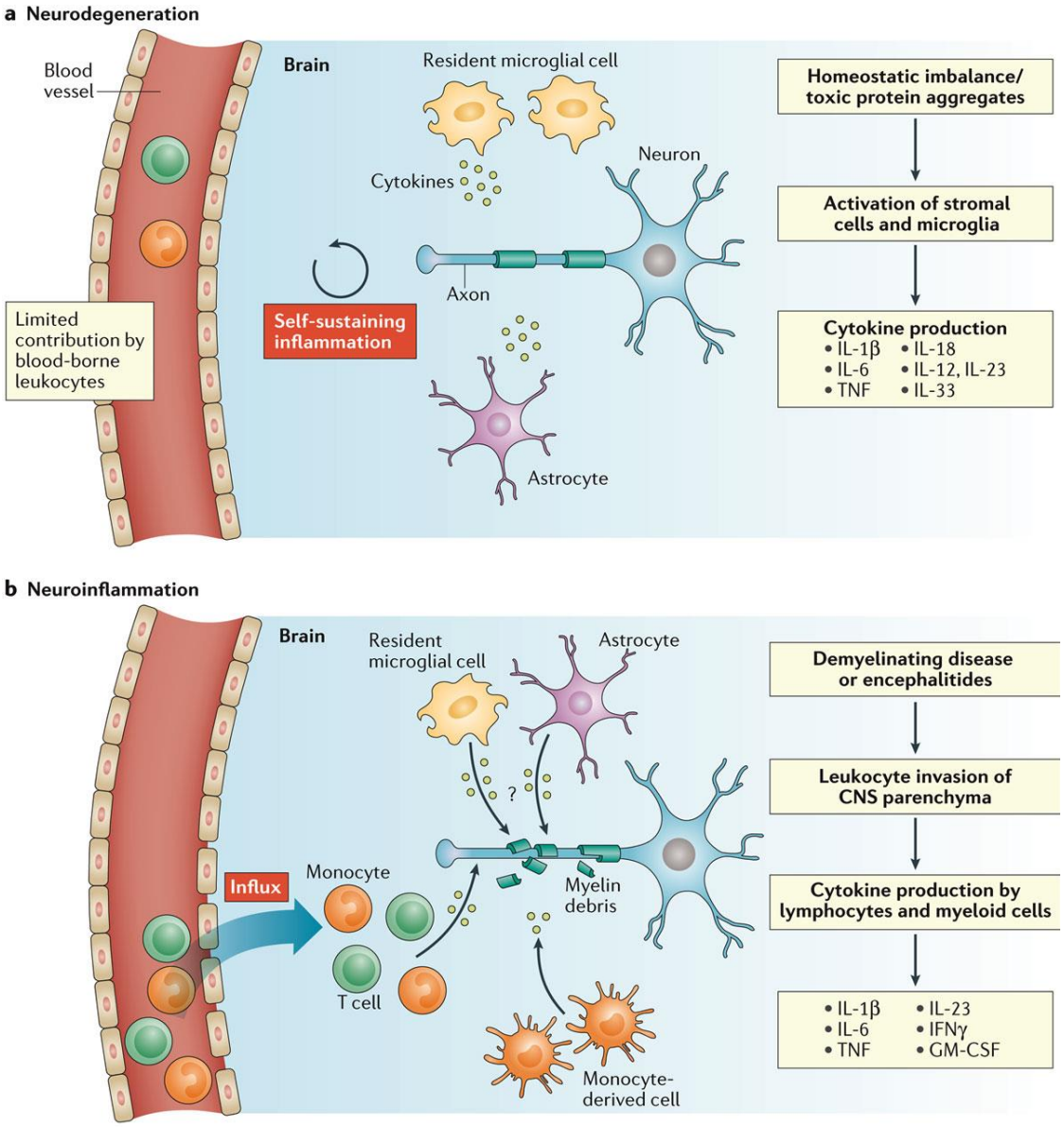

Figure 1. Mechanisms triggered by neurodegeneration and neuroinflammation disorders.

a) Resident microglia cell and astrocytes are activated by proteins aggregate which induce the cytokines production contributing to the neurodegenerative mechanisms in the brain. Most of the inflammatory cells are recruited from the brain without any involvement of leucocytes from the peripheral blood circulation. **b)** Neuroinflammation is triggered by an internal defect such as demyelination which activates mechanisms mediated by astrocytes and microglia resulting in the invasion of lymphocytes and monocytes coming from the peripheral circulation (Becher *et al.*, 2017).

1.1 The immune response in the CNS

In the CNS the first line of defence is accomplished by the Blood-Brain Barrier (BBB), a selectively permeable membrane that controls the CNS microenvironment and homeostasis

(Fig. 2). The BBB separates the brain from the circulating blood by specialized endothelial cells which are attached to each other via peculiar junctions. This tight barrier prevents the entrance of infectious agents and toxic factors to protect alteration of the CNS.

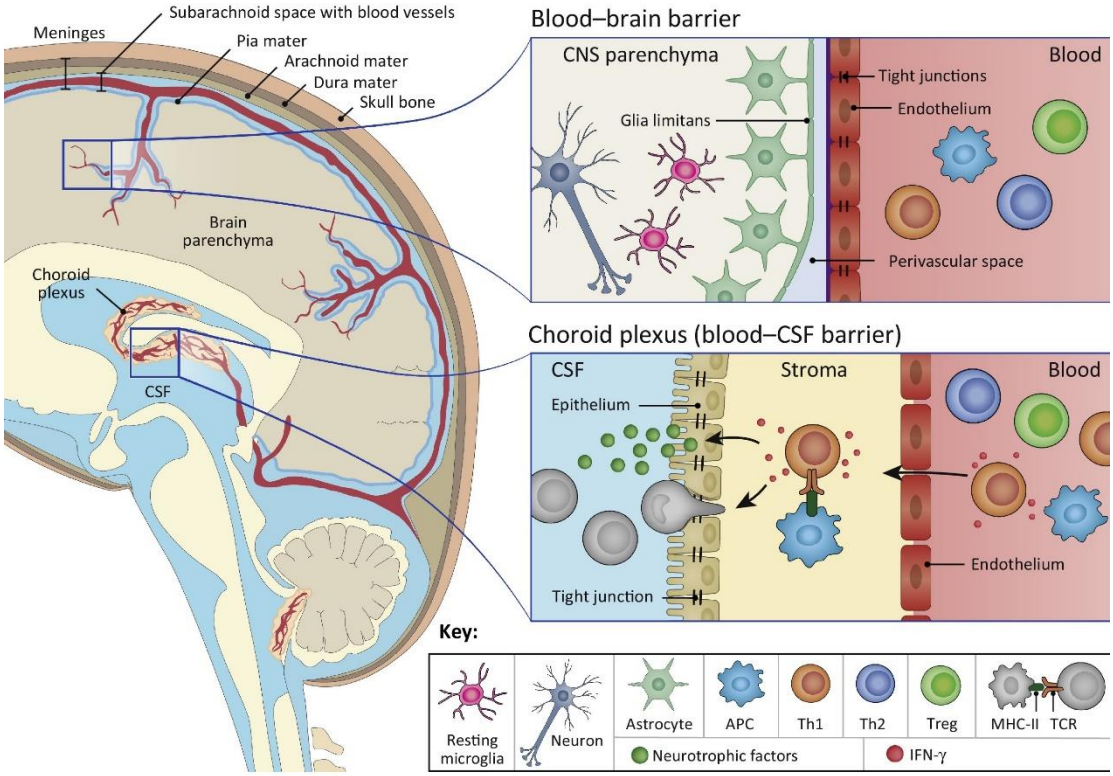

Figure 2. Structure of the blood barrier in the central nervous system.

CNS is protected from the external environment by two barriers located around the brain and the choroid plexus. The blood-brain barrier (BBB) is composed of endothelial cells and astrocytes which maintain well separated the blood circulation and the brain parenchyma. Similar to the BBB, the blood-CSF barrier has a stroma layer between blood and CSF which role is to control the leucocytes trafficking and the production of neurotrophic factors (Deczkowska *et al.*, 2016).

In several pathological conditions such as infections, injuries, or traumas, even slight alterations of the BBB expose the SNC to molecules that trigger the activation of the innate immunity. These molecules include proteins from the bacterial membrane, intracellular proteins, and molecules such as ATP, urea and nucleic acid (Kumar *et al*., 2011) which are recognized by germline-encoded pattern recognition receptors (PRRs). Three groups of receptors belong to PRRs family: Toll-like receptors (TLRs), Nod-like receptor (NLRs), and RIG1-like receptors (RLRs). These receptors expressed by microglia, astrocytes,

oligodendrocyte, endothelial cells, and even neurons activate a specific pathway and release cytokines mainly involved in disease progression, particularly TNF-α, IL-1β, and INF-γ.

1.2 Neuroglia

The term of "neuro-glia" (*nerve-cement*) was coined for the first time way back in 1858 from Rudolph Virchow, a German pathologist. With this name, Virchow denominated all the material present in CNS between neurons. Substantially, he described the real "cement" which binds the nervous elements together that constitutes a tissue different from the other connective tissue (Virchow R, 1978).

Today, the term neuroglia, better known as glial cells, indicates a number of cells, including microglia, astrocytes, oligodendrocytes, and Schwann cells. They are distinguished from each other by their different morphology, lineage, properties, and functions. Glial cells play an essential role in development, synaptic plasticity, and regeneration, ensuring the highest performance for the brain and spinal cord.

Microglia

Microglia represent the 5-20% of the total population of glial cells in the entire CNS. These cells are considered complementary to macrophages, given their ability to fulfil phagocytosis, release cytotoxic factors and begin an immune response (Hanisch and Kettenmann, 2007).

There are two major functional roles of microglia: immune defence and CNS maintenance (Hanisch and Kettenmann, 2007; Colton CA, 2009; Hanisch, 2013). Microglia are sentinels that recognise pathogens invasion and damage, under the inflammatory condition, they react but also tone down the damage to the CNS, delete debris, dead cells, and support remodelling and tissue repair (Lloyd *et al*., 2017). Another feature of microglia are their ability in controlling neuronal proliferation and differentiation (Graeber *et al*., 2010; Hughes *et al*., 2012), besides contributing to synaptic structures formation and elimination (Tremblay *et al*., 2010).

The presence of microglial cells have been described for the first time during early development, suggesting that microglia arise from embryonic progenitors. These progenitors were first proposed to be meningeal macrophages infiltrating into the brain during early embryonic development (Ginhoux *et al.,* 2013).

At murine embryonic stage E8.5, yolk sac (YS) produces early primordial macrophages and erythrocytes as part of the process of primitive hematopoiesis. In addition, multilineage erythromyeloid progenitors (EMP) and lymphomyeloid progenitors also emerge in the YS as a second wave (Fig. 3). Later, at E9.5 YS macrophages migrate to colonize the brain rudiment, become microglial precursors, and starting from E13 they give rise to microglial cells during the brain development. On the other hand, the generation of definitive hematopoietic stem cells (HSCs) occurs in the aorta–gonad–mesonephros (AGM) region of the embryo around E10.5. These AGM-derived HSCs then migrate to the foetal liver (FL) and bone marrow (BM) and differentiate into all lineages (Cumano and Godin, 2007). Afterwards, HSC-derived myeloid cells, such as monocytes, are produced abundantly in the FL only from E12.5/E13.5 (Fig. 3). As a result, the brain contains YS-derived macrophages, but not HSC or maternal macrophages, suggesting that microglia have different origins from the other haematopoiesis lineages.

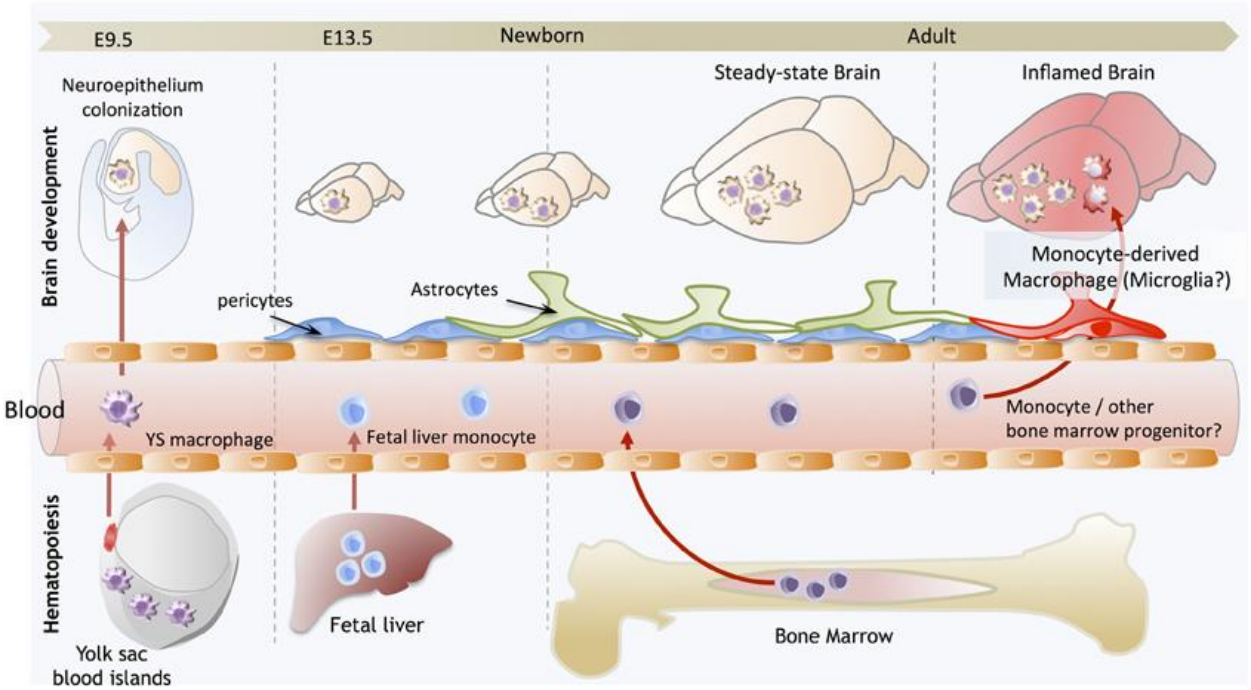

Figure 3. Microglial and hematopoiesis cells differentiation during development.

In the early stage of mice development macrophages are originated from the yolk sac (YC). Later, they migrate through the blood to reach and colonize the rudimental brain. Here, YC-macrophage differentiates in microglia together with the brain maturation (Ginhoux et al., 2013). In parallel, from the foetal liver (FL) and later from the bone marrow (BM), monocytes migrate in the blood through which they can reach any tissue and organs. In

addition, inflammatory brain stimuli can recruit blood circulating monocytes, which after reaching the brain are able to offer support in re-establishing the physiological conditions (Ginhoux *et al.,* 2013).

A similar pattern of events may occur in humans. In human foetuses, microglia-like cells with a range of different morphologies can be detected as early as 13 weeks of estimated gestational age (Hutchins *et al.,* 1990). However, it appears that maturation of the microglial compartment is ongoing throughout the majority of gestation. Colonization of the spinal cord begins at around 9 weeks, the major influx and distribution of microglia commence at about 16 weeks, and ramified microglia take up to 22 weeks to become evenly distributed within the intermediate zone (Rezaie and Male 1999; Rezaie *et al.,* 2005). In fact, it is only close to term, at 35 weeks, that well-differentiated microglial populations can be detected within the developing human brain (Esiri *et al.,* 1991; Rezaie and Male 2002; Rezaie *et al.,* 2005; Verney *et al.,* 2010).

In physiological conditions, microglia are distributed ubiquitously throughout the CNS, with the highest densities in the hippocampal formation, the olfactory telencephalon, and in some areas of the basal ganglia, such as the substantia nigra. One of the main peculiarities of microglia are the ability in changing their morphology and appearance upon certain physiological or pathological states. This morphology, mainly characterized by the extent of branching patterns, differs among brain regions, or when comparing cells located in the grey or white matter (Lawson *et al.*, 1990). The microglial immunophenotype commonly associated with resting or activated microglia is influenced by the chemical composition of the microenvironment, reflecting the physiological or pathological conditions of the surrounding tissue. In the healthy adult brain, microglia are usually highly branched (ramified) with a small amount of perinuclear cytoplasm and a small, dense, heterochromatic nucleus.

This structure is associated with resting microglia (quiescent) (Fig. 4). On the opposite, in pathological conditions in particular associated with inflammation, microglia reduce the branches toward the amoeboid type (reactivate). In addition, microglia produce neurotoxic molecules, such as nitric oxide, glutamate, reactive oxygen and nitrogen species, and pro-inflammatory cytokines, contributing to the so-called secondary damage following injured or diseased CNS (Leong and Ling, 1992).

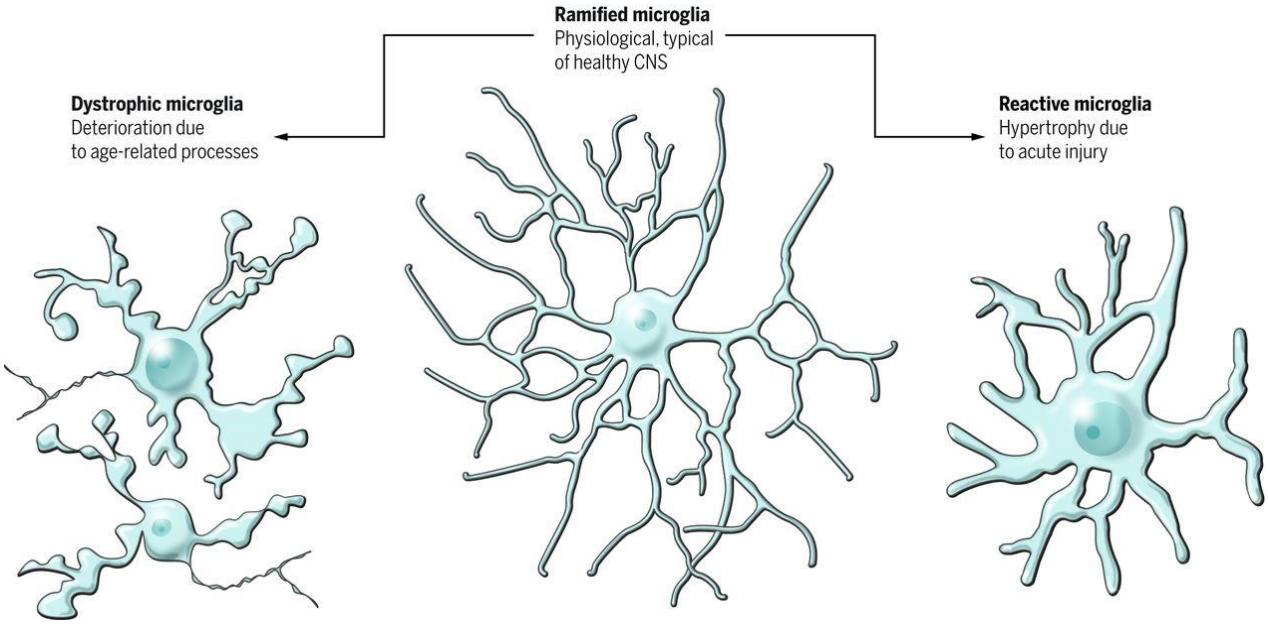

Figure 4. Different microglia morphology

Resting microglia are characterized by long a numerous branches which confer them the typical ramified shape. Inflammatory and injured stimuli induce microglia activation which is represented by an amoeboid morphology, promoting the phagocytosis of debris and dead cells. Moreover, microglia can active mechanisms in order to deteriorate their body and became dystrophic microglia. (Ransohoff, 2016).

Astrocytes

In the nineteenth century, two distinct classes of astrocytes were identified for the first time: protoplasmic astrocytes and fibrous astrocytes (Andriezen, 1893). The protoplasmic astrocytes are distributed homogenously within cortical grey matter, appearing as complex structures with numerous fine processes. Whereas fibrous astrocytes are less complex and organized along white matter area with fewer branching processes. Later studies reported the presence of specialized astrocytes within different brain area: the Bergmann glia of the cerebellum, or the Muller cells of the retina (Kettenmann and Verkhratsky, 2008).

Glial fibrillary acidic protein (GFAP), an intermediate filament protein expressed by astrocytes, has been used to identify astrocytes within the SNC (Eng, 1985) although it is well known that not all types of astrocytes express this marker.

Astrocytes have a plethora of functions, from neuronal support during development, maturation and injuries in the CNS, to promoting forms of synaptic signalling and plasticity. Astrocytes can be activated thus becoming larger and up-regulating GFAP and other

intermediated filament proteins (Pekny and Nilsson, 2005). This mechanism promotes astrocytes mobility, in order to reach and contact active synapses.

The different classes of astrocytes originate from glial progenitor cells. Gliogenesis occurs in the perinatal phase in the germinal niches of the CNS, the ventricular (VZ) and subventricular zones (SVZ) (Levison *et al.*, 1999). Radial cells in the VZ and glial progenitor cells in the SVZ develop into distinct pools of astrocytes. Radial cells are multipotent and persist also postnatally, giving rise to a subset of cortical astrocytes (Malatesta *et al.*, 2003; Goldman, 1995). Alternatively, astrocytes are generated from distal-less homeobox 2 (Dlx2) glial progenitor cells, and postnatally from $NG2^+$ glial progenitor cells (Marshall and Goldman, 2002). This process governs the formation of protoplasmic, cortical and white matter astrocytes (Beckervordersandforth *et al.*, 2010).

Likewise, in the spinal cord astrocytes follow the same path. Especially, $Olig2^+$ progenitors arise from a particular ventricular zone of the spinal cord named the motor neuron progenitor domain (pMN), which give rise to ventral horn astrocytes (Masahira *et al.*, 2006). Recent studies have demonstrated three distinct domains of the ventral ventricular zone, which generate distinct white matter astrocyte subpopulations in the spinal cord (Hochstim *et al.*, 2008).

Oligodendrocytes

Oligodendrocytes are defined as the cells that produce the myelin sheaths around the axons of several neurons. Rio Hortega classified oligodendrocytes into types I to IV, according to the characteristics of the number and orientation of their cellular processes, the shape and size of their soma, the size of the axons they were associated with, and their distributions within the CNS (Simons and Nave, 2015).

Type I and II oligodendrocytes are quite similar. They have more than three fine primary processes that myelinate 10-30 axons < 2 μm in diameter. Type III oligodendrocytes have large cell bodies with primary processes that branch and myelinate less than five axons, forming a sheath with a diameters ranging from 4 to 15 μm. They are mainly localized in the cerebral and cerebellar peduncles, the medulla oblongata, and the spinal cord. Quite similar, type IV units are formed by a single long myelin sheath over large-diameter fibres which are found near the entrance of nerve roots into the CNS (Simons and Nave, 2015).

Differences among large- and small-diameter fibres are mainly due to their protein composition (Hildebrand *et al.,* 1993). In fact, myelin basic protein (MBP) and proteolipid protein (PLP) are expressed more intensely in small- and large-diameter fibres, respectively (Hartman *et al.,* 1982). Moreover, differences are also identified in the adult rat anterior medullary velum (Butt and Berry, 2000), concerning of the expression of carbonic anhydrase (CA) II and the S-isoform of myelin-associated glycoprotein (MAG).

During development and maturation, the four classes of oligodendrocytes are derived from precursors named Oligodendrocyte Progenitor Cells (OPCs) (Butt *et al.,* 1997). Type III/IV oligodendrocytes that differentiate prior to birth, myelinate the large-diameter fibres (≥4 μm) early in development. Whereas type I/II oligodendrocytes that differentiate in the first postnatal weeks, myelinate the small-diameter fibres (≤2 μm) later in development. Oligodendrocytes initially contact a large number of immature thin axons, and most of these processes are lost during myelination. In addition, another class of progenitors is associated with oligodendrocytes generated during development and the following demyelination in the adult brain (Dawson *et al.,* 2000). These cells called NG2-glia for the expression of the NG2 chondroitin sulfate proteoglycan a potent inhibitor of axon regeneration carry out a principal role during injuries protecting the surrounding neurons from further damage (Butt and Berry, 2000).

Schwann cells

The major population of peripheral glial cells is represented by the Schwann cells which are similar to oligodendrocytes in terms of structure, molecular composition and functions. Two main populations are derived from neural crest, the myelinating and not myelinating Schwann cells, distinguished by their ability to contact group of small or one large axon (Dong *et al.,* 1999). Schwann cells have a peculiar role in forming myelin, a specialized structure that allows the conduction of action potentials. In particular, they are responsible for maintaining the internodal insulating myelin sheath as well as to the structural and molecular organization of the node of Ranvier (Bennett *et al.,* 1997). Other kinds of Schwann cells with different role have been described; the perisynaptic Schwann cell of the neuromuscular junction and terminal Schwann cell-like cells of the sensory system (Dong *et al.,* 1999).

The Schwann cells lineage start from Schwann cell precursors originate from neural crest cells. These precursors give rise to immature Schwann cells in a process that starts after 3 weeks of mouse embryonic development around birth. Hence, three major developmental steps lead to the maturation of Schwann cells after leaving the neuronal crest. Since crest cells can generate several cell types, the first steps involve a fate choice in which kind of cells it should become. The second transition, in contrast, represents lineage progression that Schwann cell precursors are fated only to become Schwann cells or die by programmed cell death. The last stage provides the differentiation in myelinated or not myelinated cells (Lobsiger *et al.*, 2002).

1.3 Microglia and astrocytes in neuroinflammation and diseases

Microglia mediate immune and inflammatory responses in the CNS. When the brain is injured or diseased, the ramified microglia tune their morphology, via retracting their processes and increasing their volume (Fig. 5). In response to microenvironment stimuli, microglia can take two different fates: pro-inflammatory or anti-inflammatory phenotypes. These phenotypes are highlighted by upregulation of specific receptors and soluble molecules; CD16 Fc receptors, CD32, CD64, CD86, IL-1β, IL-6, IL-12, IL-23, tumor necrosis factor (TNF)-α, inducible nitric oxide synthase (iNOS), and chemokine for the pro-inflammatory state; arginase (Arg)-1, mannose receptor (CD206), insulin-like growth factor (IGF)-1, triggering receptor expressed on myeloid cells 2 (TREM2), chitinase 3-like 3 (Ym-1) for the anti-inflammatory phenotype (Jha *et al.*, 2016).

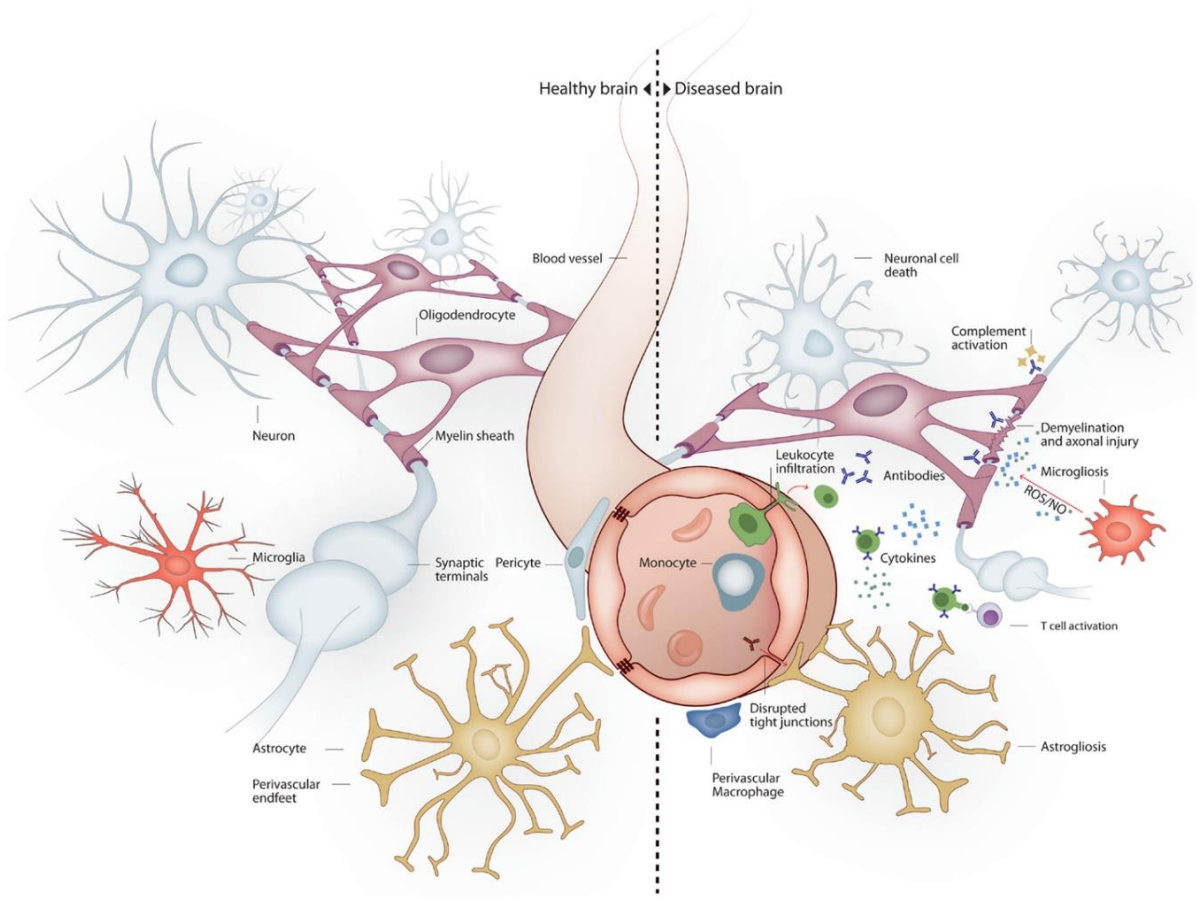

Figure 5. The synergic work between microglia and astrocytes in diseases

Changes in microenvironment cause the activation of microglia and astrocytes, altering neuronal functions by releasing cytokines and chemokines. In physiological conditions, microglia is in a quiescent status useful for homeostasis processes. Once activated by stimuli coming from pathogenic agents, microglia in the first instance induce the weakness of neuronal synapses, contributing later to neuronal dysfunction (Sankowski *et al.*, 2015).

In damaged or reactive tissue, microglia proliferate in response to specific factors such as macrophage-colony stimulating factors (M-CSF), granulocyte macrophage-colony stimulating factors (GM-CSF), multi-CSF [interleukin-3 (IL-3)], microglial mitogen-1 (MM1), and microglial mitogen-2 (MM2) (Giulian and Ingeman,1988; Giulian *et al.*, 1991).

The expression of the chemokine receptors such as CCR1, CCR2, CCR3, CCR5, CXCR4, and CX3CR1, allow the microglia to move during the active state, in order to reach the inflammatory area (Gebicke-Haerter *et al.*, 2001).

When microglia are activated in response to specific stimuli which involve debris and dying cells, they transform themselves into phagocytes, in order to engulf dead neurons and damaged

tissue. The presence of phagocytes has been observed in AD, PD, MS, ischemia, and trauma. In addition, in this activated state microglia produce and secrete a variety of deleterious factors including reactive oxygen species (ROS). Thus, one of the more toxic is represented by the nitric oxide (NO) that in turn reacts with superoxide anion to produce peroxynitrite. These radicals inhibit respiratory enzymes, oxidize the SH group of proteins, and enhance DNA injury, finally resulting in neuronal cell death. In the AD β-amyloid, in the presence of interferon-γ (INFγ), synergistically stimulates the production of NO and TNF-α in microglia. Furthermore, TNF-α causes cell death and, for instance, oligodendrocytes and myelin give rise to the inflammation reaction typically associated with MS (Liu *et al.,* 1998).

On the opposite, microglia may play a protective role in the pathological condition, including spinal cord injuries, compression injuries, and ischemia (Dougherty *et al.,* 2000; Ikeda *et al.,* 2001; Lee *et al.,* 2002). Even in this case activated microglia release a specific class of neuroprotective factors and cytokines.

Nerve growth factor (NGF), brain-derived neurotrophic factor (BDNF), neurotrophin-3 (NT-3), and NT-4/5 belong to the neurotrophins family which plays an essential protective role on various types of neurons in the CNS and the peripheral nervous system (PNS). Furthermore, other factors such as fibroblast growth factor 2 (FGF2: bFGF), insulin-like growth factor-I (IGF-I), IGF-II, and hepatocyte growth factor (HGF) promote neuronal survival in various types of neurons in pathological conditions.

Astrocytes are involved in many important processes such as controlling the environment by regulating pH, ion homeostasis, blood flow, and modulating oxidative stress. Together with microglia, astrocytes are involved in the neuroinflammatory response. After specific signals such as injury or damage, astrocytes rapidly induce important changes in their morphology and function, reminiscent of what observed for microglial cells. Reactive gliosis is a self-perpetuating process by which astrocytes may also exacerbate the injury, instead of protecting the damaged tissue. Thus, when astrocytes lose their helpful properties, they contribute to neurodegenerative mechanisms (Steardo *et al.,* 2015).

The mechanisms leading to the activation of these cells are actually unclear, and many factors that are involved in neurodegenerative diseases can trigger the response of these cells. As microglial cells, astrocytes also can phagocytose and degrade amyloid-beta in AD.

1.4 Cytokines network in neuroinflammation

Cytokines are small proteins that are involved in several cells signalling such as cell growth and differentiation, tissue homeostasis and repair, and immune and inflammatory responses in the CNS. In fact, they regulate molecules that modify the neuronal microenvironment. In addition, cytokines are pleiotropic molecules able to induce the production of other cytokines, initiating a complex mechanism of action (Boulanger, 2009; Benveniste, 1998).

Most of our comprehension of the effects of cytokine release in the nervous system has been obtained by studies in primary cultures and in animal models of severe neurological diseases. The latter include experimental autoimmune encephalomyelitis (EAE) models for the inflammatory, de-myelinating diseases multiple sclerosis; models of chronic neurodegenerative disorders, such as AD and prion disease; and SOD1 mutant mice, a model for ALS (Glass *et al.*, 2010; Chen *et al.*, 2016). Many studies have been conducted using human brain material or cerebrospinal fluid (CSF) from neurological patients, providing important knowledge on the role of cytokines in MS (Czubowicz *et al.*, 2017; Burm *et al.*, 2016). On the other hand, *in vitro* studies often generated conflicting results on cytokine sources and targets in the CNS, owing to the fact that astrocytes and microglia cultures are able to influence each other and neuronal cultures without the contribution of the peripheral system.

Interferons

The interferons (IFNs) are a family of proteins produced and released in response to pathogens infections. They are classified into two different types: the type I composed by interferon-α and -β (IFN-α/β), and type II associated with interferon-γ (IFN-γ). The type I is the product of a combination of genes that are produced by many cell types in response to viruses or double-stranded RNA. Alternatively, type II is the product of a single gene mainly produced by $CD8^+$ cytotoxic T cells, a subset of $CD4^+$ T helper cells (Th1), and natural killer (NK) cells.

IFN-α/β are released by glial cells following the contact with viruses and induce an antiviral resistance from CNS cells. In addition, they have also been detected in reactive microglia and astrocytes during neurodegenerative processes (Akiyama *et al.*, 1994; Rho *et al.*, 1995). Furthermore, both subtypes are used in the therapy of many neuroinflammatory dysfunctions; lethal neurotropic viral infection and MS, respectively (Wang *et al.*, 2002a).

Contrarily from the previous ones, IFN-γ plays a protective role against neurotropic pathogens. In particular, it has been found in high levels in inflammatory pathologies in which are involved demyelination and neurodegeneration (Owens *et al.*, 2001; Wang *et al.*, 2002a). In addition, the presence of IFN-γ is supported by tissue infiltration and activation of NK, $CD8^+$ cytotoxic, and Th1-type T cells (Owens *et al.*, 2001).

When INF-γ binds to specific microglia receptors, it activates a signal transduction cascade which induces the transcription of several immune genes via the transcription factor STAT-1. Moreover, IFN-γ potentiates the production of cytokines, chemokines, proteases, NO, and ROS, during activation of microglia-mediated by lipopolysaccharide (LPS) and CD40 ligation. In addition, IFN-γ acts also on astrocytes and Schwann cells, promoting expression of major histocompatibility complex (MHC) and adhesion molecules. The opposite effects exerted by INF-γ is chiefly attributable to its activity expressed at local and system level. Locally, INF-γ plays a pro-inflammatory role, while at the systemic level it exerts immunosuppressive and protective effects, observed especially in EAE model. In particular, a downstream immunosuppressive suggested effector molecule is NO, usually induced by INF-γ (Duong *et al.*, 1994; Ferber *et al.*, 1996; Willenborg *et al.*, 1996).

Colony-Stimulating Factors

Colony-stimulating factors (CSFs) are hematopoietic cytokines that regulate the growth and differentiation of bone marrow progenitor cells. IL-3, macrophage-CSF (M-CSF), granulocyte-macrophage CSF (GM-CSF), and granulocyte-CSF (G-CSF) are included in this class of cytokines. M-CSF is released during infectious, autoimmune, and neurodegenerative diseases and together with GM-CSF stimulate microglia proliferation, differentiation, and activation in health and disease conditions (Raivich *et al.*, 1999). Besides, GM-CSF is increased in microglia following nerve injury, promoting phagocytic capability and antigen-presenting function (Re *et al.*, 2002). Furthermore, IL-3 supports the proliferation of microglia and may serve as a neurotrophic/neuroprotective factor, highly accumulated during EAE and in peripheral neuropathies.

Transforming Growth Factor-β Family

Additional cytokines that regulate the cell proliferation, differentiation, migration, and apoptosis are called transforming growth factor-β (TGF-β). These include TGF-βs, bone morphogenetic proteins, and activins. Three mammalian TGF-β isoforms, TGF-β1, -β2 and -β3, are principally expressed in the SNC that usually interact with at least three receptors. All three TGF-β isoforms have been detected in macrophages/microglia and reactive astrocytes in multiple sclerosis lesions. In particular, TGF-β1 mRNA is expressed predominantly in an area with leukocytes and microglia after brain injury and in EAE (Kiefer *et al.*, 1998). In addition, also Schwann cells increase the TGF-β1 mRNA after peripheral nerve lesion, whereas in Alzheimer's, Parkinson's, and prion diseases, high level of TGF-β1 and/or TGF-β2 isoform are increased. On the contrary, studies conducted on animal model have revealed that TGF-β could also have anti-inflammatory and protective effects (Owens *et al.*, 2001).

Tumor Necrosis Factor Family

The Tumor Necrosis Factor Family comprises 20 members mainly involved in the regulation of immune responses, inflammation, tissue homeostasis, and development. TNF is principally produced by macrophage and its action occurs after binding to functionally distinct receptors: TNFR1 (p55 TNF receptor) and TNFR2 (p75 TNF receptor). The most expressed isoform in the CNS is TNF-α which induces synthesis of adhesion molecules and chemokines implicated in leukocyte recruitment, cell proliferation, and apoptosis.

TNF-α plays a role in microglia activation contributing to the pathogenesis of multiple sclerosis, EAE (Centonze *et al.*, 2009; Owens *et al.*, 2001), and to early neuronal injury following acute brain damage (Allan and Rothwell, 2001). One of the major potent stimuli for induction of TNF-α in microglia is mediated by lipopolysaccharide (LPS) through binding and activation of Toll-like receptors (TLR)-4 (Aloisi, 2001). In contrast, it has been shown that TNF-α exhibit distinct functions that can be beneficial as well (Kruglov *et al.*, 2011).

Interleukin Family

Interleukin family are composed by a large mixture of cytokines with a different role as pro- and anti-inflammatory effects such as interleukin-1, -6, -17, and Interleukin-4, -10, -13, respectively.

Interleukin-1 (IL-1) comprises two molecules, IL-1α and IL-1β which have similar affinity for the type I IL-1 receptor (IL-1R). Both IL-1 are produced as precursors called pro-IL-1 that are cleaved by the enzyme which in turn generate the final active molecule. IL-1 is a pro-inflammatory cytokine that is produced predominantly by monocyte/macrophage after binding to the IL-1R, resulting in the amplification of the inflammatory responses.

Interleukin-4 (IL-4) is produced by mature Th2 cells, mast cells and basophil. It is released in response to allergic diseases and it has a crucial role as in suppressing macrophage activation. Many levels of this cytokine have also been detected in autoimmune diseases such as MS and EAE model (Owens *et al.*, 2001). Their protective role is due to its ability to inhibit NO and pro-inflammatory cytokines and to stimulate NGF releasing (Chao *et al.*, 1993).

Members of the interleukin-6 (IL-6) family comprises LIF, IL-6, IL-11, ciliary neurotrophic factor (CNTF), oncostatin M (OSM), cardiotrophin-1, and growth-promoting activity. The principal member is represented by IL-6 whose functions include pro-inflammatory actions and regulation of hematopoiesis, B cell growth, and antibody production. On the other hand, it can also act as an anti-inflammatory cytokine, blocking the strong production of pro-inflammatory molecules. The IL-6 receptor is expressed in neurons and astrocytes and is increased during CNS inflammation.

Interleukin-10 (IL-10) is a cytokine with major immunosuppressive and anti-inflammatory activities that downregulates cellular immunity by acting directly on T cells. In particular, IL-10 production is induced in following infection and acute injury and during autoimmunity. *In vitro,* IL-10 inhibits the ability of microglia to function as antigen-presenting cells and to produce pro-inflammatory mediators (Aloisi, 2001).

1.5 Inflammation in neurodegenerative and neuroimmunological disorders

Neuroinflammation is a peculiar condition characterized by several sequential signals which in turn induce the release of cytokines and inflammatory mediators as a result of the activation of microglia and astrocytes. There is increasing evidence that neuroinflammation might contribute to the increase and the progression of several neurodegenerative disorders (Glass *et al.*, 2010). One of the major challenges for scientists in this field is to understand deeply the mechanisms involved in the neuroinflammation in order to develop new strategies and therapies. One important example is represented by MS.

Multiple Sclerosis (MS)

Different from AD, PD, and ALS, MS is an autoimmune and not hereditary disease characterized by inflammation, demyelination, and axon degeneration in the CNS (Fig. 6). The pathology occurs when immune system cells trigger an inflammatory response toward the myelin sheath. Afterwards, the infiltration of lymphocytes, the increasing in microglia and astrocytes, and demyelination into the perivascular region of the brain and spinal cord white matter promote axonal degeneration and neuronal loss (Lassmann *et al.,* 2001; Frohman *et al.,* 2006). The symptoms of MS are associated with defects in sensation and in the motor, autonomic, visual, and cognitive systems.

MS is typically diagnosed by supporting medical imaging and laboratory testing. In fact, magnetic resonance imaging (MRI) of the brain and spinal tissue may show plaques or lesions associated with demyelinated neurons.

The development of MS is thought to be principally due to environmental factors, triggering an autoimmune response that targets the myelin sheath surrounding nerves (Fig. 6).

Since MS is not considered a hereditary disease, its pathogenesis is closely correlated with viral and bacterial infections because regions of pathogen-associated proteins resemble myelin proteins, such as MBP. The onset of the disease occurs when naïve T cells recognize as antigen MBP presented by dendritic cells, macrophages, and microglia. A crucial role in the pathogenesis of MS is given by Th17 cells a subset of Th1 helper T cells (Cua *et al.,* 2003). Th17 cells secrete the pro-inflammatory cytokine IL-17 that plays a key role in infection by pathogens (Korn *et al.,* 2009). More in detail, the demyelination phenomenon is due to the loss of oligodendrocytes, resulting in the breakdown of the axons and loss of electrical signals efficient propagation. In the majority of cases, remyelination could take place in early phases of the disease, but the oligodendrocytes are unable to restore completely the myelin sheath. Furthermore, repeated attacks toward myelin increase the damage around the axons, inducing the formation of new plaques (Chari, 2007; Compston and Coles, 2002).

EAE animal model has been induced with peptide sequences from infectious agents that share structural homology with myelin components (Libbey and Fujinami, 2010).

Integrin α4β1 (VLA4) is an adhesion molecule that allows autoreactive T cells to break the BBB and migrate into the brain parenchyma. In fact, an antibody directed against very late

VLA-4 are used as a therapeutic strategy to inhibit EAE and reduces the frequency of lesion formation in MS (Miller *et al.*, 2003).

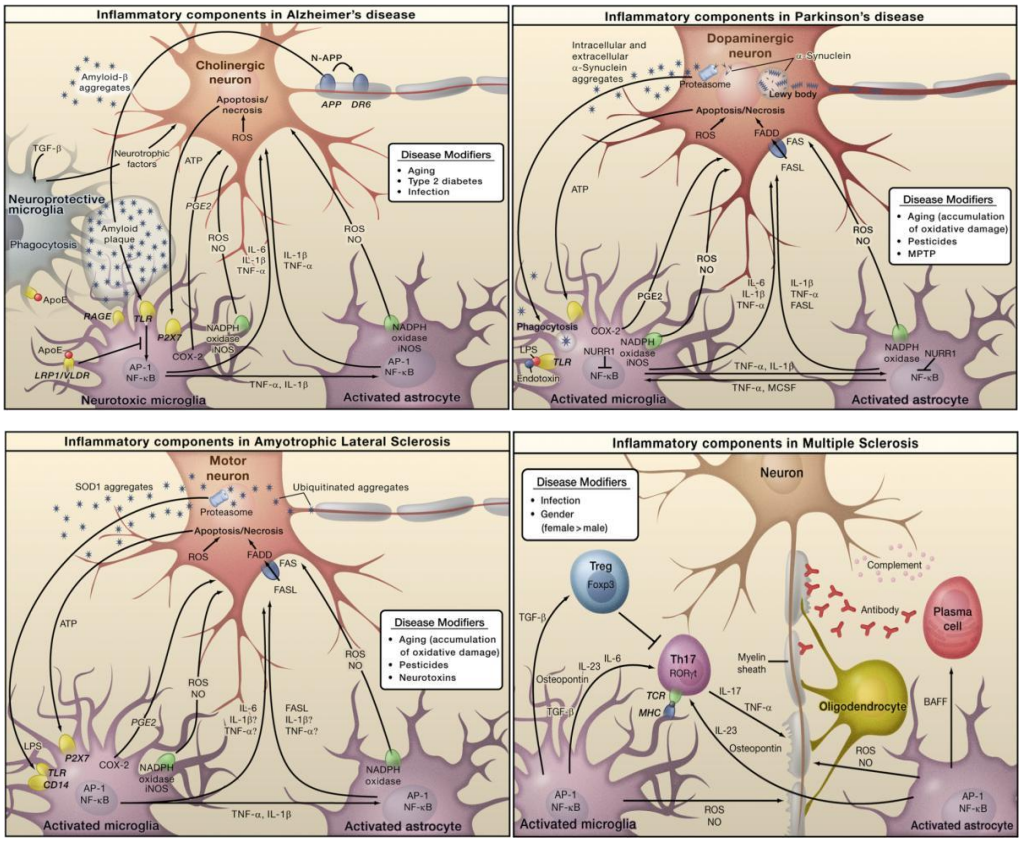

Figure 6. Neuroinflammatory mechanisms in the neurodegenerative diseases.

Neurodegenerative diseases such as AD, PD, ALS, and MS involve inflammatory mechanisms which contribute to degeneration and neuronal death. Different damage stimulate activation of both microglia and astrocytes which release several inflammatory factors, including NO, cytokines, chemokines, and ATP. These neuroinflammatory agents are crucial for activation of immune cells, recruitment of peripheral blood cells, and neuronal-glial communication (Glass *et al.*, 2010).

1.6 Neuroinflammation and neuronal activity

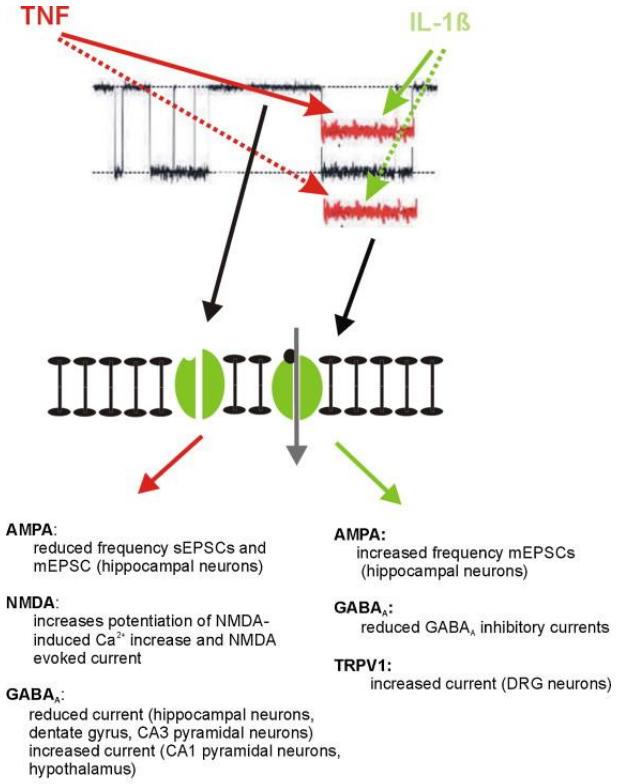

Figure 7. Cytokines action on ionotropic and metabotropic receptors.

TNF-α and IL-1β are able to act different effects on AMPA and GABA receptors located in the separate area in the SNC. In particular, thanks to the modification in increasing or decreasing of the receptors expressed on neurons, cytokines are able to influence the frequency of the neuronal currents signal. Moreover, many evidences have demonstrated a further action operated exclusively by TNF-α on the NMDA receptors (Schäfers and Sorkin, 2008)

Astrocytes and microglia contribute to the development, plasticity and maintenance of neuronal circuits controlling neuronal signalling. In response to changes in the environment, activated microglia release NO, trophic factors, or cytokines, all known to control neuronal function and synaptic transmission. Studies conducted on neuronal cultures or acute brain slices stimulated by LPS have shown an increase of the excitatory post-synaptic currents (EPSCs) (Pascual *et al.*, 2012). In fact, LPS-toll-like receptor 4 (TLR4) microglia activation release ATP that induce astrocytes-glutamate releases. As a result, glutamate enhances the AMPA glutamate receptor-mediated PSCs frequency giving to microglia a specific role in the modulation of excitatory neurotransmission (Pascual *et al.*, 2012). In addition, ATP can also

increase miniature EPSCs (mEPSCs) frequency in hippocampal cultures apparently regulating structural features of synapses such as the probability of presynaptic vesicle release (Antonucci *et al.,* 2012).

Pro-inflammatory cytokines may also specifically interact with receptor and ion channels regulating neuronal excitability, synaptic plasticity and injury (Fig. 7).

The pro-inflammatory cytokine tumor necrosis factor-α (TNF-α) was found to initiate the activation cascade of other cytokines and growth factors (Schäfers and Sorkin, 2008). In addition, TNF-α induces an increase in the expression on neurons surface of AMPA receptors (AMPARs). In fact, blockade of TNF-α signalling reduces the surface level of AMPARs, suggesting that TNF-α plays a crucial role in the regulation of synaptic strength at excitatory synapses (Tancredi *et al.,* 1992; Beattie *et al.,* 2002). Moreover, additional TNF-α effects are observed also on the $GABA_A$ receptors, whose expression is reduced on the surface of hippocampal neurons (Stellwagen *et al.,* 2005). In particular, through the TNFR1, TNF-α is able to regulate both AMPA and $GABA_A$ receptors trafficking by controlling mechanism of exocytosis and endocytosis, resulting in the alteration of excitatory and inhibitory transmission (Stellwagen *et al.,* 2005). Furthermore, several effects on the expression of NMDA receptor are known as well (Wheeler *et al.,* 2009).

Interleukin-1β (IL-1β) is another potent pro-inflammatory cytokine that is produced and secreted under conditions that are associated with inflammation and degeneration. Similar to TNF-α, IL-1β is able to affect glutamate and GABA receptors, increasing the NMDA- and reducing $GABA_A$-mediated transmission. In EAE similar changes in neurotransmission are reported to occur in the cerebellum where pro-inflammatory cytokines, in particular, IL-1β, are released from infiltrated lymphocytes (Mandolesi *et al.*, 2015). On the contrary, IL-1β inhibits the activity of preoptic area/anterior hypothalamus neurons by increasing the presynaptic release of GABA through IL-1R signalling (Tabarean *et al.*, 2006).

2. Spinal cord networks

2.1 Structure and function of the spinal cord

The spinal cord is considered as a gateway for information transfer between the peripheral body and the brain consisting of complex neuronal circuits that integrate and coordinate sensory, motor and autonomic functions (Hochman, 2007).

The spinal cord is organized in segments and each segment is associated with a group of sensory neurons, whose cell bodies form the dorsal roots ganglia (DRG), from which axons leave to reach the periphery. In humans, depending on where they are localized, these segments are divided into cervical, thoracic, lumbar, and sacral. In addition, the segmental organization within the spinal cord is divided in white and grey matter. White matter surrounds the cord and comprises the axon tracts that relay signals to and from the brain and between spinal segments and consists almost of myelinated motor and sensory axons. Whereas, the grey matter with their peculiar butterfly shape is divided in dorsal and ventral horns that contain sites of termination of primary afferent neurons, neurons descending from the brain, interneurons, and ascending tract cells projecting to higher CNS levels (Fig. 8). Furthermore, it includes microglia, astrocytes, oligodendrocytes and unmyelinated axons as well (Hochman, 2007).

The several hundred thousand neurons per segment are housed within cytoarchitectonically defined anatomical layers called laminae (I-X). Commonly, they are classified into three distinct groups: the sensory dorsal horn (laminae I-VI), the intermediate grey (lamina VII), and the ventral horn (VII-IX). Motor neurons are located in lamina IX. Moreover, dorsal and ventral horn consist of specific and complex systems that differ from each other by their distinct function and structure; the sensory system in the dorsal horn and the motor system in the ventral horn.

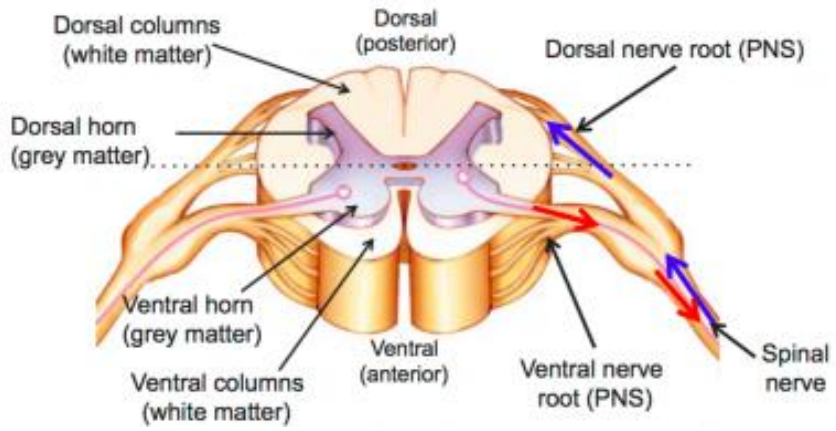

Figure 8. Segmental organization of the spinal cord

Ventral and dorsal horn spinal organization with the presence of white and grey matter. Fibres arise from grey matter neurons are spread to the periphery that form the spinal nerves. These nerves send the signals from the ventral zone and the stimuli from the periphery come to the dorsal neurons located in the grey matter as well (studyblue)

The somatosensory system

The somatosensory system is a complex circuit that allows the organism to perceive a wide range of heterogeneous signals arising from the periphery thanks to various types of receptors widespread in the body. Depending on the type of signal, the receptors are classified in: chemoreceptors, thermoreceptors, mechanoreceptors and nociceptors, which translate physical stimuli into electrical signals. Moreover, the receptors have a corresponding anatomical representation in the spinal cord. Once reached the corresponding neuron, the signal transmitted and mapped along sensory pathways that enable a representation of the sensory stimulus to specified regions in the cortex (Craig, 2003).

Somatosensory information starts when stimuli arise from multiple sensory modalities converge and interact spatiotemporally on spinal neurons whose response is transmitted to other behaviourally relevant regions such as the brain or segmental motor systems. This process is controlled by the interneurons that in the dorsal horn are glutamatergic (excitatory) and GABA or GABA/glycinergic (inhibitory) interneurons. Primary afferents release glutamate as a main neurotransmitter to evoke fast postsynaptic responses composed of early AMPA/kainate and late NMDA receptor-mediated components. The continuous signal coming from the periphery is well controlled to avoid an excess of transmission. In fact, depolarization

of their terminals via negative feedback depression of activated afferents lead to a reduction of the neurotransmitter release (Jankowska, 1992). One of the most important roles played by dorsal horn is to integrate and relay pain information.

Glutamate is not the only neurotransmitter involved in the nociceptive signal. In fact, some primary afferents are able to co-release a variety of neurotransmitters including substance P, calcitonin gene-related peptide, galanin and neuropeptide Y (Millan, 2002).

The motor system

The ventral horn is composed by lamina VII-IX whose area is occupied by interneuronal populations divided into glutamatergic excitatory neurons and GABA/glycinergic inhibitory neurons. In addition, especially in the lamina IX, a wide range of cholinergic motor neurons are located, which send axons out of the ventral root to innervate skeletal muscle fibres. These motor neurons are divided into two distinct types: α-motor neurons that supply extrafusal muscle fibres responsible for movement; γ-motor neurons that innervate intrafusal muscle fibres to control muscle tone by regulating the sensitivity of muscle spindles to stretch.

A peculiar mechanism used by the spinal cord to control the correct functioning of the motor outputs is represented by the reflex system. Spinal reflexes are involuntary responses to sensory stimuli arising from muscle, joints, and skins to determine stereotyped muscles recruitment. The mechanism is due to a correct excitation and inhibition combination between motor and interneurons in order to generate flexors and extensors contraction-release (Fig. 9).

An intrinsic localized neuronal network called central pattern generator (CPG) resides in the spinal cord that can generate rhythmic pattern outputs such as walking, breathing, flying, and swimming in the absence of sensory inputs or descending commands from the brain cortex. Its role is to control the timing and pattern of the muscle activity underlying locomotion. In mammals, CPG is situated throughout the ventromedial portion of the lower thoracic and lumbar spinal cord (Kiehn and Kjaerulff, 1996; Cowley and Schmidt, 1997; Kremer and Lev-Tov, 1997). Research conducted on invertebrate species, such as lamprey and *Xenopus* tadpole, has provided a detailed complex structure of CPGs controlling the locomotor movements (Grillner, 2003, McLean *et al.,* 2000, Roberts *et al.,* 1998). Despite this, less is known about locomotor CPGs in mammals.

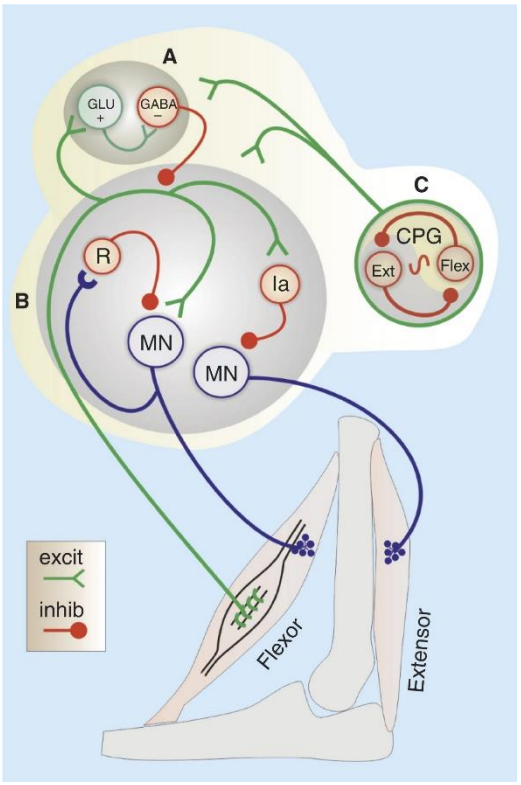

Figure 9. Motor control network in the spinal cord

Scheme of the motor system characterized by CPG in order to generate stimuli on motor neurons and interneurons. A) The interaction between glutamatergic and GABAergic neurons are able to control neural network for presynaptic inhibition of muscle spindle afferents. B) Inhibitory signals from Renshaw cells (R) and inhibitory interneurons (Ia) reduce the motor neurons (MN) transmission direct to the peripheral muscles. C) The CPG induces the activation of the neuronal network important for the alternation to flexor and extensor muscles (Hochman, 2007).

2.2 Molecular and cellular development of the spinal cord

Spinal cord development is regulated by specific genes that control cell proliferation, migration and patterning as well as later events such as neuronal circuit formation and synaptogenesis (Salie *et al.*, 2005). Formation and maturation of spinal cord neurons occur along the three basic spatial axes of the embryonic body plan: rostral-caudal, dorsal-ventral, and medial-lateral (Fig. 10).

The rostrocaudal formation is coordinated by a specific gradient of fibroblast growth factor (FGF) and retinoic acid (RA) concentrates in the opposite area, caudal and rostral respectively (Dasen *et al.*, 2008). Indeed, the medial-lateral axis is separated into progenitor cells, medially, and differentiating progeny, laterally. The dorsal-ventral axis is driven ventrally by Sonic

hedgehog (Shh) produced by the floorplate, and dorsally by bone morphogenetic proteins (BMPs) and Wnts (integrin family) signals from the roof plate. These different morphogens form gradients, in turn, activates a specific transcriptional response which proteins can be divided into two classes: the class I are inhibited by Shh whereas the class II are contrarily activated by Shh (Briscoe *et al.*, 2000; Jessell, 2000; Alaynick *et al.*, 2011). This contrasted function between class II and class I proteins allows the consolidation of progenitor identity. These progenitor cells are divided into five ventral progenitor domains termed p0, p1, p2, pMN and p3, which in turn give rise to interneuron subtypes and motor neurons (Fig. 10).

The Wnt signalling was also shown to be involved in the formation of DRG sensory neurons at early stage (Lee *et al.*, 2004). In vertebrate, Wnt drives the correct direction undertaken by axons projection in the rostrocaudal axis in order to reach their target in the brain. In particular, this role is mediated by Wnt4 which drives axons toward either posterior or anterior path (Salie *et al.*, 2005).

Heterogeneous classes of interneurons during spinal cord development

The heterogeneous classes of spinal interneurons play a major role in integrating sensory and motor signals in the spinal cord. One of the spinal research challenges is to identify the afferent input, output, and the specific role played by the different classes of interneurons in the spinal network (Grillner *et al.*, 1998).

Five classes of genetically distinct ventral neurons are generated by progenitor cells through the progressive changes in Shh concentration: V0, V1, V2, V3 interneurons and motor neurons (Goulding *et al.*, 2002; Sapir *et al.*, 2004; Alvarez *et al.*, 2005; Nissen *et al.*, 2005). In particular, the Shh gradient is driven by homeodomain proteins express by ventral progenitor cells; Pax7, Dbx1, Dbx2, Irx3 and Pax6 (Class I); Nkx6.1 and Nkx2.2 (class II) (Briscoe *et al.*, 2000) (Fig. 10). Post-mitotic neurons generated from these different progenitor domains induce differentiation leading to the segregation of the various classes (Jessell, 2000; Goulding *et al.*, 2002; Nissen *et al.*, 2005).

From ventral progenitor domains, p0 and p1 derive V0 and V1 that express Evx1/2 and En1 respectively. Afterwards during the maturation V0 persists whereas the loss of V1 occurs gradually. V2 neurons that express Chx10 arise from the p2 domain. Finally, the region between floor plate cells and motor neurons generates Sim1 V3 interneurons, defined by

expression of Nkx2.2 which derived from cells within the p3 domain (Ericson *et al.*, 1997a; Pierani *et al.*, 1999; Briscoe *et al.*, 2000; Jessell, 2000).

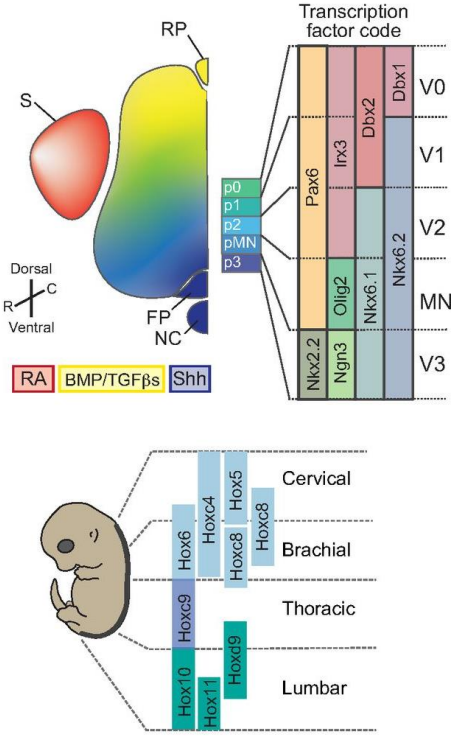

Figure 10. Transcriptional spinal cord development and neuronal formations.

Different transcriptional factors are responsible for the gradient of proteins such as RA, BMP, and Shh, distributed according to the dorsal-ventral axis. The dissimilar progenitors area including p0, p1, p2, pMN, and p3 give rise to the specific spinal neurons. In addition, the temporal expression of a wide range of transcriptional factors delimits the four segmental spinal zone (Davis-Dusenbery *et al.*, 2014).

Previous work conducted on spinal neurons demonstrated that a different class of V0 interneurons is responsible for left-right coordination during locomotion. In fact, glutamatergic interneurons located in lamina VIII are capable of generating rhythmic membrane potentials in phase with rhythmic motor outputs (Lanuza *et al.*, 2004; Hinckley *et al.*, 2005; Wilson *et al.*, 2005). Otherwise, V1 neurons generate Ia inhibitory interneurons as well as Renshaw Cells (RC). This class of neurons exhibits different concentration and distribution of the GABA/glycine phenotypes from embryos to adult phase. Briefly, embryonic spinal interneurons express a high level of GABA, particularly in the ventral horn, which is downregulated immediately after birth followed by the increasing of glycinergic interneuron (Sauressig *et al.*, 1999; Pierani *et al.*, 2001; Sapir *et al.*, 2004). In addition, it was suggested

that V1 neurons take part of the CPG by regulating the duration of locomotor step cycle and hence the speed of locomotion in mammals (Gosgnach *et al.* 2006). V2 are ipsilaterally projecting interneurons that extend axons caudally across several segments. They derive from progenitors residing dorsally to pMN domain and are divided in two different classes: V2a is glutamatergic while V2b is inhibitory which expresses both glycine and GABA. Finally, V3 interneurons are predominantly glutamatergic neurons expressing Sim1 and VGluT2 which arise from the ventral p3 progenitor domain. The 80–85% of these cells project contralaterally and a lower proportion remains ipsilateral (Zhang *et al.*, 2008).

GABAergic and glycinergic changes in the developing spinal networks

The interplay between the glycinergic and GABAergic synapses changes throughout development and is essential for the maturation of the spinal cord. GABA and glycine are neurotransmitters involved in the fast synaptic chloride-mediated transmission in the spinal cord. From the embryonic to the early postnatal phase, GABA and glycine act as depolarizing transmitters due to the high intracellular Cl^- concentration (Reichling *et al.*, 1994).

Crucial for the formation of the interneuronal spinal synaptic connections is the interneurons heterogeneity, as well as the essential interaction of excitatory glutamatergic and inhibitory GABAergic/glycinergic synaptic transmission (Grillner *et al.*, 1995, 2000).

In the embryonic mouse spinal cord, the early glycinergic transmission sustains the propagation of activity bursts throughout contiguous spinal segments, while their generation locally relies on a network formed by motor neurons and GABAergic interneurons (Hanson and Landmesser, 2003; Moody and Bosma, 2005). Nevertheless, existing evidence suggests that GABA is the most important transmitter in the generation of early prenatal miniature currents in rodent motor neurons (Gao *et al.*, 2001).

During mouse embryogenesis, precisely at E13, glycine levels are higher than GABA ones, which progressively augment between E17 and P3, suggesting an already abundant presence of glycinergic neurons. Likewise, a gradual increase between E14 and P3 has been noted for the GABA neurons too (Miranda-Contreras *et al.*, 2002). An extensive loss of glycinergic synapses in addition to a lower pronounced loss of GABAergic synapses occur during the first week, precisely between P3 and P7 (Miranda-Contreras *et al.*, 2002).

The spatial and temporal development of GABA in the embryonic spinal cord has received much attention over the last two decades (Sibilla *et al.*, 2009). The first GABA-immunoreactive (GABA-ir) *somata* have been noted in rat at E12.5, following by a transient peak in the ventral region differently from the stable GABA-ir density in the dorsal horn (Ma *et al.*, 1992, Tran and Phelps, 2000). In addition, the intracellular distribution of glutamic acid decarboxylase (GAD) proteins, is shifted from somatic and proximal axon to distal axons and terminal-like varicosities during spinal development (Tran *et al.*, 2003).

In the mouse spinal cord, a slight difference in terms of temporal expression occurs in the GABAergic neurons. In fact, the first GABA-ir *somata* occurs at E11.5, following by a rostro-caudal gradient of maturation, as well as the increase in the dorsal area (Allain *et al.*, 2004). This 1-day delay is essentially due to the different gestation time in the two species: 22 days for rat and 19 days for mouse.

From E13.5 in mouse, the ventral area exhibits a large amount of GABA-ir cells, which is partially transposed at E17.5 with a higher GABA-ir density in the dorsal area (Allain *et al.*, 2004). After birth, precisely at P0, a drastic reduction of ventral GABA cells occurs, following by an increase of the glycine density until the mature phase. In fact, Gao *et al.* (2001) suggest that only neurons expressing GABA phenotype at early stage of development maintain mature ventral position. Otherwise, neurons which fail to express GABA may switch phenotype to glycine ones.

The functional role of GABAergic ventral synapses in the embryonic rat spinal cord is related to the connection between left and right sides, to the depolarization mediated by $GABA_A$ receptors, and to the generation of synchronous spontaneous burst of activity (Nakayama *et al.*, 2002). Later, from E18.5, glycine receptors take over the role of $GABA_AR$ in modulating the left-right alternation and mediate the inhibition between the two sides of spinal segments.

A major of GABAergic and glycinergic function is represented by their excitatory effect carried out in the early spinal cord. In fact, during the foetal period, the high intracellular concentration of Cl^- ions provides a depolarizing activity, resulting in the elevated Ca^{2+} concentration in the spinal neurons (Cherubini *et al.*, 1991; Ziskind-Conhaim, 1998). Using this mechanism, GABA and glycine promote neuronal development, control outgrowth and differentiation, induce synaptogenesis, crucial for establishing the inhibitory pathway between

the rhythm-generating networks (Ziskind-Conhaim, 1998; Phelps *et al.*, 1999; Gao *et al.*, 2001).

The switch from the excitatory to the inhibitory transmission of GABA/glycine occurs in the entire CNS during development as well as in the maturation of the spinal cord. Especially in the mouse, the first evidence of this transition appears after E14.5 persevering for the first two weeks (Branchereau *et al.*, 2002; Deply *et al.*, 2008). The mechanism underlying this switch is related to changes in the intracellular Cl^- concentration, resulting in the shift from depolarizing action of GABA/glycine toward a hyperpolarizing activity. In particular, the intracellular Cl^- concentration depends on the reverse expression of the Na^+-K^+-$2Cl^-$ co-transporters isoform 1 (NKCC1) and the K^+-$2Cl^-$ type 2 co-transporters (KCC2). Typically, immature neurons are designated by a higher intracellular Cl^- concentration associated with higher NKCC1 levels, which profile is completely reversed in mature cells (Fiumelli and Woodin, 2007; Ben-Ari *et al.*, 2012).

2.3 Synaptic activity and cytokines effect on the spinal networks

Cytokines (CKs) are a large family of proteins released by immune cells in response to tissue damage or infections. CKs are powerful neuromodulatory molecules capable of influencing synaptic transmission and neuronal excitability (Schäfers and Sorkin, 2008). The effects of cytokines on neuronal networks are mediated indirectly, by the release of neuroactive molecules from glia, such as neurotransmitters, nitric oxide, and neurotrophins (Allan and Roshwell, 2001), or directly by activating neuronal receptors (Viviani *et al.*, 2007; Zhang *et al.*, 2014). Regardless the CKs role in triggering the immune response, cytokines exerts physiological functions in the immature CNS related to its growth and development. Nevertheless, any over-expression of CKs in the tissue leads to neuronal dysfunctions associated with neurodegenerative diseases (Glass *et al.*, 2010; Burm *et al.*, 2016; Chen *et al.*, 2016; Czubowicz *et al.*, 2017).

In the last decade, research on this subject has led to a deep understanding of the role of CKs in driving synaptic function and plasticity. Especially, TNF-α, IL-1β, and IL-6 are attracting considerable interest due to their implication in a wide range of synaptic dysfunctions typically concerning neurological disorders (Kawasaki *et al.*, 2008; Centonze *et al.*, 2009; Glass *et al.*, 2010).

The focus of recent research has been mainly on TNF-α and IL-1β which affect all principal classes of voltage-gated channel (VGCs), such as Na^+ channels (Nav), Ca^+ channels (Cav) and K^+ channels (Kv), as well as receptor-operated ionic channels (Vitkovic *et al.,* 2000; Viviani *et al.,* 2007).

TNF-α modulates glutamate and GABA receptors at the neuronal membrane, resulting in increased excitotoxicity stress and neuronal death. In particular, TNF-α can exhibit its function affecting AMPARs by TNF-R1 (Beattie *et al.,* 2002; Stellwagen *et al.,* 2005; Ferguson *et al.,* 2008). In addition, TNF-α can also modify extracellular glutamate levels by inducing glutamate release from microglia and as well as blocking the astrocytic glutamate re-uptake (Zou and Crews, 2005; Takeuchi *et al*., 2006).

More recent evidence highlights that acute application or incubation of spinal cord slices with TNF-α modulates excitatory and inhibitory synaptic transmission (Kawasaki *et al.,* 2008) precisely in the spinal cord dorsal horn (DH). Zhang *et al*. (2010) have demonstrated that TNF-α increases the frequency of spontaneous EPSCs (sEPSCs) and also produce a robust decrease in the frequency of spontaneous IPSCs (sIPSCs). This enhancement is principally mediated through TNF-R1, but not TNF-R2, followed by the activation of neuronal p38 MAPK signalling. Hence, GABAergic neurons display a decrease in the spontaneous action potentials accompanied by a lowering of I_h currents which provide to the development of neuropathic and inflammatory pain. In addition, the main involvement of TNF-α in peripheral nerve injury is well delineated. In fact, the control of presynaptic TTX sensitive sodium channel activity by TNF-α increased the sensitivity of presynaptic TRPV1 receptors in the primary afferent fibres after injury (Spicarova *et al.,* 2011).

Similar to TNF-α, IL-1β plays a crucial role in synaptic modulation by binding to the IL-1 receptor 1 (IL-1R1) and regulating the surface expression of NMDA receptors (Viviani *et al.,* 2003; Gardoni *et al.,* 2011). This leads to the enhancement of Ca^{2+} influx through NMDARs, which in turn promote neuronal network hyperexcitability in *vitro* DRG and spinal slices (Viviani *et al.,* 2003; Yan and Weng, 2013). Different studies conducted on lamina II neurons isolated from spinal slices have demonstrated that IL-1β increases frequency and amplitude of AMPA receptors, including modulation of NMDARs. Furthermore, IL-1β also reduces frequency and amplitude of the sIPSCs acting on GABA- and glycine-induced currents (Kawasaki *et al.,* 2008).

In the spinal ventral horn, GABA and glycine provide the fast synaptic inhibitory transmission essential for motor outputs coordination (Kiehn *et al.*, 1997). The GABA/glycine system mature from foetal stages via expressing important changes related to the locomotor spinal pattern development. Most of the motor circuits in the ventral spinal cord depend on the interplay between excitation mediated by glutamate and inhibition regulated by GABA/glycine. Especially in the adult spinal cord, GABA appears to have a crucial role in the optimization of motor patterns innervating the motor pattern-generating neurons (Christenson *et al.*, 1990).

CKs with their ability in modulating ion channels, receptors, and synapsis may contribute to altering motor synaptic function provoking a wide range of symptoms commonly expressed in several neurodegenerative disorders.

3. Organotypic spinal cord cultures

3.1 Ex-vivo spinal cord model from mouse embryos

Organotypic spinal cord slices represent an *ex vivo* model of segmental microcircuit development in which subsets of interneurons can be directly investigated at different growth-time *in vitro* (Streit *et al.*, 1991; Gähwiler *et al.*, 1997). Many studies conducted in our laboratory have shown that these long-term cultures preserve the basic tissue architecture, synaptic connections and dorsal-ventral orientation of the spinal segment (Rosato-Siri *et al.*, 2002; Avossa *et al.*, 2003; Furlan *et al.*, 2007). Differently, from others *in vitro* models, the organotypic spinal slices have many peculiar characteristics. In fact, processes as synaptogenesis and formation of myelin take place in these cultures. In addition, these cultures are characterized by a variety of neurons and glial cells and maintain the presence of DRG and their incoming output (Streit *et al.*, 1991; Ballerini and Galante, 1998; Ballerini *et al.*, 1999) (Fig. 11). Despite the absence of afferent and supraspinal inputs, this preparation represents a useful model for studying the dynamics of intra-segmental maturation processes which evidently rely on propriospinal circuits.

In the mouse spinal cord, spontaneous rhythmic activity appears emerges at early developmental stages, before the completion of muscle innervations. The generation of this activity relies on the depolarizing drive of GABA and glycine receptor-mediated activity,

(Hansen and Landmesser, 2003), combined with synaptic short-term depression (O'Donovan *et al*., 1998).

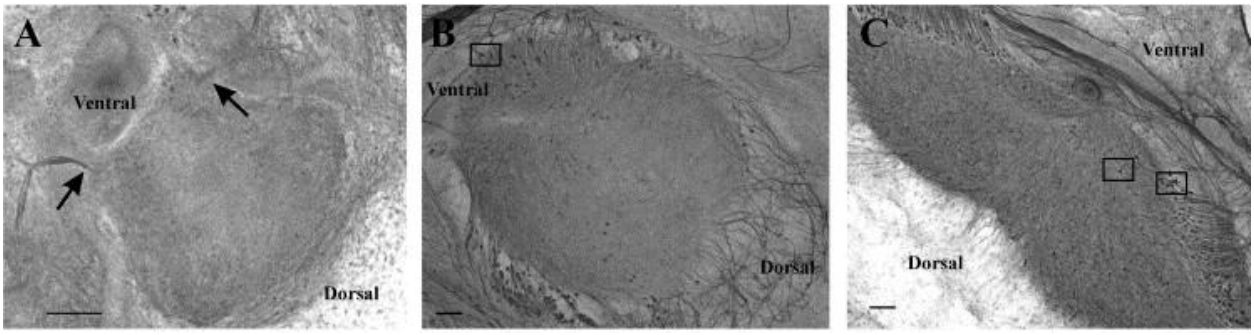

Figure 11. Immunocytochemistry of organotypic cultures with the anti-NF-H antibody SMI32

A) The culture at 8 DIV labelled with SMI32 show processes exiting bilaterally from the ventral part of the slice (arrows). DRG cells present in the top part of the picture. B) The culture at 14 DIV show motoneurons located in the ventral region, bilaterally to the ventral fissure. C) Slice at 21 DIV notes motor neurons and DRG neurons in the ventral horn. All the images show the correct ventral-dorsal orientation typical of the spinal cord (Avossa *et al.,* 2003).

Since ontogeny and functional development of GABAergic interneurons observed *in vivo* is maintained in cultured spinal slices (Avossa *et al.*, 2003; Furlan *et al.*, 2005; Furlan *et al.*, 2007), validating the crucial importance of GABAergic connections for circuit assembly and activity (Barbeau *et al.*, 1999).

In the organotypic spinal slices, five different types of ventral interneurons have been identified, on the basis of their discharge patterns: tonic cells, that fired action potentials (APs) without apparent accommodation; adapting cells, that discharged an early burst of APs followed by adaptation; delay cells, that generated APs after a lag; irregular cells without discernible discharge patterns; transient cells, that generated a single AP only (Furlan *et al.*, 2007). Interestingly, the distribution of the five neuronal classes is maturation-dependent and reflects in addition to the heterogeneous nature of neuronal types of the spinal cord (Jankowska, 2001).

The organotypic spinal model replicates some aspects of the *vivo* environment (Ravikumar *et al.,* 2012). There are several advantages of using this model:

i. interneurons are easily visualized based on their shape and localization, allowing to conduct electrophysiological patch clamp experiments useful to observe the spinal network activity;
ii. slices maintain the correct ventral-dorsal orientation providing the possibility to focus on a specific spinal area;
iii. the correct structure of the pre-motor circuits is preserved along with the complex interplay between interneurons and motor neurons, supported by the DRG and their incoming output;
iv. the ability to reproduce suitable inflammatory responses mediated by microglia, astrocytes, and oligodendrocytes following in vitro neuroinflammatory activation;
v. the advantage of isolating a specific mediated-receptor current, such as excitatory (AMPA and NMDA) and inhibitory (GABA and glycine) transmission by pharmacological block.
vi. the possibility to test pharmacological target fundamental for many neuroinflammatory diseases.

Electrophysiological experiments such as patch clamp recordings, local field potential recordings and multi-electrode arrays combined with immunohistological tools can detect changes in neural mechanisms and activity when interfaced to different pathological environments.

For all these reasons, this model allows elucidating the potential effects due to the alteration of spinal network, which is principally responsible for several inflammatory and degenerative diseases.

In summary, the combination of a developing spinal network supported by different cell populations, complex synapses, and the interneurons electrical profile make the organotypic spinal slices an excellent model to clarify several mechanisms underlying network dysfunctions (Rosato-Siri *et al.*, 2002; Avossa *et al.*, 2003; Medelin *et al.,* 2016; Medelin *et al,* 2018).

4. Fast inhibitory synaptic networks: the GABAergic transmission

Fast inhibitory neurotransmission is modulated by two different neurotransmitters: GABA (γ-aminobutyric acid) and glycine. GABA plays a crucial role in adjusting several functions

including sensory and motor processing, central autonomic control, sleep-wakefulness, emotions, and cognition. Moreover, GABA is capable of binding to ionotropic ($GABA_AR$) and metabotropic ($GABA_BR$) receptors, ubiquitously expressed in the CNS (Barnard *et al.*, 1998; Bowery *et al.*, 2002). Alteration in the GABAergic system leads to a wide range of neurological disorders, such as epilepsy, anxiety, ethanol dependence, and schizophrenia (Coulter *et al.*, 2001; Malizia *et al.*, 1999; Morrow *et al*., 2001; Blum and Mann, 2002). In particular, $GABA_A$ receptors represent a major site of action for clinically important drugs, including benzodiazepines, barbiturates, and some general anaesthetics (Rudolph and Antkowiak, 2004), as well as ethanol, and endogenous modulators, notably endozepines (Christian *et al.*, 2013) and neurosteroids (Hosie *et al.*, 2006). The endogenous modulators, in large part derived from glial cells, are implicated in the regulation of many functions under both physiological and pathological conditions.

4.1 $GABA_A$ receptors: structural composition and function

$GABA_AR$ belongs to a superfamily ligand-gated ion channels able to mediate fast inhibitory transmission by gating Cl^- ions through the cell membrane. This receptor is a pentameric subunit-complex and consists of a hydrophilic extracellular N-terminal domain containing the Cys-loop, followed by four transmembrane sequences (M1–M4) which are arranged around a central pore. In mammals, there are 21 different subunits, including α1–6, β1–4, γ1–4, δ, ρ1–3, θ, π, ε (Barnard *et al.*, 1998; Whiting, 1999) which make the $GABA_AR$ very heterogeneous when compared to any other ligand-gated ion channel. The majority of $GABA_ARs$ contain two α- and two β-subunits, and one γ-subunit variant (Fig. 12), with the α1β2γ2 combination representing the largest population of $GABA_AR$, followed by α2β3γ2 and α3β3γ2. The γ2 subunit can be substituted by γ1 or γ3 subunits or by δ, and possibly ε, subunits.

Pharmacological studies of $GABA_AR$ allowed distinguishing between the various $GABA_AR$ subunits. Precisely, the α1-, α2-, α3-, and α5-subunit correspond to diazepam-sensitive receptors, whereas the α4- and α6-subunit are insensitive to diazepam (Benson *et al.*, 1998; Wingrove *et al.*, 2002). The $GABA_ARs$ are discriminated further by their affinity to zolpidem, a selective allosteric modulator belonging to the nonbenzodiazepine of the imidazopyridine class (Mohler *et al.*, 1996). Aside from this classical pharmacological characterization, neurosteroids, which are positive allosteric modulators of $GABA_ARs$ (Lambert *et al.*, 2001),

are most selective on receptors containing the δ-subunit (Wohlfarth *et al.*, 2002). It is also important to note, that, depending on the α-subunit expressed, $GABA_AR$s may display differences in the kinetics of receptor deactivation (Hutcheon *et al.*, 2000).

$GABA_AR$ subunit molecular heterogeneity allows to generate two distinct forms of inhibitory transmission, phasic or tonic, depending on their postsynaptic or extrasynaptic localization, respectively (Farrant and Nusser, 2005; Belelli *et al.*, 2009; Brickley and Mody, 2012). Importantly, these two major populations of $GABA_AR$s are molecularly distinct, with postsynaptic receptors containing mainly the α1, α2 and α3 subunits, along with β and γ2 subunit, and extrasynaptic receptors composed by α4, α5 and α6 subunits, often combined with the δ subunit as an alternative to γ2 subunit.

In the adult brain and spinal cord, the expression of $GABA_A$ receptor subunits exhibits a remarkable region- and cell-specificity, suggesting that individual subunits are necessary for the distinct neuronal circuits. The segregated distribution of α1- and α2-$GABA_AR$s is correlated with the differential kinetics of deactivation. Indeed, α1-$GABA_AR$s are responsible for the faster kinetics of deactivation, as opposed to α2-$GABA_AR$s (Brussaard *et al.*, 1997; Hutcheon *et al.*, 2000; Jüttner *et al.*, 2001; Vicini *et al.*, 2001).

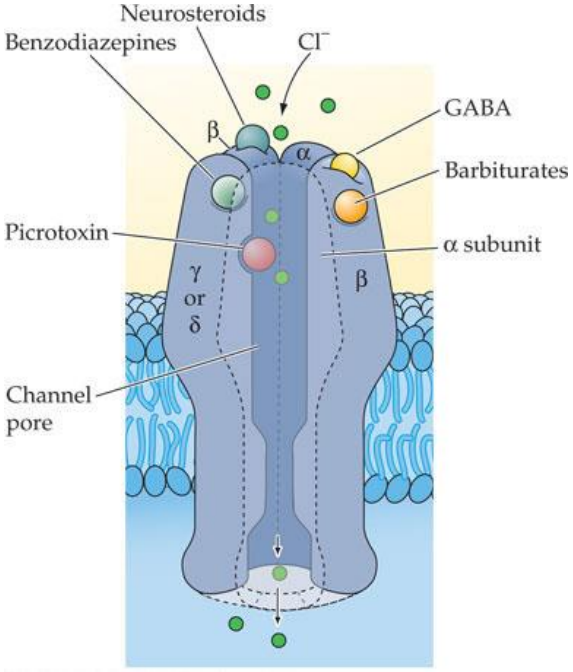

Fig. 12. $GABA_A$ receptor subunits: structure and composition.

Typical schematic representation of $GABA_AR$ characterized by the 5 subunits composition usually 2α2β1γ, resulting in the formation of pore core channel designed for the Cl^- and HCO_3^- ions transfer. The cartoon show also the spots used for binding different molecules such as GABA, neurosteroids, benzodiazepine, barbiturates, and picrotoxin, which are capable of modulating the $GABA_A$-gated receptors (Meyer and Quenzer, 2013).

$GABA_ARs$ function is mainly characterized by their dependence on ion mechanisms, which provide the exchange of Cl^- and $HCO3^-$ (Blaesse *et al.*, 2009). Hence, the effects of $GABA_ARs$ on the resting membrane potential, independently of their subunit composition, are determined by the action of K^+/Cl^- co-transporters and carbonic anhydrases. In fact, the increasing of KCC2, the main Cl^- extrusion transporter, during the maturation of neurons leads to the switch from depolarising to hyperpolarising $GABA_AR$ actions (Ben-Ari, 2002). $GABA_AR$-mediated transmission regulates multiple steps of neuronal development and maturation during ontogenesis and adult neurogenesis, including control of stem/precursor cell proliferation, cell fate decision, migration of precursor cells, survival of immature neurons, dendritic growth, and synaptogenesis (Platel *et al.,* 2007; Dieni *et al.,* 2013).

4.2 $GABA_ARs$ post-synaptic organization and plasticity

In terms of molecular organisation, GABAergic post-synaptic sites consist of specific proteins which contribute to the trafficking and anchoring of $GABA_ARs$ in a subtype-specific manner. More recent evidence proposes that $GABA_ARs$ also clustered by gephyrin scaffold formation at postsynaptic sites (Sassoè-Pognetto *et al.,* 2000; Saiepour *et al.,* 2010). Gephyrin together with direct binding proteins, such as collybistin and NL2, represents the principal protein accountable for regulating $GABA_AR$ trafficking and GABAergic synapse formation (Luscher *et al.,* 2011, Fritschy *et al.,* 2012), α1, α2, and α3 subunits can interact directly with gephyrin via essential motifs located in their main intercellular loop, and hence be clustered postsynaptically (Tretter *et al.,* 2008; Mukherjee *et al.,* 2011; Kowalczyk *et al.,* 2013).

The formation and function of GABAergic synapses are due to the palmitoylation of the γ2 subunit crucial for membrane anchoring of $GABA_ARs$. Consequently, multiple mechanisms such as phosphorylation of various $GABA_ARs$ subunits, are responsible for regulating kinetic properties, or for stability, delivery, or further internalization of $GABA_ARs$ (Jacob *et al.,* 2008; Houston *et al.,* 2009a, 2009b; Vithlani *et al.,* 2011). Thus, gephyrin plays a key role as an anchor scaffold for protein kinase that regulates the efficiency of the inhibitory transmission.

Internalization of $GABA_AR$s is a key mechanism fundamental for the plasticity of synaptic transmission (Kittler and Moss, 2001; Kneussel, 2002). In fact, most synapses dynamically regulate synaptic receptor density by endocytosis, recycling, and degradation (Lin *et al.*, 2000; Barnes *et al.*, 2001).

A major mechanism associated with recycling and degradation of membrane proteins is the clathrin-dependent endocytosis. This process is supported by the interaction between the clathrin adaptor protein (AP2) and the intracellular domains of β1-, β2-, and γ2-subunits, but not the α-subunits. In addition, Kittler *et al.*, (2000) have shown that a large increase of mIPSCs amplitude occurs after blocking of clathrin-dependent endocytosis mechanism in neuron cultures.

Neurotrophins, such as BDNF, play a role in excitatory synaptic plasticity by activation of TrkB signalling pathways. Likewise, BDNF produces a bi-phasic effect on the $GABA_AR$-mediated transmission via interference with the trafficking processes (Jovanovic *et al.*,2001). Particularly in the amygdala, BDNF causes the internalization of α1-$GABA_AR$s followed by a rapid degradation of gephyrin (Mou *et al.*, 2013). In the hippocampus, on the contrary, an increased receptor expression on cell surface has been shown to be mediated by BDNF via the phosphorylation of γ2-subunit (Vithlani *et al.*,2013). In addition, other molecules, such as tyrosine kinase, ROS, and benzodiazepine are implicated in the regulation of trafficking and internalization of $GABA_AR$s (Ali and Olsen, 2001; Henneberger *et al.*, 2002; Accardi *et al.*, 2014).

4.3 The dynamic of intracellular chloride regulation

In the brain and spinal cord, fast-synaptic inhibition is mediated by Cl^- currents, supported by GABA and glycine receptors. Synaptic inhibition efficiency due to Cl^- current flow, may emerge from the degree of GABA and glycine receptor activation or from the driving force of Cl^- ions. The ionotropic GABA and glycine receptors associated channels are permeable to Cl^- and the flow of the negatively charged chloride ions usually inhibits postsynaptic cells since the reversal potential for Cl- is more negative than the threshold for neuronal firing. In physiological conditions Cl^- driving force is stable, but in the certain pathological conditions, the intracellular Cl^- concentration ($[Cl^-]_i$) may be tuned by differential operations of membrane co-transporters.

The individual concentrations of chloride ions outside and inside the cell define the chloride reversal potential (E_{Cl^-}), as described by the Nernst equation. E_{Cl^-} in the health, mature neurons, is approximate -85/-70 mV (Arosio *et al.*, 2010). $[Cl^-]_i$ is maintained at low concentrations (around 5 mM) that enable the influx of Cl^- ions *via* opening of ionotropic GABA or glycine receptors (Payne *et al.*, 2003; Ben-Ari *et al.*, 2012; Kayla *et al.*, 2014). This low concentration is maintained by the KCC2 co-transporter which extrudes Cl^- ions against its gradient. KCC2 takes advantage of the electrochemical K^+ gradient due to the sodium-potassium ATPase, which is energy dependent (Fig. 13). Conversely, another co-transporter, named NKCC1, is essential for internalizing Cl^- ions in the neurons. Particularly, NKCC1 allows Na^+, K^+, and Cl^- transition inside the cell, using the same process of KCC2, thus exploiting the Na^+/K^+ ATPase.

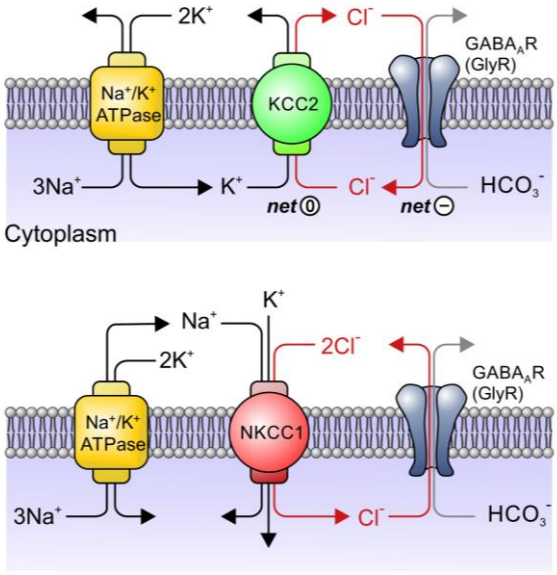

Fig. 13. Schematic Cl^-/HCO_3^- regulation.

Cl^-/HCO_3^- flux through GABA/glycine receptors inside or outside the cell. Mechanisms associated with the cotransporters NKCC1/KCC2 important for the correct balance of the ion equilibrium. In addition, the energetic role carried out by Na^+/K^+ ATPase exploited by both cotransporters (Doyon *et al.*, 2016).

In immature neurons, the expression of KCC2 is low and KCC1 govern the Cl^- membrane-transport, generating typically a high (around 30 mM) $[Cl^-]_i$, fundamental for expressing depolarizing $GABA_AR$ mediated responses (Achilles *et al.*, 2007; Fig. 14).

The expression profile of KCC2 mRNA is correlated with the sequential maturation of neurons (Li *et al.*, 2002; Wang *et al.*, 2002b; Stein *et al.*, 2004). Generally, the ontogeny of KCC2

mRNA in mouse is similar to rat, with the singular difference concerning delays of 2 days in rat embryos (Li *et al.,* 2002).

Mouse spinal cord and brainstem show the earliest development of Cl^- homeostasis. Expression of KCC2 mRNA starts at E10.5 while the KCC2 transcripts are found in the ventral motor as early as E12.5 (Hübner *et al.,* 2001) and in sensory nuclei at later stages, E15.5 (Stein *et al.,* 2004). In mouse embryonic spinal cord, both KCC2 and NKCC1 are expressed and functional early in development (E11.5–E13.5), when $GABA_AR$ activation mediates excitatory responses (Delpy *et al.,* 2008). After E15.5, NKCC1 progressively reduces its activity in motor neurons while KCC2 increases its function and provides more negative E_{Cl^-}, responsible of the inhibitory role of GABA and glycine receptor activation in the majority of spinal neurons at E17.5 (Branchereau *et al.,* 2002). This switch corresponds to the transition phase in which the locomotor networks start to generate alternating flexor and extensor motor activities as well as the network expression of left-right alternation, indicating the presence of functional network inhibition (Delpy *et al.,* 2008).

4.4 Chloride regulation in CNS disorders

Several pathological disorders in the CNS involve alterations in GABAergic synaptic signalling, affecting the physiological Cl^- ion fluxes. These alterations may include (1) mutations in the $GABA_AR$ subunits composition and (2) dis-regulation in the NKCC1/KCC2 balance (Lewis *et al.,* 2005; Bavelier *et al.,* 2010; Ben-Ari *et al.,* 2012; Kaila *et al.,* 2014).

$GABA_AR$ mutations specifically of α, β3, γ2, and δ subunit are commonly correlated with various idiopathic epilepsies syndrome. In particular, the majority of this mutation is implicated in altering the orderly processes of trafficking and clustering (Bouthour *et al.,* 2012).

GABAergic transmission also regulates neuronal plasticity by controlling the inhibitory-excitatory balance in neuronal networks and is key in regulating the proper development of the CNS

Potential dysfunctions of $GABA_AR$ are also implicated in a range of diseases which might be treated with benzodiazepine site ligands. This is the case of pathologies concerning the neuropathic pain. In fact, the anti-hyperalgesic effects mediated by certain benzodiazepine site

ligands take place via stimulation of α2-$GABA_AR$ in the spinal cord dorsal horn (Paul *et al.*, 2013).

Alterations in the maturation of NKCC1/KCC2 balance during development have been correlated to various diseases, from childhood epilepsy to autism spectrum disorders (Ben-Ari *et al.*, 2012; Kaila *et al.*, 2014). In particular, mutations in the KCC2 gene have been associated with a partial or complete loss of chloride extrusion, which result in several modifications of the neuronal network activity (Stödberg *et al.*, 2015; Fig. 14).

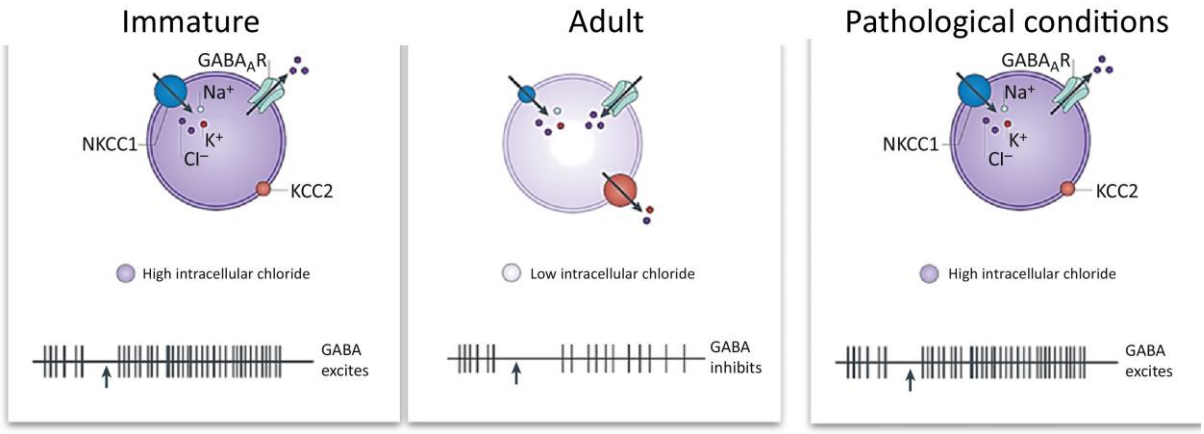

Fig. 14. NKCC1/KCC2 expression during neuronal development and diseases.

Divergent expression of NKCC1/KCC2 co-transporters in immature and adult neurons, which drive the $[Cl^-]_i$ important for the excitatory-inhibitory GABAergic transmission. In the mature neurons, physiological conditions are characterized by high KCC2 and low KCC1 expression, which maintain low $[Cl^-]_i$. In contrast, during disease the NKCC1/KCC2 expression reflexes the same profile exhibit by early embryonic neuron, contributing to a $GABA_AR$-mediated excitatory response (Ben-Ari, 2017).

A similar loss of function of KCC2 has been reported in spinal cord dorsal horn, which therefore interferes with the sensory signalling associated with neuropathic pain pathologies (Doyon *et al.*, 2013; Prescott, 2015). Many studies have shown that BDNF signalling via TrkB receptors is responsible for the KCC2 down-regulation. In fact, in experiments conducted on chronic pain models, BDNF appears to arise from microglia (Ferrini and De Koninck, 2013). Intriguingly, impaired Cl^- homeostasis is also present in various pathological conditions of the brain and spinal cord, such as injury, neuroinflammation, and stress.

Since a wide range of diseases are associated with Cl^- dis-regulation, responsible for the failure of $GABA_A$-mediated inhibitory transmission, several strategies have been developing in order

to restore the physiological low $[Cl^-]_i$ inside the neurons. One of these strategies is characterized by taking advantages of positive allosteric modulators, able to enhance the $GABA_AR$ (Knabl *et al.,* 2008). Given that, the $GABA_AR$ allows the transition of both Cl^- and HCO_3^- ions reducing the inward currents generated by HCO_3^- efflux representing an alternative strategy to restore inhibition (Prescott, 2015).

In addition, emerging tools to re-establish the normal ion homeostasis provide the use of pharmacological drugs that act on NKCC1. In particular, bumetanide a powerful blocker of NKCC1 has been revealed potentially useful to treat some developmental seizure-prone conditions, as well as reducing the severity of autism symptoms (Dzhala *et al.,* 2005; Lemonnier *et al.,* 2012). New strategies focused on the excess of KCC2, which might lead to a huge extracellular K^+ accumulation, ultimately increasing the network excitability (Doyon *et al.,* 2011; Krishnan and Bazhenov, 2011).

Aims of the thesis

The principal aim of my thesis was to investigate the mechanisms underlying neuroinflammation which are able to interfere with the synaptic transmission. Since several neurodegenerative disorders involving spinal cord circuits are frequently accompanied by an inflammatory profile, the consequences of which result in neuronal defects, I focused my attention on a specific area of the SNC, the ventral spinal cord. For these reasons, my goal was to understand the key role of inflammation and resident cells in affecting the regular spinal pre-motor networks.

I used a combination of two distinct elements to integrate both inflammation and spinal circuits:

1. the organotypic spinal cultures obtained from mice embryos which represent an excellent model well characterized in our laboratory;
2. a specific cytokines cocktail composed by TNF-α, IL-1β, and GM-CSF whose are reported to be highly concentrated in blood and CSF from MS patients and EAE model.

In the first part of my work, by using the patch clamp voltage-mode technique I recorded the synaptic activity from visually identified interneurons located in the pre-motor microcircuits. In particular, I addressed my study in understanding the effect of CKs, and later LPS, on $GABA_A$ receptor-mediated currents. In doing so I also monitored the astrocytes and microglia responses under inflammatory stress conditions by immunohistological methods.

In the second part of my work, I assessed more specifically the mechanisms involved in the alteration brought about by CKs of $GABA_A$ receptor-mediated currents, dissecting experimentally the following potential mechanisms:

1. disequilibrium in the intracellular chloride homeostasis associated with alterations in the chloride co-transporters (NKCC1 and KCC2);
2. variation in the α-subunit $GABA_AR$ composition due to exchange mechanisms between membrane and cytoplasm.

Medelin et al. Molecular Brain (2018) 11:3
DOI 10.1186/s13041-018-0347-x

Molecular Brain

RESEARCH Open Access

Bridging pro-inflammatory signals, synaptic transmission and protection in spinal explants in vitro

M. Medelin[1,2], V. Giacco[2], A. Aldinucci[3], G. Castronovo[4], E. Bonechi[3], A. Sibilla[3], M. Tanturli[4], M. Torcia[5], L. Ballerini[2*], F. Cozzolino[4] and C. Ballerini[3*]

Abstract

Multiple sclerosis is characterized by tissue atrophy involving the brain and the spinal cord, where reactive inflammation contributes to the neurodegenerative processes. Recently, the presence of synapse alterations induced by the inflammatory responses was suggested by experimental and clinical observations, in experimental autoimmune encephalomyelitis mouse model and in patients, respectively. Further knowledge on the interplay between pro-inflammatory agents, neuroglia and synaptic dysfunction is crucial to the design of unconventional protective molecules. Here we report the effects, on spinal cord circuits, of a cytokine cocktail that partly mimics the signature of T lymphocytes sub population Th1. In embryonic mouse spinal organ-cultures, containing neuronal cells and neuroglia, cytokines induced inflammatory responses accompanied by a significant increase in spontaneous synaptic activity. We suggest that cytokines specifically altered signal integration in spinal networks by speeding the decay of $GABA_A$ responses. This hypothesis is supported by the finding that synapse protection by a non-peptidic NGF mimetic molecule prevented both the changes in the time course of GABA events and in network activity that were left unchanged by the cytokine production from astrocytes and microglia present in the cultured tissue. In conclusion, we developed an important tool for the study of synaptic alterations induced by inflammation, that takes into account the role of neuronal and not neuronal resident cells.

Keywords: Organotypic spinal slices, Network activity, Cytokines, Neuroinflammation, Neuroprotection, NGF-mimetic

Introduction

Inflammatory mechanisms have been closely linked to the pathogenesis of heterogeneous diseases of the Central Nervous System (CNS), including multiple sclerosis (MS), Alzheimer's disease (AD), amyotrophic lateral sclerosis (ALS) and Parkinson's disease (PD) [1, 2]. In these pathologies, inflammatory cytokines (CKs) can be either delivered by activated microglia and astrocytes (CNS resident cells) or by peripheral immune cells able to infiltrate the CNS parenchyma (lymphocytes, neutrophils and mast cells). CKs release affects neurons and synapses, contributing to gray matter pathology. In experimental multiple sclerosis the harmful action of microglia on synaptic activity is mediated by tumor-necrosis factor-alfa (TNF-α) and interleukin-1beta (IL-1β), and pro-inflammatory conditions in general have been reported to tune post-synaptic NMDA and AMPA glutamate receptors, enhancing excitatory transmission and inhibiting the GABAergic one [3–5]. These observations have led to the awareness that multiple sclerosis pathophysiology, traditionally viewed as a genuine white matter autoimmune disorder with only secondary neurodegenerative components [6], involves diffuse synaptic dysfunction and loss, i.e. synaptopathy, that concurrently with demyelination contributes to grey matter atrophy. Inflammatory-dependent synaptopathy, reviewed by Mandolesi et al. (2015), has been detected in MS patients, representing a novel and promising target for future therapies [7].

Nerve growth factor (NGF), extensively studied as neuro-protector agent in neurodegenerative diseases [8], is involved in neuronal survival and reparative processes. NGF has been reported to confer CNS protection in

* Correspondence: ballerin@sissa.it; clara.ballerini@unifi.it
[2]International School for Advanced Studies (SISSA/ISAS), 34136 Trieste, Italy
[3]Department NEUROFARBA, University of Florence, 50139 Florence, Italy
Full list of author information is available at the end of the article

experimental autoimmune encephalomyelitis (EAE) [9]. Recently, Xu et al. (2016) described the neuroprotective effects of a molecule (T-006) that mimic NGF activities and potentiates NGF-protection against glutamate-induced excitotoxicity [10]. In accordance to these strategies, the strongest rationale behind mesenchymal stem cell (MSC) transplantation as an effective therapeutic approach in MS, AD, PD and ALS, resides also in MSCs ability to secrete neurotrophic factors, preventing neuronal damage induced by the inflammatory insult [11]. In the development of novel therapies, the design of trophic molecules able to cross the blood brain barrier (BBB) and thus to directly target neurons, shielding them from synaptic alterations, is a timely placed issue.

Mechanistic studies of the interplay between the release of CKs, the activation of microglia, the emergence of synaptic dysfunction and the role of novel protective molecules, may require sophisticated in vitro models tested in the laboratory to investigate CNS responses at synaptic resolution.

Organotypic slice cultures developed from the embryonic mouse spinal cord represent a complex in vitro model where sensory-motor cytoarchitecture, synaptic properties and spinal cord resident cells are retained in a 3D–fashion [12, 13]. By the use of this model, we have recently shown that in the $SOD1^{G93A}$ mouse, a genetic ALS model, spinal synapses retain greater GABA and glycine co-release than in the wild types and these changes influenced synaptic integration [14].

Here, we further exploit organotypic cultures from the embryonic mouse spinal cord to monitor the emergence of synaptopathy in pre-motor circuits following CKs transient exposure, and to test the neuroprotective efficacy of NGF-mimetic molecule MT2 [15].

We monitored synaptic activity by patch-clamp recording of visually identified ventral interneurons. Spinal cultured tissue exposed to a cocktail of pro-inflammatory CKs displayed a significant increase in spontaneous synaptic activity characterized by a speeding up of the decay phase of GABAergic inhibitory currents, that may affect temporal precision at post-synaptic site and synaptic control of network excitability. These changes were accompanied by significant production of cytokines and chemokines, astrogliosis and microglia activation. Although these inflammatory features were untouched by MT2 applications, this drug reverted all synaptic changes, suggesting the need of specific neuro-protective strategies during chronic inflammation in the CNS.

Results

Organotypic spinal cord cultures express TrkA and TrkB receptors

Organotypic spinal slices represent a biological model useful for studying the dynamics of intra-segmental processes that evidently rely on resident neuroglial cells, propriospinal neurons and circuits [12–14]. To investigate the impact of inflammation on spinal synaptic networks we used co-cultured mouse DRG and spinal cord explants after 2 weeks of in vitro growth (Fig. 1a). These cultures contain heterogeneous cell populations belonging to the neuronal and neuroglial phenotypes [12], including GFAP-positive astrocytes and Iba1-positive microglia (Fig. 1b). We exploited this model to evaluate the NGF-mimetic molecule MT2 ability to prevent synaptic modulation brought about by neuroinflammation, the latter induced by incubating (for 4 and 6 h) the tissue with pro-inflammatory CKs (TNF-α, IL-1β and GM-CSF, 10 ng/mL) [16]. Since MT2 is a ligand of TrkA and TrkB receptors, we first checked the expression of these receptors in the cultured slices. Figure 1c shows the western blot analysis obtained under basal conditions and upon CK stress in the presence or in the absence of MT2 (10 μM). We found that both receptors are expressed by organotypic cultures, and the levels of expression were comparable in all the experimental conditions. By immunofluorescence labeling (Fig. 1d) we observed that TrkA and TrkB are mainly expressed by DRG neurons and with TrkB, in part, by astrocytes (Fig. 1e).

NGF-mimetic MT2 counteracts CKs induced increase in synaptic activity in organotypic slices

We triggered the neuro-inflammatory stress by incubating organotypic cultures with a cocktail of CKs. To directly assess the presence of changes at the level of spinal network activity we patch clamped visually identified ventral interneurons and compared, under voltage clamp mode, the emergence of heterogeneous spontaneous post-synaptic currents (sPSCs; Fig. 2a) between control (CTRL; $n = 48$) and treated cultures (CKs4H and CKs6H; $n = 32$ and $n = 34$, respectively). Organotypic spinal slices display prominent spontaneous electrical activity in the ventral, premotor area [13, 14]. To enable a meaningful comparison of the shifts in communication dynamics in networks exposed to CKs, we selected the 2 WIV stage, where neurons are known to exhibit an intense synaptic activity [13, 14]. In all culture groups, sPSCs were represented by heterogeneous inward currents of variable amplitudes (Fig. 2a and b). CKs treatments did not affect neuronal passive membrane properties (see Methods), however both CKs incubation protocols significantly increased the frequency of sPSCs. The plot in Fig. 2c shows (small symbols) data for six different culture series (between 5 and 8 cells in CTRL and CK4H or CK6H for each series), and the difference in mean values, reported as larger symbols, is statistically significant (19.1 ± 12.7 Hz CTRL; 29.6 ± 10.0 Hz CKs4H; 31.7 ± 14.7 Hz CKs6H; $^{**}P = 0.0048$ CTRL vs CKs4H and $^{**}P = 0.0002$ vs CKs6H, two-way ANOVA). This result is in agreement with previous works reporting

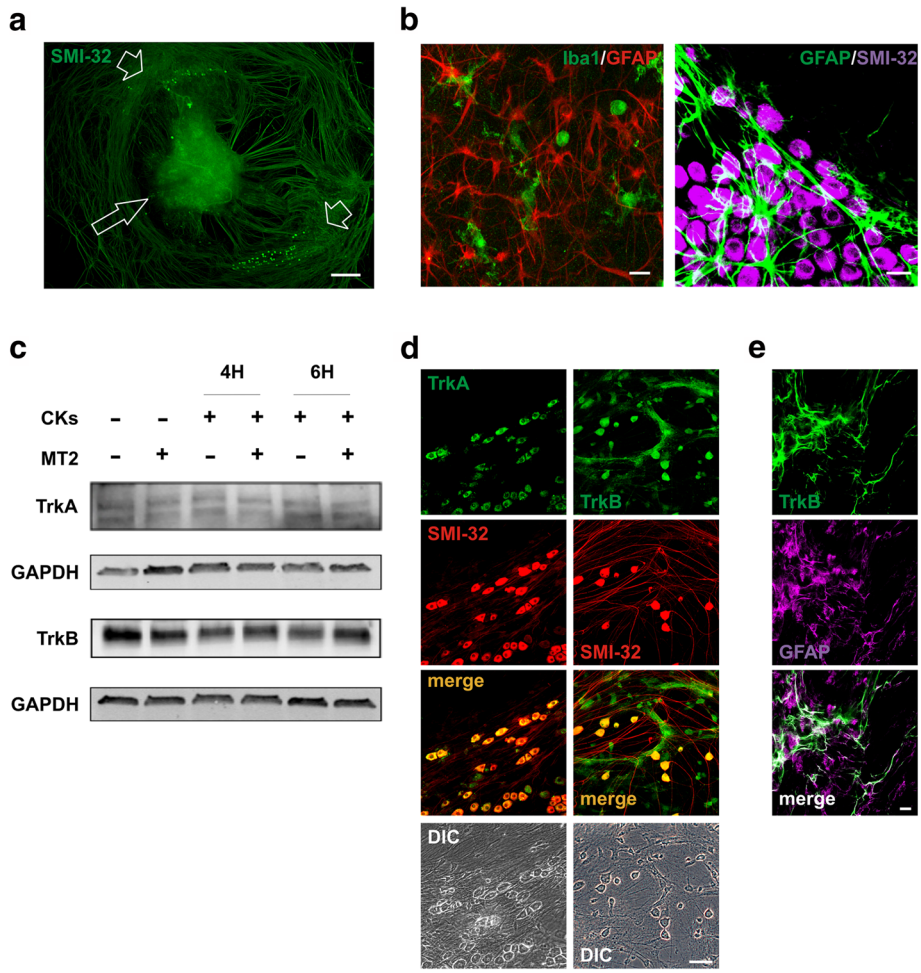

Fig. 1 TrkA/B receptor expression in organotypic spinal cord cultures. **a** Low magnification immunofluorescence for SMI32 (green) of an organotypic spinal cord slice cultured for 2 weeks. The arrow indicates the ventral fissure, localizing the ventral horns. Note the co-cultured DRGs (arrow heads). Calibration bar 500 μm. **b** High magnification immunofluorescence labeling for microglia, astrocytes, and neurons, details of the ventral horn (left) or DRG (right) are shown. Left) green: Iba1 (microglia); red: GFAP (astrocytes). Right) green: GFAP (astrocytes); magenta: SMI-32 (neurons). Calibration bar 20 μm. **c** Western blot analysis of Tropomyosin receptor kinases A and B (TrkA and TrkB) expression in organotypic cultures stimulated with a cocktail of pro-inflammatory CKs (TNF-α, IL-1β and GM-CSF, 10 ng/ml each) for 4 or 6 h in the presence or in the absence of NGF-mimetic molecule MT2 (10 μM). GAPDH was used as house-keeping gene. Each well of the electrophoresis gel was loaded with an equal amount of proteins extracted from a pull of $n = 5$ organotypic slices. Note that TrkA and TrkB expression is not affected by treatments. This experiment is representative of 3 independent ones. **d** Immunofluorescence confocal and differential interference contrast (DIC) images for TrkA and TrkB expression in DRG neurons. Green: TrkA (left panel), TrkB (right panel). Red: SMI-32. Yellow: merge. Calibration bar 50 μm. **e** Immunofluorescence confocal images for TrkB and GFAP in the ventral horns. Green: TrkB; magenta: GFAP Calibration bar 20 μm

the ability of pro-inflammatory CKs, such as TNF-α or IL-1β, to enhance synaptic transmission in spinal cord acute slices [17–19]. However, differently from other studies [20, 21], the neuroinflammatory milieu did not affect the frequency and amplitude of miniature (recorded in the presence of TTX, 1 μM), pharmacologically isolated (in the presence of bicuculline 20 μM and strychnine 1 μM), AMPA-glutamate receptor-mediated excitatory PSCs (mEPSCs; CTRL $n = 37$, CKs4H $n = 20$, CKs6H $n = 20$; Fig. 2d). mEPSCs are independent of network function and should primarily help to localize observed changes in synaptic transmission to pre- and/or post-synaptic level. Our results suggest that CKs treatments were not affecting network activity by tuning excitatory synapses at the pre-synaptic level, increasing the probability of release or the number of release sites, or at the post-synaptic one, altering the properties of glutamate receptors [22].

In parallel, we tested the effects of MT2 applications prior and during CKs 4H and 6H treatments (Fig. 2b). MT2 did not affect the passive properties of CTRL spinal neurons (see Methods) that exhibited a variable and slight, although not significant ($P = 0.3292$), increase in sPSCs frequency (24.5 ± 14.1 Hz CTRL + MT2, $n = 43$), as summarized in the plot of Fig. 2c. In the presence of MT2,

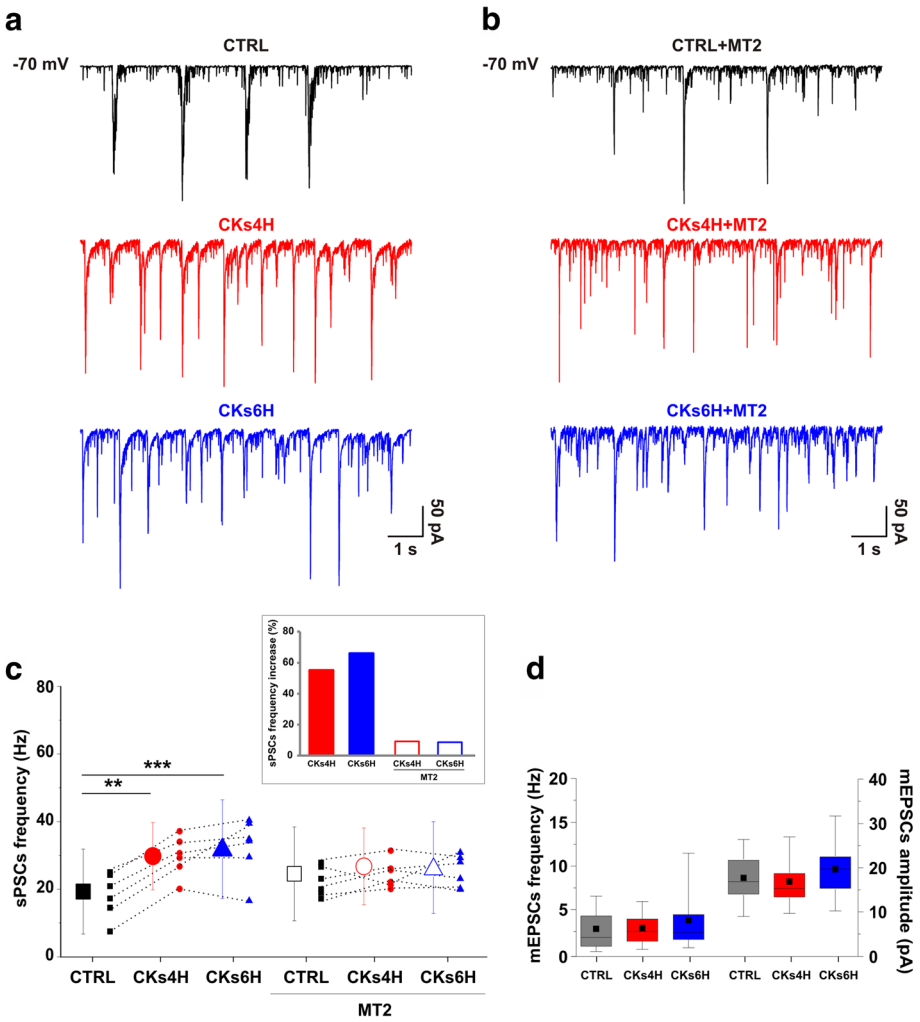

Fig. 2 Pro-inflammatory CKs modulation of synaptic activity in organotypic spinal cord cultures is prevented by MT2. In (**a**) and (**b**) Spontaneous PSCs (sPSCs) recorded from organotypic spinal cord ventral interneurons in control (CTRL) or after CKs treatments in the absence in (**a**) or in the presence in (**b**) of MT2. Note that CKs ability to increase sPSCs occurrence is prevented by MT2 applications. **c** The plot summarizes the frequency of sPSCs prior and after CKs incubation, note the significant increase in network activity, and the frequency of sPSCs prior and after CKs incubation in the presence of MT2, note the absence of significant changes in network activity. Small symbols depict data for six different culture series (between 5 and 8 cells each); larger symbols report mean values. In the inset: the frequency of sPSCs is expressed in respect to each control group, note the increase by 55.27% in CKs4H and by 65.94% in CKs6H. Virtually no increases were observed in MT2: 9.20% in CKs4H + MT2 and 8.63% in CKs6H + MT2. **d** Box-plots summarize the mEPSC event frequency and amplitude values in control or after CKs treatments. Note that CKs applications did not affect these parameters. See the Additional file 1: Figure S1 for mEPSCs in MT2 control and MT2 CKs-treated organotypic slices

CKs treatments at both 4H ($n = 40$) and 6H ($n = 40$) did not further boost sPSCs frequency (26.8 ± 11.5 Hz CKs4H + MT2; 26.6 ± 12.8 Hz CKs6H + MT2). MT2 ability to control the increase in sPSCs frequency brought about by CKs treatments is summarized in the inset of Fig. 2c, where the frequency of synaptic currents is expressed as % of each control.

mEPSCs frequency and amplitude were unchanged when measured in the presence of MT2, with or without CKs (see Additional file 1: Figure S1). These results support the hypothesis that MT2 prevented the increase in network activity caused by the inflammation milieu, apparently without targeting at the pre or post-synaptic level the AMPA receptor mediated synapses.

In the next set of experiments we explored fast Cl^- mediated synaptic transmission and, because of the relatively low frequency of glycinergic events at this developmental stage in culture [13], we compared CTRL ($n = 16$) vs CKs treated $GABA_A$ receptor-mediated synaptic events (IPSCs), recorded in the presence of CNQX (10 μM), APV (25 μM) and strychnine (1 μM). Upon CKs treatments at 4H ($n = 13$) and 6H ($n = 11$) IPSC frequency (4.6 ± 3.0 Hz CTRL; 4.9 ± 2.3 Hz CKs4H; 4.7 ± 3.1 Hz CKs6H) and amplitude (20.1 ± 8.9 pA CTRL; 20.7 ± 9.5 pA CKs4H;

25.2 ± 13.6 pA CKs6H) were not changed by the inflammatory conditions in control or in the presence of MT2 (sample tracings in Fig. 3a and b; box plots in Additional file 2: Figure S2; CTRL + MT2 $n = 16$, CK4H + MT2 $n = 14$, CK6H + MT2 $n = 18$).

Superimposed IPSCs in Fig. 3a (right), show that their decay time constant (τ) becomes progressively shorter with CKs treatments. In Fig. 3c the box plot summarizes the measured τ values (32.3 ± 7.8 ms CTRL; 24.3 ± 4.7 ms CKs4H; 21.8 ± 5.6 ms CKs6H; $^{*}P = 0.020$ CTRL vs CKs4H, $^{**}P = 0.0014$ CTRL vs CKs6H, two-way ANOVA; scaled IPSCs average are superimposed, top). The absence of a significant correlation between IPSC rise time vs decay time values (CTRL $r = 0.3693$; CKs4H $r = -0.1897$; CKs6H $r = 0.3419$; CTRL + MT2 $r = 0.3629$; CKs4H + MT2 $r = 0.4652$; CKs6H + MT2 $r = 0.4420$; plots in Additional file 2: Figure S2) suggests that differences in recording conditions, location of synapses or electronic filtering are unlikely to have affected our observations. We extend our characterization to the properties of miniature IPSCs (mIPSCs; recorded in the presence of TTX). The results in this group of cells confirm that upon CKs treatments mIPSCs differ in their decay kinetics (45.0 ± 8.6 ms CTRL; 31.2 ± 10.4 ms CKs4H; 21.9 ± 2.1 ms CKs6H; $^{*}P = 0.024$ CTRL vs CKs6H, $n = 4$ for each of the three groups, one-way ANOVA; Additional file 3: Figure S3) in a manner similar to that of spontaneous IPSCs. In the presence of MT2, IPSCs show comparable τ in all CKs treatments, as exemplified by the superimposed events in Fig. 3b. The τ values are summarized in the box plot of Fig. 3c (27.5 ± 7.7 ms CTRL + MT2, 27.8 ± 4.7 ms CKs4H + MT2, 26.8 ± 7.2 ms CKs6H + MT2; scaled IPSCs average are superimposed, bottom). The changes in GABAergic

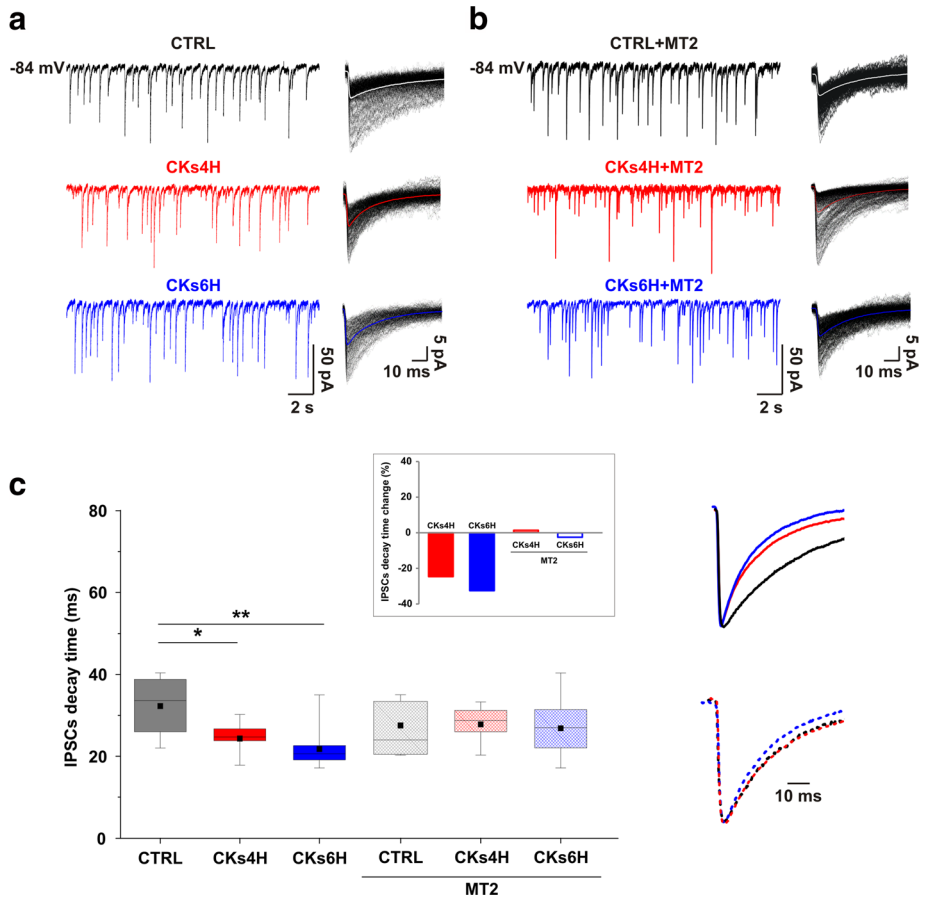

Fig. 3 Pro-inflammatory CKs modulation of $GABA_A$ receptor-mediated event time course is prevented by MT2. Representative traces of IPSC recorded from organotypic spinal slices prior and after CKs treatments in control (**a**) and in the presence of MT2 (**b**). Note that while CKs did not increase IPSC frequency, they affected IPSC time course (superimposed tracings). **c** Box-plots summarize the decay time constant values in all conditions, in the insets the scaled and superimposed average IPSC are depicted (control in black, CKs 4H in red and 6H in blue) in the absence or in the presence of MT2. Note that in the presence of MT2 no changes in the IPSC time course were detected following CKs treatments. In the inset: the τ is expressed as % in respect to each control group, note the reduction by 24.59% in CKs4H and by 32.48% in CKs6H. Virtually no decreases were observed in MT2: slight increase by 1.12% in CKs4H + MT2 and slight reduction by 2.44% CKs6H + MT2. See the Additional file 2: Figure S2 for GABAergic PSCs in the absence or in the presence of MT2

τ induced by CKs treatments are summarized in the inset of Fig. 3c, reported as % of changes in respect to each control.

We can hypothesize that the MT2 was actually able to protect inhibitory synapses from pro-inflammatory stimulation.

Both CKs and MT2 are not interfering with spinal neurons excitability

To elucidate the neuronal mechanisms mediating neuro-inflammatory increase in spinal activity, we addressed whether CKs changed neuronal excitability. In current clamp mode, recorded interneurones did not differ in terms of resting membrane potential and firing threshold (see Methods). Ventral interneurons in organotypic slices have been identified on the basis of their discharge patterns [13]. We identified four different classes of interneurons on the basis of their firing pattern (Fig. 4a) [13, 23–26]: 'transient' cells, that generated a single AP only; 'adapting' cells, that discharged an early burst of APs followed by adaptation; 'irregular' cells without discernible pattern of AP discharge; 'tonic' cells, that continuously fired APs without apparent accommodation. A fifth category (i.e. 'delay' cells, that generated APs after a lag) [13] was rarely (< 4%) observed and thus was not quantified in these series of experiments.

We used depolarizing current steps (0.1 and 0.2 nA amplitude) [13] to induce the firing patterns. The histograms depicted in Fig. 4b report the similar distribution of discharge patterns in CTRL and CK4H (CTRL 16% transient, 64% adapting, 10% irregular, 10% tonic, $n = 31$; CKs4H 24% transient, 44% adapting, 16% irregular, 16% tonic, $n = 25$) and such a

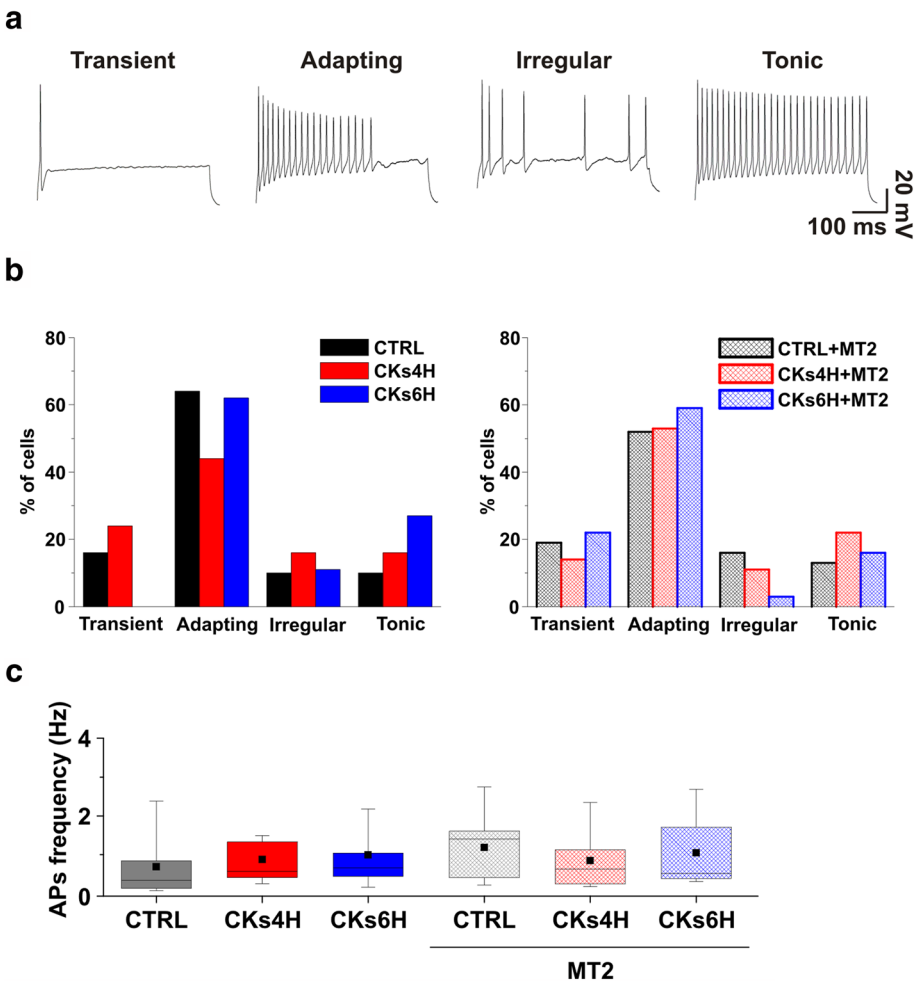

Fig. 4 Pro-inflammatory CKs and MT2 do not alter neuronal excitability in organotypic spinal slices. **a** Discharge patterns of ventral interneurons. The 500 ms depolarizing current commands induced different discharge patterns that identified four cell categories: transient, adapting, irregular and tonic. **b** Bar-charts illustrate the probability distribution (expressed as percentage of sampled population) of each cell type in the various conditions in the absence (left) or in the presence (right) of MT2. **c** Box-plots illustrate the absence of changes in the frequency of spontaneous action potentials in all conditions tested

distribution was not affected by MT2 treatments (CTRL + MT2 19% transient, 52% adapting, 16% irregular, 13% tonic, $n = 31$; CKs4H + MT2 14% transient, 53% adapting, 11% irregular, 22% tonic, $n = 36$). The only different value observed was the virtual absence in CKs6H of transient firing cells, on the contrary well represented in CKs6H + MT2 (CKs6H 0% transient, 62% adapting, 11% irregular, 27% tonic, $n = 26$; CKs6H + MT2 22% transient, 59% adapting, 3% irregular, 16% tonic, $n = 37$).

The box plots in Fig. 4c quantify the frequency of spontaneous APs, and also in this case no differences were detected among CTRL and CKs treated (CTRL 0.7 ± 0.8 Hz, $n = 14$; CKs4H 0.9 ± 0.8 Hz, $n = 14$; CKs6H 1.0 ± 1.1 Hz, $n = 12$) or CTRL + MT2 and CKs + MT2 (CTRL + MT2 1.3 ± 0.9 Hz, $n = 14$; CKs4H + MT2 0.8 ± 0.8 Hz, $n = 18$; CKs6H + MT2 1.0 ± 1.0 Hz, $n = 13$).

These results suggest that cell excitability was not affected by CKs or MT2.

Inflammatory stress modifies cytokine and chemokine production and induces astrogliosis

We evaluated the production of cytokines and chemokines by organotypic spinal cord slices in response to pro-inflammatory stress. The summarizing plots of Fig. 5a show that the exposure to Th1 cytokine cocktail significantly increases the release of IL6 and IL10, key players in regulating inflammation, as well as the release of CXCL1, CXCL2 and CCL2, chemokines implicated in the recruitment of innate immune cells (*$0.01 < P < 0.05$; **$0.001 < P < 0.01$; ***$P < 0.001$; one-way ANOVA). CXCL10, a T cell chemoattractant, is not affected by these treatments. MT2, independently on the inflammatory stimulation, does not exert any effect in the release of any analyzed soluble factor. As expected, the altered cytokine profile induced by pro-inflammatory stress is accompanied by marked astrogliosis and microglia activation, qualitatively illustrated in the example of Fig. 5b (compare with Fig. 1b).

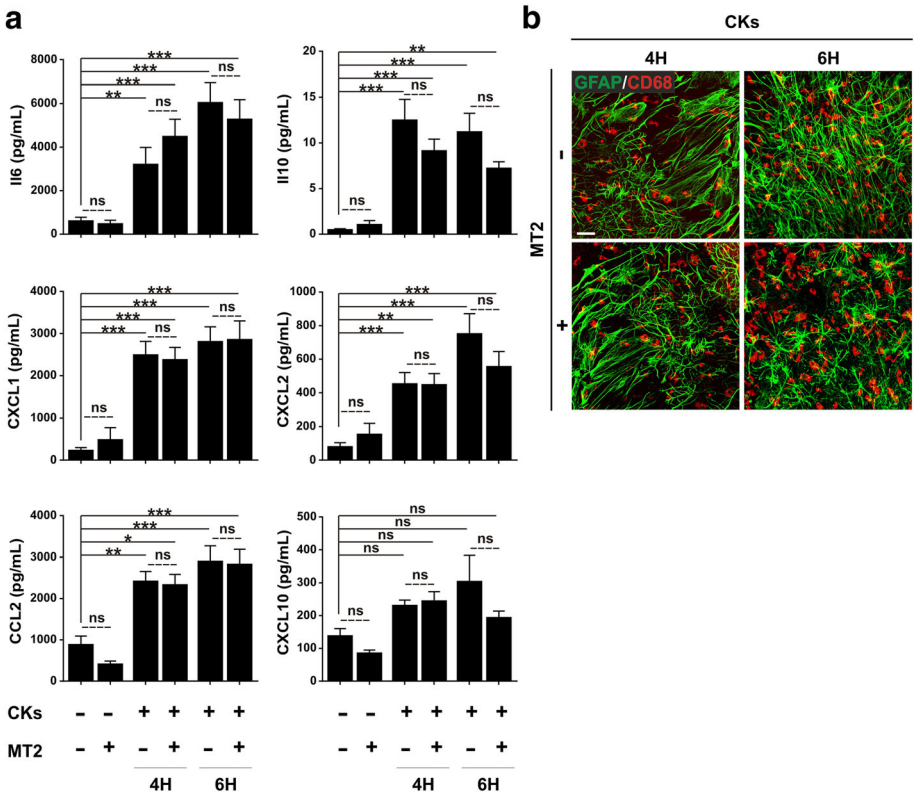

Fig. 5 Effects of pro-inflammatory stress on soluble factor production and on astro/microglia morphology in organotypic spinal slices. **a** Production of cytokines (IL6; IL10) and chemokines (CXCL1; CXCL2; CCL2; CXCL10) determined by Milliplex assay in organotypic culture supernatants after stimulation with the pro-inflammatory cytokine cocktail (CKs) for 4 or 6 h in the presence or absence of MT2. Column graphs report mean values ± SEM of 25 independent experiments. The pro-inflammatory stimulus significantly increases the release of IL6, IL10, CXCL1, CXCL2 and CCL2 compared to control (first column), both after 4 and 6 h of treatment. MT2 treatment did not alter the soluble factor production. **b** Immune fluorescence staining for astrocytes (GFAP, green) and microglia (CD68, red). The pro-inflammatory stress (CKs) induces astrocyte spreading and microglia activation, as indicated by the amoeboid shape. MT2 treatment did not affect these cellular patterns. The pictures show one field representative of 5 randomly analyzed ones (one experiment representative of 5 independent ones). Calibration bar 20 μm

MT2 modulates p38 MAPK activation induced by cytokine stress

It is generally accepted that many highly conserved serine/threonine mitogen-activated protein kinases (MAPK), including p38 MAPK, are activated in response by environmental and cellular stresses including CKs [15]. We investigated the interplay between MT2 treatment and p38 MAPK activation in organotypic slices undergoing pro-inflammatory cytokines incubation. Fig. 6a shows the result of western blot analysis with specific antibody to phospho-p38 MAPK performed in lysates of organotypic slices subjected to CKs stimuli. The data show a de-phosphorylation of p38 MAPK in MT2 treated slices. To better understand the modulation of p38 MAPK activation elicited by MT2, we tested whether MKP-1, a phosphatase highly specific for p38 MAPK and also for JNK, could have a role in this setting. Figure 6b shows that, at 6H CKs treatment, MT2 caused an increase in MKP-1 expression. Taken together these data suggest that MT2 has trophic effects on slices undergoing metabolic derangement induced by pro-inflammatory cytokines.

Discussion

The dogma of the CNS immune-privilege is progressively weakening. In the last decade, an increasing amount of results suggested that, notwithstanding its being surrounded by the BBB, the CNS is a highly immunological active organ, characterized by complex immune cell activation [27] resulting in beneficial (protective) as well as harmful (degenerative) responses [28].

Inflammation, synaptic transmission and neuronal damage are ultimately linked [7]. In this work we have investigated pro-inflammatory CKs effects in spinal microcircuits developed in organotypic cultures containing microglia, astrocytes and neurons, focusing on synaptic activity and measuring soluble factor production. Last, we exploited this model to demonstrate the synaptic protective role of neurotrophins by treating the culture with a non-peptidic mimetic molecule (MT2) that binds TrkA/B receptors.

We selected a CKs cocktail able to mimic an inflammatory reaction that spreads in CNS containing IL-1β, well known determinant of neuropathy [3, 7], TNF-α, that is ubiquitary present during Th1/Th17 mediated inflammatory reactions, and GM-CSF, key cytokine responsible of pro-inflammatory effects in the CNS of MS animal models [29]. GM-CSF receptors are expressed in microglia, therefore the use of this soluble factor allows targeting resident microglial cells, present within the organotypic spinal explanted tissue. Indeed, one of our aims was that to address synaptic function in CNS circuits in the presence of astrocytes and microglia exposed to CKs. We used factors known to be released in EAE and able to directly and indirectly (via activation of resident cells) target neuronal functions. We adopted relatively acute treatments, which triggered inflammatory responses, without affecting neuronal membrane properties or inducing direct neurotoxicity, yet still able to alter synaptic transmission. This protocol has allowed unmasking subtle early changes in GABAergic synaptic currents, a significant player in the excitation/inhibition balance of pre-motor outputs.

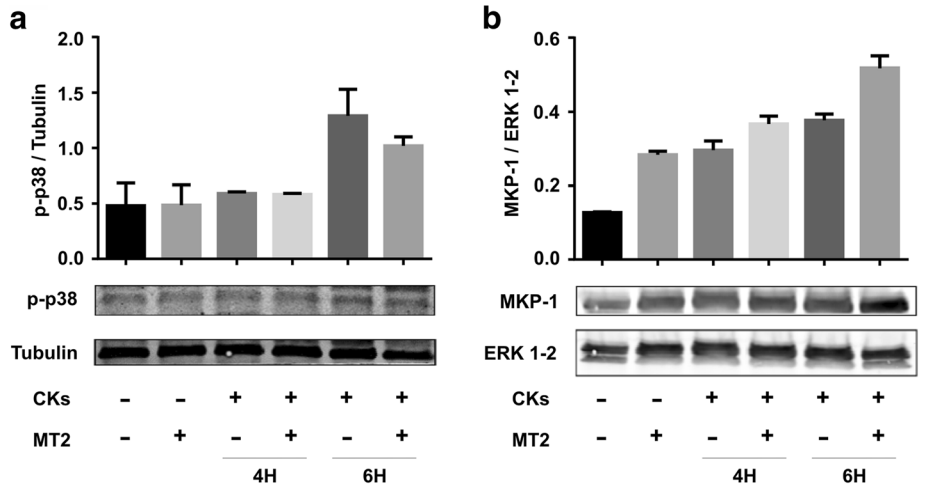

Fig. 6 Effects of MT2 on MAP Kinase pathway in organotypic spinal slices. Organotypic cultures were stimulated with pro-inflammatory CKs cocktail for 4 or 6 h, in the presence or in the absence of MT2. **a** Slices lysates were blotted with rabbit anti-P-p38 and mouse anti-Tubulin as loading control. Bar-charts represent the data of densitometric analysis and are expressed as the ratio between phospho-p38 and Tubulin proteins. **b** Slices lysates were blotted with rabbit anti-MkP-1 and rabbit anti-ERK 1/2 as loading control. The bar-charts represent the data of densitometric analysis and are expressed as the ratio between MKP-1 and ERK 1/2 proteins

Pro-inflammatory CKs tune the excitability of organotypic pre-motor circuit

In organotypic spinal tissue we confirmed the presence of heterogeneous neuroglial cells after 2 weeks of in vitro growth [9], and we further documented the expression and cell-localization of TrkA/B receptors (see below). In the present study, we have used a CKs cocktail and set a tissue exposure protocol to these agents that did not alter TrkA/B receptor expression, however such agents induced a reliable release of cytokines and chemokines, mostly due to the local generation and delivery of inflammatory factors. In fact, upon CKs stimulus, we reported clear inflammatory tissue reactivity expressed as IL6 and monocytes recall-chemokines release, likely requiring the involvement of the heterogeneous cell types present in the slice culture. Our experimental model is ideally suited to dissect spinal resident cells ability in modulating local synapses, in the absence of any contributions from the peripheral infiltrating cells, this mimics early phases of multiple sclerosis where immune cells in brain perivascular spaces activate and produce inflammatory CKs that easily diffuse before cells enter the CNS [30]. In particular, CNS cultured explants allow investigating complex synaptic networks preserving the basic cytoarchitecture of the original CNS area [31], but, differently from acute slices, long term culturing allows the complete recovery from the altered metabolic state caused by the tissue dissection and promotes the effective clearance from the tissue debris, due to the slicing procedure [32, 33].

We recorded from interneurons to assess how the pro-inflammatory stress may regulate the ventral (pre-motor) [14] circuit activity, and this was done within a time-frame where the inflammatory pathological process did not progress to the extent of excitotoxicity. The lack of clear cell damage was supported by the absence of changes in the values of resting membrane potential, input resistance, cell capacitance and AP threshold in the treated neurons in respect to control ones [34–36].

The present data show that, after 4 and 6 h CKs treatments, the frequency of sPSCs was increased. An increased synaptic transmission is a described feature of pro-inflammatory stress in neural circuits, reported form ex-vivo CNS slices isolated from EAE mouse models or from healthy slices exposed to cerebrospinal fluid from multiple sclerosis patients [3, 5, 37] as well as from acute spinal cord slices transiently exposed to various pro-inflammatory molecules [17–19]. Such increases in synaptic transmission have been attributed to the up-regulation of the glutamatergic system [3, 5, 37], to the down-regulation of inhibitory transmission [17, 18, 38] or to altered cell excitability [19, 39]. In spinal cultured slices we did not detect the signatures of any of these mechanisms. To understand the reason for the observed boost in spinal network activity, we examined the miniature excitatory currents [22] that did not suggest the presence of changes in pre-synaptic release probability and in the number of synaptic contacts or in post-synaptic receptor sensitivity in glutamatergic synapses due to CKs exposure, we also excluded alterations in single cell excitability. We equally ruled out variations in the general distribution of firing patterns [13, 19] and in the frequency or amplitude of IPSCs.

We focused our attention to the fast Cl^--mediated neurotransmission due to $GABA_A$ receptor activation, recently indicated as a specific CKs target in spinal circuits [17, 19, 39]. Intriguingly, we found that both IPSCs and mIPSCs from 4 and 6 h CKs slices decayed faster than those from controls, in the absence of any other changes, including differences in release synchronization [14]. This is, to our knowledge, the first time that such a modulation of GABAergic activity is reported due to pro-inflammatory CKs exposure. We did not further investigate in the present work the mechanisms responsible for the altered kinetic properties of GABAergic receptors and therefore the IPSC time course, which can involve differences in the intracellular chloride concentration [40, 41] as well as changes in the receptor subunit composition [42].

Regardless the mechanisms involved, our experimental conditions unmasked a sophisticated and specific synaptic regulation during inflammatory states that may contribute to the increase pre-motor circuit excitability via network-mediated mechanisms. In fact, the faster decaying GABAergic PSCs will lead to weaker and shorter-lasting inhibition, resulting in a reduction in charge transfer in the range 28–35%, perhaps associated with increased network activity. This hypothesis is in agreement with the MT2 ability to control both the CK-mediated increase in network activity and the reduction in IPSC decay. It is tempting to speculate that the different CKs cocktail, the duration of the exposure used here, longer than in the previous studies on acute spinal slices [17, 19, 39], and, in particular, the presence of resident cells, are all factors ultimately responsible of this divergence from previous results. In addition, when compared to acute slicing, the presence of full metabolic recovery from dissection in organ cultures, might also play a significant role.

Interestingly, in previous reports, in dissociated cultures exposed to inflammatory cues [38], the involvement, during chronic EAE phases, of perturbed GABAergic transmission, was suggested together with the need of alternative neuroprotective strategies.

MT2 protective effect on spinal organotypic cultures

With the aim to restore spinal network activity following the neuroinflammatory treatment, we turned our attention to NGF. NGF is a well-known regulator of neuronal differentiation and plasticity [43]. More recently, NGF

has been associated to inflammation and autoimmune diseases. NGF, via TrkA receptors, down-regulates inflammatory CKs production while inducing the release of anti-inflammatory mediators [44]. Moreover, administration of NGF in vivo in EAE animals delays the onset of clinical symptoms and prevents the full development of EAE lesions [45–48]. Despite these exciting reports, the therapeutic use of neurotrophins is a daunting task, due to their limited ability to diffuse in tissues [15]. Therefore, the design of small molecules able to interact with neurotrophins receptors is of great therapeutic interest. In our cultures, TrkA is specifically expressed in DRG and other neurons; on the other hand, we found TrkB expression also in astrocytes. TrkB expression in cultured DRG was not unexpected [49], reviewed in [50]; the finding of TrkB expression in astrocytes is, although surprising for cultured tissue, reminiscent of the complexity of the CNS in vivo. In fact, in the adult rodent spinal cord TrkB expression has been described in reactive astrocytes [51–53]. We did not detect TrkB in CD68+ microglia, present in our culture mostly in amoeboid (activated) form after CKs treatments, in agreement with a previous report on the spinal cord [54–56]. Notwithstanding TrkB expression in the organotypic GFAP-positive astrocytes, (probably the main source of IL-6), the sole addition of MT2 did not modify CK profile in the supernatants, neither directly nor by neuron mediated immune modulation [57]. However, MT2 controlled the CKs electrophysiological signature, namely the induced increase in the sPSCs frequency and the modulation of IPSC time course. To note, MT2 provoked a slight increase in synaptic activity per se, although not significant, and one could argue that in this manner the CKs potentiating effect was simply occluded. Against this interpretation, we also reported the efficacy of MT2 in preventing IPSC decay time modulation. Previous observations [15] suggested the possibility of relatively fast transduction events, after engaging the tyrosine kinase receptors; such mechanisms may explain the short time (no more than 4 h) needed in order to observe the MT2 counteracting effect on electrophysiological alterations. We also reported a trend of decrease in p-p38 accompanied by an increase in MKP-1. These results are, although preliminary, suggestive of such pathways involvement in rescuing GABAergic PSCs.

In conclusion, we developed an important tool for the study of spinal cord alterations induced by inflammation, that takes into account the role of resident cells: neuronal and not neuronal populations, this tool allowed us to test a potential therapeutic molecule.

Methods

Preparation of spinal cord organotypic cultures and neuroinflammation treatments

Briefly, organotypic slice cultures of spinal cord and dorsal root ganglia (DRG) were obtained from mouse embryos (C57BL/6 J of either sex) at days 12–13 of gestation as previously described [13, 14, 58, 59]. Pregnant mice were sacrificed by CO_2 overdose and fetuses delivered by caesarean section. Isolated fetuses were decapitated and their backs were isolated from low thoracic and high lumbar regions and transversely sliced (275 μm) with a tissue chopper. After dissecting the spinal cord slices from the surrounding tissue, slices were embedded into a thick matrix obtained by chicken plasma (Rockland) and thrombin (Sigma) clot. Slices were cultured in plastic tubes with 1 mL medium [14]. The tubes were kept in a roller drum rotating 120 times per hour in an incubator at 37 °C in the presence of humidified atmosphere, with 5% CO_2. Experiments were performed on spinal cultures at 2-weeks in vitro (WIV). The day of the experiment, organotypic spinal cord slices were incubated with standard medium (Control, CTRL) or, for 4 or 6 h (4H and 6H), with a cocktail of the following mouse recombinant cytokines: TNF-α (R&D Systems, #210-TA/CF), IL-1β (R&D Systems, #M15330), and granulocyte-macrophage colony-stimulating factor (GM-CSF; R&D Systems, #P04141), 10 ng/mL each, in order to induce an inflammatory state (Hanisch, 2002). CKs were removed after 4H and 6H, prior to electrophysiological recordings. In sister cultures, controls and the incubation with the CKs cocktail was done in the presence or absence of MT2, a NGF mimetic non-peptidic TrkA and TrkB ligand, kind gift from MimeTech srl, Rome, Italy. MT2 (10 μM for 4H) was tested in the same three conditions (CTRL, CKs4H and CKs6H; in CKs6H condition, MT2 was added after the first 2H of the CKs treatment).

Immunofluorescence and microscopy

Organotypic cultures were fixed in 4% formaldehyde (prepared from fresh paraformaldehyde; Sigma) in PBS for 1 h at room temperature (RT; 20–22 °C), washed in PBS and incubated at RT for 1 h in blocking/permeabilizing solution consisting of 3% FBS and 3% BSA (Sigma) and 0.3% Triton-X 100 (Sigma) in PBS. Then, slices were incubated over night at 4 °C with a combination of the following primary antibodies, diluted in blocking/permeabilizing solution: mouse monoclonal anti-glial fibrillary acidic protein, (GFAP; Sigma, #G3893, RRID:AB_477010, 1:200); rabbit polyclonal anti-ionized calcium-binding adapter molecule 1, (Iba1; Wako, #019–19,741, RRID:AB_839504, 1:400); rat monoclonal CD68 (Abcam, #ab53444, RRID:AB_869007, 1:200), rabbit polyclonal against Tropomyosin receptor kinase A (TrkA), (Santa Cruz, #SC-14024, RRID:AB_2298807, 1:200); rabbit monoclonal against Tropomyosin receptor kinase B (TrkB), (Cell Signaling Technologies, #4607S, RRID:AB_2155128 1:100); mouse monoclonal anti-Neurofilament H Non-Phosphorylated (SMI-32; EMD-Millipore, #NE1023, RRID:AB_2043449, 1:200). Subsequently slices were PBS-washed and

incubated with secondary antibodies diluted in blocking/permeabilizing solution for 2 h at room temperature (RT) in the dark. The secondary antibodies we used were: Alexa 635 goat anti-mouse (Invitrogen, #A31574, RRID:AB_2536184, 1:250); Alexa 488 goat anti-mouse (Invitrogen, #A11001, RRID:AB_2534069, 1:400); Alexa 546 goat anti-mouse (Invitrogen, #A11003, RRID:AB_141370, 1:400); Alexa 488 donkey anti-rabbit (Abcam, #ab150061, RRID:AB_2571722, 1:300). Samples were PBS-washed and mounted on glass slides with ProLong® Diamond Antifade Mountant with DAPI (Thermo Fisher Scientific). Stained samples were examined with 20× and 40× magnification on a Laser Scanning Confocal Microscopy (LSM 5109 Meta, ZEISS); sections were acquired at different focal planes every 1 μm. The image analyses were performed using the ImageJ software (http://rsbweb.nih.gov/ij/).

Western blot analysis

Organotypic slices ($n = 5$ for each experimental condition) were lysed with RIPA buffer (50 mM Tris-HCl, pH 7.4; 150 mM NaCl; 2 mM EDTA; 1 mM NaF; 1 mM sodium orthovanadate, 1% NP-40) in the presence of phosphatase inhibitor cocktail 2 and 3, protease inhibitor cocktail (Sigma Aldrich) and centrifuged at 12.000 r.p.m. for 15 min. 40 μg of total proteins were loaded into SDS-PAGE and blotted onto nitrocellulose filters (GE Healthcare, Fairfield, CT, USA). Membranes were stained with rabbit anti-TrkA, anti-TrkB, anti-MKP-1, anti-ERK ½, anti-P-p38 (Cell Signaling), mouse anti-GAPDH (Cell Signaling), mouse anti-α-tubulin (Santa Cruz Biotechnology); all the antibodies were used at 1:1000, final dilution. HRP-coniugated anti-rabbit IgG (GE Healthcare) or HRP-conjugated anti mouse IgG (Santa Cruz Biotechnology) were used as secondary antibodies at 1:2000 final dilution. The reactions were visualized by the ECL detection system as recommended by the manufacturer (GE Healthcare).

Electrophysiological recordings

For patch clamp recordings (whole-cell) a coverslip with the spinal culture was positioned in a recording chamber, mounted on an inverted microscope (Nikon Eclipse TE200 and Nikon Eclipse Ti-U), and superfused with a standard saline solution containing (in mM): 152 NaCl, 4 KCl, 1 $MgCl_2$, 2 $CaCl_2$, 10 HEPES and 10 glucose. The pH was adjusted to 7.4 with NaOH (osmolarity 305 mOsm). Visually identified ventral interneurons were patched with pipettes (4–7 MΩ) filled with a solution of the following composition (in mM): 120 K gluconate, 20 KCl, 10 HEPES, 10 EGTA, 2 $MgCl_2$, 2 Na_2ATP. The pH was adjusted to 7.3 with KOH (295 mOsm). All recordings were performed at RT.

Under voltage clamp configuration, the voltage values indicated are corrected for the liquid junction potential (−14 mV) [14] if not otherwise indicated. Series resistance values were < 10 MΩ enabling recordings of synaptic currents without significant distortion, and were not compensated for [13]. Recordings were performed from ventrally located spinal interneurones identified on the basis of previously reported criteria [13, 60, 61]. Electrophysiological responses were amplified (EPC-7, HEKA; Multiclamp 700B, Axon Instruments), sampled and digitized at 10 kHz with the pCLAMP software (Axon Instruments) for offline analysis.

In voltage-clamp recordings, single spontaneous post-synaptic currents (sPSCs) were detected by the use of the AxoGraph X (Axograph Scientific) event detection program [62] and by the Clampfit 10 software (pClamp suite, Axon Instruments). On average, ≥ 400 events were analysed from each cell in order to obtain mean kinetic and amplitude parameters. From the average of these events we measured the rise time defined as the 10–90% time needed to reach the peak of the synaptic current, the peak amplitude and the decay time constant (expressed as τ) by fitting a mono-exponential function.

We detected no differences in membrane capacitance (45 ± 21 pF CTRL, 46 ± 19 pF CKs4H, 48 ± 18 pF CKs6H; $n = 55$, 41, 39, respectively; and 48 ± 21 pF CTRL + MT2, 43 ± 16 pF CKs4H + MT2, 46 ± 24 pF CKs6H + MT2; $n = 53$, 47, 47, respectively) and input membrane resistance (417 ± 247 MΩ CTRL, 415 ± 328 MΩ CKs4H, 424 ± 404 MΩ CKs6H; and 400 ± 354 MΩ CTRL + MT2, 430 ± 309 MΩ CKs4H + MT2, 407 ± 244 MΩ CKs6H + MT2) of ventral spinal interneurons recorded in the different conditions. GABAergic post-synaptic currents (IPSCs) were recorded at −84 mV holding potential in the presence of CNQX (10 μM; Sigma), strychnine (1 μM; Sigma) and APV (25 μM; Sigma) and tetrodotoxin (TTX; 1 μM, Latoxan) was used to isolate $GABA_A$ receptor-mediated miniature events (mIPSCs). $GABA_A$ receptor-mediated PSCs were fully blocked by the application of 10 μM SR-95531 (Sigma). AMPA-glutamate receptor-mediated PSCs were recorded at −70 mV holding potential in the presence of strychnine (1 μM; Sigma) and bicuculline (10 μM; Sigma), and TTX (1 μM, Latoxan) was used to isolate AMPA-glutamate receptor-mediated miniature events (mEPSCs). AMPA-glutamate receptor-mediated PSCs were fully blocked by the application of 10 μM CNQX (Sigma).

During current clamp recordings, bridge balancing was continuously monitored and adjusted [13]. Action potentials (APs) were isolated off line by setting an appropriate threshold (−34 mV). The fast (~ 3 ms duration) voltage transients that crossed this threshold were identified as APs. The spontaneous firing frequency for each neuron was calculated on a sample of at least 5 min of continuous recording at −74 mV resting membrane potential. APs threshold was experimentally determined by depolarizing current steps [63].

Induced AP discharge patterns were investigated by delivering depolarizing current steps (500 ms duration) of 0.1–0.2 nA amplitude while keeping the cells at −74 mV resting potential with steady intracellular current injection. We did not detect differences between all the conditions tested in neither interneuron resting membrane potential (−64 ± 9 mV CTRL, −65 ± 9 mV CKs4H, −63 ± 12 mV CKs6H; n = 21, 16, 16, respectively; and −66 ± 8 mV CTRL + MT2, −68 ± 6 mV CKs4H + MT2, −64 ± 7 pF CKs6H + MT2; n = 24, 21, 22, respectively), nor in the spike threshold (−53 ± 4 mV CTRL, −54 ± 5 mV CKs4H, −53 ± 5 mV CKs6H; and −51 ± 5 mV CTRL + MT2, −53 ± 4 mV CKs4H + MT2, −52 ± 3 mV CKs6H + MT2). Electrophysiological data were obtained from 20 different culture series.

Cytokines and chemokines measurement

IL6, IL10, CCL2, CXCL1, CXCL10 and CXCL2 concentrations were measured in organotypic culture supernatants by Milliplex assay (Merck Millipore, #MCYTOMAG-70 k), using the Bio-Plex apparatus (Biorad), according to the manufacturer's recommendations.

Statistical analysis

All values from samples subjected to the same experimental protocols were pooled together and results are presented as mean ± S.D., if not otherwise indicated; n = number of neurons. Two-way analysis of variance (two-way ANOVA) and one-way ANOVA were used to determine significance when multiple groups were compared. Statistical significance was determined at $P < 0.05$.

Additional files

Additional file 1: Miniature excitatory PSCs were not affected by MT2 prior or after CKs treatments. The box plots summarize the mEPSCs frequency (A) and amplitude (B) in control and CKs-treated organotypic slices. (TIFF 294 kb)

Additional file 2: The frequency and amplitude of GABAergic PSCs were not affected by CKs treatments in the absence of in the presence of MT2. Box-plots summarize the frequency (A) and the amplitude (B) of IPSCs prior and after CKs incubation in both the absence and the presence of MT2. (C) The plots show the absence of linear correlation between the decay time constant and rise time of IPSCs in all the conditions tested. (TIFF 777 kb)

Additional file 3: Miniature inhibitory PSCs were faster after CKs treatments. Box-plots summarize the decay time constant values of mIPSCs in all conditions (A). Note the speeding up of the event time course following CKs treatments. (TIFF 89 kb)

Abbreviations

AP: Action potential; BBB: Blood brain barrier; CKs: Cytokines; DRG: Dorsal root ganglia; EAE: Experimental autoimmune encephalomyelitis; GFAP: Glial fibrillary acidic protein; GM-CSF: Granulocyte-macrophage colony-stimulating factor; Iba1: Ionized calcium-binding adapter molecule 1; IL-1β: Interleukin-1beta; IPSCs: $GABA_A$-receptor mediated inhibitory post-synaptic currents; mEPSCs: AMPA-receptor mediated miniature excitatory post-synaptic currents; mIPSCs: $GABA_A$-receptor mediated miniature inhibitory post-synaptic currents; MSC: mesenchymal stem cell; NGF: Nerve growth factor; RT: Room temperature; SMI-32: Neurofilament H non-phosphorylated; sPSCs: Spontaneous post-synaptic currents; TNF-α: Tumor-necrosis factor-alfa; TrkA: Tropomyosin receptor kinase A; TrkB: Tropomyosin receptor kinase B; TTX: Tetrodotoxin; WIV: Week in vitro

Acknowledgements

Not applicable

Funding

We acknowledge financial support from the NEUROSCAFFOLDS-FP7-NMP-604263 and PRIN-MIUR n. 2012MYESZW.

Availability of data and materials

The datasets supporting the conclusion of this article are included within the article (and its additional files). The datasets generated and/or analysed during the current study are stored in a public repository and are available from the corresponding author on reasonable request.

Authors' contributions

MM performed the electrophysiology and the voltage- and current-clamp analysis; VG contributed to the electrophysiology in voltage-clamp experiments; AA performed the immunohistochemistry, the microscopy, the Milliplex assays and the relative analysis; GC, EB and AS performed the WB and the kinase pathways experiments and analysis; MT, MT and CF design the MT2 molecule and provide the MT2 molecule for experiments: LB and CB conceived the idea, design the experiments and wrote the MS. All authors read and approved the final manuscript.

Ethics approval

All experiments were performed in accordance with the EU guidelines (2010/63/UE) and Italian law (decree 26/14) and were approved by the local authority veterinary service and by our institution (SISSA) ethical committee. All efforts were made to minimize animal suffering and to reduce the number of animal used. Animals use was approved by the Italian Ministry of Health, in agreement with the EU Recommendation 2007/526/CE.

Consent for publication

Not applicable

Competing interests

The authors declare that they have no competing interests.

Publisher's Note

Author details

[1]Department of Life Sciences, University of Trieste, 34127 Trieste, Italy. [2]International School for Advanced Studies (SISSA/ISAS), 34136 Trieste, Italy. [3]Department NEUROFARBA, University of Florence, 50139 Florence, Italy. [4]Department of DSBSC, University of Florence, 50134 Florence, Italy. [5]Department of DMSC, University of Florence, 50134 Florence, Italy.

Received: 22 November 2017 Accepted: 4 January 2018
Published online: 15 January 2018

References

1. Glass CK, Saijo K, Winner B, Marchetto MC, Gage FH. Mechanisms underlying inflammation in neurodegeneration. Cell. 2010;140:918–34.
2. Chen W-W, Zhang X, Huang W-J. Role of neuroinflammation in neurodegenerative diseases. Mol Med Rep. 2016;13:3391–6.
3. Centonze D, Muzio L, Rossi S, Cavasinni F, De Chiara V, Bergami A, et al. Inflammation triggers synaptic alteration and degeneration in experimental autoimmune encephalomyelitis. J Neurosci. 2009;29:3442–52.
4. Pascual O, Ben Achour S, Rostaing P, Triller A, Bessis A. Microglia activation triggers astrocyte-mediated modulation of excitatory neurotransmission. PNAS. 2012;109:E197–205.
5. Rossi S, Furlan R, De Chiara V, Motta C, Studer V, Mori F, et al. Interleukin-1β causes synaptic hyperexcitability in multiple sclerosis. Ann Neurol. 2012;71:76–83.

6. Frischer JM, Bramow S, Dal-Bianco A, Lucchinetti CF, Rauschka H, Schmidbauer M, et al. The relation between inflammation and neurodegeneration in multiple sclerosis brains. Brain. 2009;132:1175–89.
7. Mandolesi G, Gentile A, Musella A, Fresegna D, De Vito F, Bullitta S, et al. Synaptopathy connects inflammation and neurodegeneration in multiple sclerosis. Nat Rev Neurol. 2015;11:711–24.
8. Cattaneo A, Calissano P. Nerve growth factor and Alzheimer's disease: new facts for an old hypothesis. Mol Neurobiol. 2012;46:588–604.
9. Zhu L, Pan QX, Zhang XJ, YM X, Chu YJ, Liu N, et al. Protective effects of matrine on experimental autoimmune encephalomyelitis via regulation of ProNGF and NGF signaling. Exp Mol Pathol. 2016;100:337–43.
10. Xu D, Chen H, Mak S, Hu S, Tsim KW, Hu Y, et al. Neuroprotection against glutamate-induced excitotoxicity and induction of neurite outgrowth by T-006, a novel multifunctional derivative of tetramethylpyrazine in neuronal cell models. Neurochem Int. 2016;99:194–205.
11. Salgado AJ, Sousa JC, Costa BM, Pires AO, Mateus-Pinheiro A, Teixeira FG, et al. Mesenchymal stem cells secretome as a modulator of the neurogenic niche: basic insights and therapeutic opportunities. Front Cell Neurosci. 2015;9:249.
12. Avossa D, Rosato-Siri MD, Mazzarol F, Ballerini L. Spinal circuits formation: a study of developmentally regulated markers in organotypic cultures of embryonic mouse spinal cord. Neuroscience. 2003;122:391–405.
13. Furlan F, Taccola G, Grandolfo M, Guasti L, Arcangeli A, Nistri A, et al. ERG conductance expression modulates the excitability of ventral horn GABAergic interneurons that control rhythmic oscillations in the developing mouse spinal cord. J Neurosci. 2007;27:919–28.
14. Medelin M, Rancic V, Cellot G, Laishram J, Veeraraghavan P, Rossi C, et al. Altered development in GABA co-release shapes glycinergic synaptic currents in cultured spinal slices of the $SOD1^{G93A}$ mouse model of ALS. J Physiol. 2016;594:3827–40.
15. Scarpi D, Cirelli D, Matrone C, Castronovo G, Rosini P, Occhiato EG, et al. Low molecular weight, non-peptidic agonists of TrkA receptor with NGF-mimetic activity. Cell Death Dis. 2012;3:e339.
16. Hanisch UK. Microglia as a source and target of cytokines. Glia. 2002;40:140–55.
17. Kawasaki Y, Zhang L, Cheng JK, Ji RR. Cytokine mechanisms of central sensitization: distinct and overlapping role of interleukin-1β, interleukin-6, and tumor necrosis factor-α in regulating synaptic and neuronal activity in the superficial spinal cord. J Neurosci. 2008;28:5189–94.
18. Zhang H, Nei H, Dougherty PM. A p38 mitogen-activated protein kinase-dependent mechanism of disinhibition in spinal synaptic transmission induced by tumor necrosis factor-α. J Neurosci. 2010;30:12844–55.
19. Zhang H, Dougherty PM. Acute inhibition of signaling phenotype of spinal GABAergic neurons by tumor necrosis factor-α. J Physiol. 2011;589:4511–26.
20. Youn D, Wang H, Jeong SJ. Exogenous tumor necrosis fator-α rapidly alters synaptic and sensory transmission in the adult rat spinal cord dorsal horn. J Neurosci Res. 2008;86:2867–75.
21. Spicarova D, Nerandzic V, Palecek J. Modulation of spinal cord synaptic activity by tumor necrosis factor α in a model of peripheral neuropathy. J Neuroinfl. 2011;8:177.
22. Raastad M, Storm JF, Andersen P. Putative single quantum and single fibre excitatory postsynaptic currents show similar amplitude range and variability in rat hippocampal slices. Eur J Neurosci. 1992;4:113–7.
23. Prescott SA, De Koninck Y. Four cell types with distinctive membrane properties and morphologies in lamina I of the spinal dorsal horn of the adult rat. J Physiol. 2002;539:817–36.
24. Szucs A, Pinto RD, Rabinovich MI, Abarbanel HD, Selverston AI. Synaptic modulation of the interspike interval signatures of bursting pyloric neurons. J Neurophysiol. 2003;89:1363–77.
25. Theiss RD, Heckman CJ. Systematic variation in effects of serotonin and norepinephrine on repetitive firing properties of ventral horn neurons. Neuroscience. 2005;134:803–15.
26. VB L, Moran TD, Balasubramanyan S, Alier KA, Dryden WF, Colmers WF, et al. Substantia Gelatinosa neurons in defined-medium organotypic slice culture are similar to those in acute slices from young adult rats. Pain. 2006;121:261–75.
27. Lampron A, Elali A, Rivest S. Innate immunity in the CNS: redefining the relationship between the CNS and its environment. Neuron. 2013;78:214–32.
28. Smith JA, Das A, Ray SK, Banik NL. Role of pro-inflammatory cytokines released from microglia in neurodegenerative diseases. Brain Res Bull. 2012;87:10–20.
29. Ifergan I, Davidson TS, Kebir H, Xu D, Palacios-Macapagal D, Cann J, Rodgers JM, Hunter ZN, Pittet CL, Beddow S, Jones CA, Prat A, Sleeman MA, Miller SD. Targeting the GM-CSF receptor for the treatment of CNS autoimmunity. J Autoimmun. 2017;84:1–11.
30. Maggi P, Macri SM, Gaitàn MI, Leibovitch E, Wholer JE, Knight HL, et al. The formation of inflammatory demyelinated lesions in cerebral white matter. Ann Neurol. 2014;76:594–608.
31. Gähwiler BH, Capogna M, Debanne D, McKinney RA, Thompson SM. Organotypic slice cultures: a technique has come of age. Trends Neurosci. 1997;20:471–7.
32. Braschler UF, Iannone A, Spenger C, Streit J, Lüscher HR. A modified roller tube technique for organotypic cocultures of embryonic rat spinal cord, sensory ganglia and skeletal muscle. J Neurosci Methods. 1989;29:121–9.
33. Lein PJ, Barnhart CD, Pessah IN. Acute hippocampal slice preparation and hippocampal slice cultures. Methods Mol Biol. 2011;758:115–34.
34. Carp JS. Physiological properties of primate lumbar motoneurons. J Neurophysiol. 1992;68:1121–32.
35. Djuric U, Cheung AY, Zhang W, Mok RS, Lai W, Piekna A, et al. MECP2e1 isoform mutation affects the form and function of neurons derived from Rett syndrome patient iPS cells. Neurobiol Dis. 2015;76:37–45.
36. Gao Y, Liu L, Li Q, Wang Y. Differential alterations in the morphology and electrophysiology of layer II pyramidal cells in the primary visual cortex of a mouse model prenatally exposed to LPS. Neurosci Lett. 2015;591:138–43.
37. Centonze D, Muzio L, Rossi S, Furlan R, Bernardi G, Martino G. The link between inflammation, synaptic transmission and neurodegeneration in multiple sclerosis. Cell Death Diff. 2010;17:1083–91.
38. Rossi S, Muzio L, De Chiara V, Grasselli G, Musella A, Musumeci G, et al. Impaired striatal GABA transmission in experimental autoimmune encephalomyelitis. Brain Behav Immun. 2011;25:947–56.
39. Zhou Y, Tang H, Liu J, Dong J, Xiong H. Chemokine CCL2 modulation of neuronal excitability and synaptic transmission in rat hippocampal slices. J Neurochem. 2011;116:406–14.
40. Funk K, Woitecki A, Franjic-Würtz C, Gensch T, Möhrlen F, Frings S. Modulation of chloride homeostasis by inflammatory mediators in dorsal root ganglion neurons. Mol Pain. 2008;4:32.
41. Moroni M, Biro I, Giugliano M, Vijayan R, Biggin PC, Beato M, et al. Chloride ions in the pore of glycine and GABA channels shape the time course and voltage dependence of agonist currents. J Neurosci. 2011;31:14095–106.
42. Ramadan E, Fu Z, Losi G, Homanics GE, Neale JH, Vicini S. GABA (A) receptor beta3 subunit deletion decreases alpha2/3 subunits and IPSC duration. J Neurophysiol. 2003;89:128–34.
43. Levi-Montalcini R. The nerve growth factor 35 years later. Science. 1987; 237:1154–62.
44. Prencipe G, Minnone G, Strippoli R, De Pasquale L, Petrini S, Caiello I, et al. Nerve growth factor downregulates inflammatory response in human monocytes through TrkA. Immunology. 2014;192:3345–54.
45. Villoslada P, Hauser SL, Bartke I, Unger J, Heald N, Rosenberg D, et al. Human nerve growth factor protects common marmosets against autoimmune encephalomyelitis by switching the balance of T helper cell type 1 and 2 cytokines within the central nervous system. J Exp Med. 2000; 191:1799–806.
46. Arredondo LR, Deng C, Ratts RB, Lovett-Racke AE, Holtzman DM, Racke MK. Role of nerve growth factor in experimental autoimmune encephalomyelitis. Eur J Immunol. 2001;31:625–33.
47. Flügel A, Matsumuro K, Neumann H, Klinkert WE, Birnbacher R, Lassmann H, et al. Anti-inflammatory activity of nerve growth factor in experimental autoimmune encephalomyelitis: inhibition of monocyte transendothelial migration. Eur J Immunol. 2001;31:11–22.
48. Makar TK, Nimmagadda VK, Singh IS, Lam K, Mubariz F, Judge SI, et al. TrkB agonist, 7,8-dihydroxyflavone, reduces the clinical and pathological severity of a murine model of multiple sclerosis. J Neuroimmunol. 2016;292:9–20.
49. Genç B, Ulupinar E, Erzurumlu RS. Differential Trk expression in Explant and dissociated trigeminal ganglion cell cultures. J Neurobiol. 2005;64:145–56.
50. Keefe KM, Sheikh IS, Smith GM. Targeting Neurotrophins to specific populations of neurons: NGF, BDNF, and NT-3 and their relevance for treatment of spinal cord injury. Int J Mol Sci. 2017;18:548.
51. Stadelmann C, Kerschensteiner M, Misgeld T, Brück W, Hohlfeld R, Lassmann H. BDNF and gp145trkB in multiple sclerosis brain lesions: neuroprotective interactions between immune and neuronal cells? Brain. 2002;125:75–85.
52. Colombo E, Cordiglieri C, Melli G, Newcombe J, Krumbholz M, Parada LF, et al. Stimulation of the neurotrophin receptor TrkB on astrocytes drives nitric oxide production and neurodegeneration. J Exp Med. 2012; 209:521–35.

53. Coulibaly AP, Deer MR, Isaacson LG. Distribution and phenotype of TrkB oligodendrocyte lineage cells in the adult rat spinal cord. Brain Res. 2014;1582:21–33.
54. Frisén J, Verge VM, Fried K, Risling M, Persson H, Trotter J, et al. Characterization of glial trkB receptors: differential response to injury in the central and peripheral nervous systems. PNAS. 1993;90:4971–5.
55. Wong I, Liao H, Bai X, Zaknic A, Zhong J, Guan Y, et al. ProBDNF inhibits infiltration of ED1+ macrophages after spinal cord injury. Brain Behav Immun. 2010;24:585–97.
56. Spencer-Segal JL, Waters EM, Bath KG, Chao MV, McEwen BS, Milner TA. Distribution of phosphorylated TrkB receptor in the mouse hippocampal formation depends on sex and estrous cycle stage. J Neurosci. 2011;31:6780–90.
57. Nakajima K, Tohyama Y, Maeda S, Kohsaka S, Kurihara T. Neuronal regulation by which microglia enhance the production of neurotrophic factors for GABAergic, catecholaminergic, and cholinergic neurons. Neurochem Int. 2007;50:807–20.
58. Fabbro A, Villari A, Laishram J, Scaini D, Toma FM, Turca A, et al. Spinal cord explants use carbon nanotubes interfaces to enhance neurite outgrowth and to fortify synaptic inputs. ACS Nano. 2012;6:2041–55.
59. Usmani S, Aurand ER, Medelin M, Fabbro A, Scaini D, Laishram J, et al. 3D meshes of carbon nanotubes guide functional reconnection of segregated spinal explants. Sci Adv. 2016;2:e1600087.
60. Ballerini L, Galante M, Grandolfo M, Nistri A. Generation of rhythmic patterns of activity by ventral interneurons in rat organotypic spinal slice culture. J Physiol. 1999;517:459–75.
61. Galante M, Nistri A, Ballerini L. Opposite changes in synaptic activity of organotypic rat spinal cord cultures after chronic block of AMPA/kainate or glycine and $GABA_A$ receptors. J Physiol. 2000;523:639–51.
62. Clements JD, Bekkers JM. Detection of spontaneous synaptic events with an optimally scaled template. Biophys J. 1997;73:220–9.
63. Ruscheweyh R, Sandkühler J. Lamina-specific membrane and discharge properties of rat spinal dorsal horn neurones *in vitro*. J Physiol. 2002;541:231–44.

Neuroinflammation by Cytokines but not by LPS shapes GABAergic currents in mouse spinal cord explants culture.

Giacco V[1], Panattoni G[1], Medelin M[1,2], Bonechi E[3], Aldinucci A[3], Ballerini C[3]*, and Ballerini L[1]*

[1] International School for Advanced Studies (SISSA/ISAS), 34136 Trieste, Italy

[2] Department of Life Sciences, University of Trieste, 34127 Trieste, Italy

[3] Dipartimento di Medicina Sperimentale e Clinica, University of Florence, 50139 Florence, Italy

*Corresponding authors: Laura Ballerini, International School for Advanced Studies (SISSA/ISAS), 34136 Trieste, Italy Email: laura.ballerini@sissa.it; Clara Ballerini: Department NEUROFARBA, University of Florence, 50139 Florence, Italy Email: clara.ballerini@unifi.it

Methods

Organotypic spinal cord cultures, pro-inflammatory treatments, and pharmacology

All experiments were performed in accordance with the EU guidelines (2010/63/UE) and Italian law (Decree 26/14) and were approved by the local authority veterinary service and by our institution (SISSA-ISAS) ethical committee. All efforts were made to minimize animal suffering and to reduce the number of animals used. Animals use was approved by the Italian Ministry of Health, in agreement with the EU Recommendation 2007/526/CE.

Organotypic spinal cord slices and dorsal root ganglia (DRG) were obtained from mouse embryos (C57BL/6J) at E12-13 of gestation as previously described (Furlan *et al.*, 2007;

Fabbro *et al.*, 2012; Medelin *et al.*, 2016; Usmani *et al.*, 2016; Medelin *et al.*, 2018). Experiments were performed on spinal cultures at 2 and 3 weeks *in vitro* (WIV).

Stimulation of neuroinflammation was achieved by incubating the cultured slices, 4 and 6 hour (4H and 6H), with the following pro-inflammatory molecules: i. a cocktail of the mouse recombinant cytokines (CKs; 10 ng/mL each; Medelin *et al.*, 2018) tumour necrosis factor-α (TNF-α; R&D Systems), interleukin-1β (IL-1β; R&D Systems), granulocyte macrophage-colony stimulating factor (GM-CSF; R&D Systems);]. ii. lipopolysaccharide (LPS; Sigma) at 1 μg/mL. For LPS we also tested a longer incubation timepoint (24H). Control cultures underwent the same medium changes, but without CKs or LPS. After incubations (4H, 6H and 24H) CKs and LPS were washed out prior to electrophysiological recordings.

Bumetanide (Sigma) was used to block the $Na^+/K^+/Cl^-$ co-transporter (NKCC1), and to inhibit chloride uptake. To decrease the cytoplasmic chloride concentration, slices were incubated for 24 hours at 37° C with bumetanide at 10 μM (BUM24H) and then the CKs cocktail was added for 4 hours (BUM24H + CKs4H).

Immunofluorescence, imaging, and analysis

Organotypic cultures were fixed with 4% formaldehyde (prepared from fresh paraformaldehyde, Sigma) in phosphate buffer solution (PBS 1×, Sigma) for 1 hour at room temperature (RT; 20 ÷ 22 °C) and washed in PBS. Free aldehyde groups were quenched in 0.1 M glycine in PBS for 10 minutes. Slices were permeabilized and blocked in PBS 1×, 5 % FBS (Sigma), 1 % BSA (Sigma), and 0.3 % Triton-X 100 (Sigma) at RT for 1 hour and then incubated overnight at 4 °C with anti-GFAP (mouse monoclonal, 1:400, Sigma), anti-Iba1 (rabbit polyclonal, 1:200, Wako), anti-SMI32 (mouse monoclonal, 1:200, EMD-Millipore), and anti-MAP2 (mouse monoclonal, 1:200, Sigma) primary antibodies.

For β-tubulin III and GAD65/67 co-immuno-labelling, fixed samples were quenched with Na (meta)periodate 2.3% in deionized water for 5 min and Na borohydride 1% in TRIS 0.1M for 10 minutes. Slices were blocked in free-floating with PBS 1×, 10 % FBS (Sigma), 1 % BSA (Sigma), 1 % fish gelatin and 0.3 % Triton-X 100 (Sigma) at RT for 1 hour and then incubated overnight at 4 °C with anti-β-tubulin III primary antibody (mouse monoclonal; 1:500, Sigma) and anti-GAD65/67 (rabbit polyclonal; 1:500, ABCAM).

Subsequently, the slices were PBS-washed and incubated with secondary antibodies diluted in blocking solution for 2h at RT in the dark. The secondary antibodies were: Alexa 488 goat anti-mouse (1:500, Invitrogen); Alexa 488 goat anti-rabbit (1:500, Invitrogen); Alexa 594 goat anti-mouse (1:500, Invitrogen); Alexa 594 goat anti-rabbit (1:500, Invitrogen); DAPI (Thermo Fisher Scientific). Samples were mounted on glass coverslips using Vectashield mounting medium (Vector Laboratories).

Images were acquired using Nikon C2 Confocal microscopes with Ar/Kr, He/NE, and UV laser with 20 ×, 40 × or 63 × oil objectives (1.4 n.a.) using oil mounting medium (1.515 refractive index). Confocal sections were acquired every 0.5 μm up to a total *Z*-stack thickness of 5 μm. For each condition, we performed n = 3 ÷ 6 independent cultures, from each culture series we used 3 ÷ 4 slices, where 3 ÷ 8 fields were randomly acquired. Offline analysis of the image Z-stack was performed using the open source image-processing package FIJI (http://fiji.sc/Fiji). Analysis of microglia morphology was performed by creating a camera lucida with Photoshop (PhotoshopCS6Portable) and then processed by NeurphologyJ FIJI plug-in (Ho *et al.*, 2011). Quantification of GAD65/67 immunoreactivity was performed measuring the intensity of fluorescence, the voxel count and the number of GAD65/67 clusters using the Volocity3D Image Analysis Software. Clusters were determined after thresholding of images. Thresholds were determined using the 'voxel spy' facility of the software and chosen such that all recognizable punctuate structures were included into the analysis (size higher than 0.03 μm^3 and separate touching objects of 0.5 μm^3).

Electrophysiological recordings and data analysis

For patch clamp recordings (whole-cell, voltage clamp mode), a coverslip with the spinal culture (2 and 3 WIV) was positioned in a recording chamber, mounted on an inverted microscope (Nikon Eclipse TE200) and superfused with a standard saline solution containing (mM): 152 NaCl, 4 KCl, 1 $MgCl_2$, 2 $CaCl_2$, 10 HEPES and 10 glucose, the pH was adjusted to 7.4 by NaOH (305 mOsm). Patch pipettes were pulled from borosilicate glass capillaries (4 ÷ 7 MΩ) and filled with intracellular solution containing (mM): 120 K gluconate, 20 KCl, 10 HEPES, 10 EGTA, 2 $MgCl_2$, 2 Na_2ATP. The pH was adjusted to 7.3 with KOH (295 mOsm). All electrophysiological recordings were performed at RT.

The reported voltage values are corrected for the liquid junction potential (−14 mV) (Medelin *et al.,* 2016). Electrophysiological responses were amplified (EPC-7, HEKA), sampled and digitized at 10 kHz with the pCLAMP software (Axon Instruments) for offline analysis. The value of series resistance was <10 MΩ enabling recordings of synaptic currents without significant distortion and thus was not compensated for (Furlan *et al.,* 2007; Medelin *et al.,* 2016). Recordings were performed from ventrally located spinal interneurons visually identified based on previously reported criteria (Galante *et al.,* 2000). Spontaneous postsynaptic currents (PSCs) were recorded at −70 mV holding potential by the Clampfit 10 software (pClamp suite, Axon Instruments). On average, ≥ 300 events were analyzed from each cell in order to obtain mean kinetic and amplitude parameters. From the average of these events, we measured the rise time defined as the 10 – 90 % time needed to reach the peak of the synaptic current, the peak amplitude and the decay time constant (τ) that was obtained by fitting a mono-exponential function.

We compared the passive membrane properties among Control, CKs- and LPS-treated spinal interneurons. We detected no differences in capacitance (51 ± 31 pF Control; 43 ± 23 pF CKs 4H; 43 ± 21 pF CKs 6H; n= 62, 47, 54 respectively; 55 ± 23 pF Control; 44 ± 18 pF LPS 4H; 48 ± 22 pF LPS 6H; n= 35, 38, 34, respectively) and input resistance (470 ± 395 MΩ Control; 587 ± 537 MΩ CKs 4H; 481 ± 414 MΩ CKs 6H; 430 ± 323 MΩ Control; 399 ± 221 MΩ LPS 4H; 439 ± 246 MΩ LPS 6H).

GABAergic postsynaptic currents (IPSCs) were recorded at −84 mV holding potential in the presence of CNQX (10 μM; Sigma), strychnine (1 μM; Sigma) and APV (25 μM; Sigma). Tetrodotoxin (TTX; 1 μM, Latoxan) was used to isolate $GABA_A$-receptor-mediated miniature events (mPSCs). $GABA_A$-receptor-mediated PSCs were fully blocked by the application of 10 μM SR-95531 (Sigma).

Recordings of the IPSCs at different holding potentials were used to measure the chloride equilibrium potential (E_{Cl}), which was determined as the x-axis intercepts point of the resulting *I-V* curve extrapolated by linear regression.

The imidazopyridine zolpidem (Sigma), a benzodiazepine ligand with high selectivity for $GABA_A$Rs containing the α1-subunit and moderate affinity to α2- or α3-subunit, (Maric *et al.,* 1999), was dissolved in water stock solution (1 mM) and diluted to the concentration of 100 nM (Chen *et al.,* 2004) in extracellular solution for bath application (15-20 min).

Cytokines and chemokines measurement

TNF-α, IL-4, IL-6, IL-10, INF-γ, CXCL1, and CXCL2 concentrations were measured in organotypic culture supernatants by Milliplex assay (Merck Millipore, #MCYTOMAG-70k), using the Bio-Plex apparatus (Biorad), according to the manufacturer's recommendations.

Statistical analysis

All values from samples subjected to the same experimental protocols were pooled together and results are presented as mean (± S.D., if not otherwise indicated, with n = number of neurons, if not otherwise indicated). In box-plots, the thick horizontal bar indicates the median value, the boxed area extends from the 25^{th} to 75^{th} percentiles while whiskers from the 5^{th} to the 95^{th} percentiles. The homogeneity of variances was assessed through the Levene's test.

Statistically significant difference between two data sets was assessed by Student's t-test for parametric data and by Mann-Whitney for non-parametric ones. Differences between the logarithmic values of the analyzed variables were assessed using one-way ANOVA and multiple comparisons were adjusted by Tukey correction.

Statistical significance was abbreviated as follows: *P<0.05, ** P<0.01, *** P<0.001.

Results

CKs and LPS differently affect GABAergic transmission in organotypic spinal slices

We exploited organotypic spinal cord and DRG co-cultures (Fig. 1 A) to model neuroinflammation *in vitro* and to investigate the impact of pro-inflammatory agents on neuronal network activity. In particular, we addressed the modulation of inhibitory, GABAergic synaptic transmission. We compared two different danger signals to trigger neuroinflammation in cultured slices: a pro-inflammatory cocktail of CKs (Medelin *et al*., 2018) and LPS. In both conditions, after 4H and 6H treatments (see methods), patched clamped ventral interneurons displayed a comparable and significant increase in the frequency of spontaneous PSCs (represented by heterogeneous inward currents of variable amplitude), in accordance with previous reports (Kawasaki *et al*., 2008; Zhang *et al*., 2010; Zhang *et al*., 2011; Medelin *et al*., 2018; Fig. S1 A-D; Control, CKs 4H, and CKs 6H; n = 62, 48, 54, respectively; Control, LPS 4H, and LPS 6H; n = 35, 38, 34, respectively

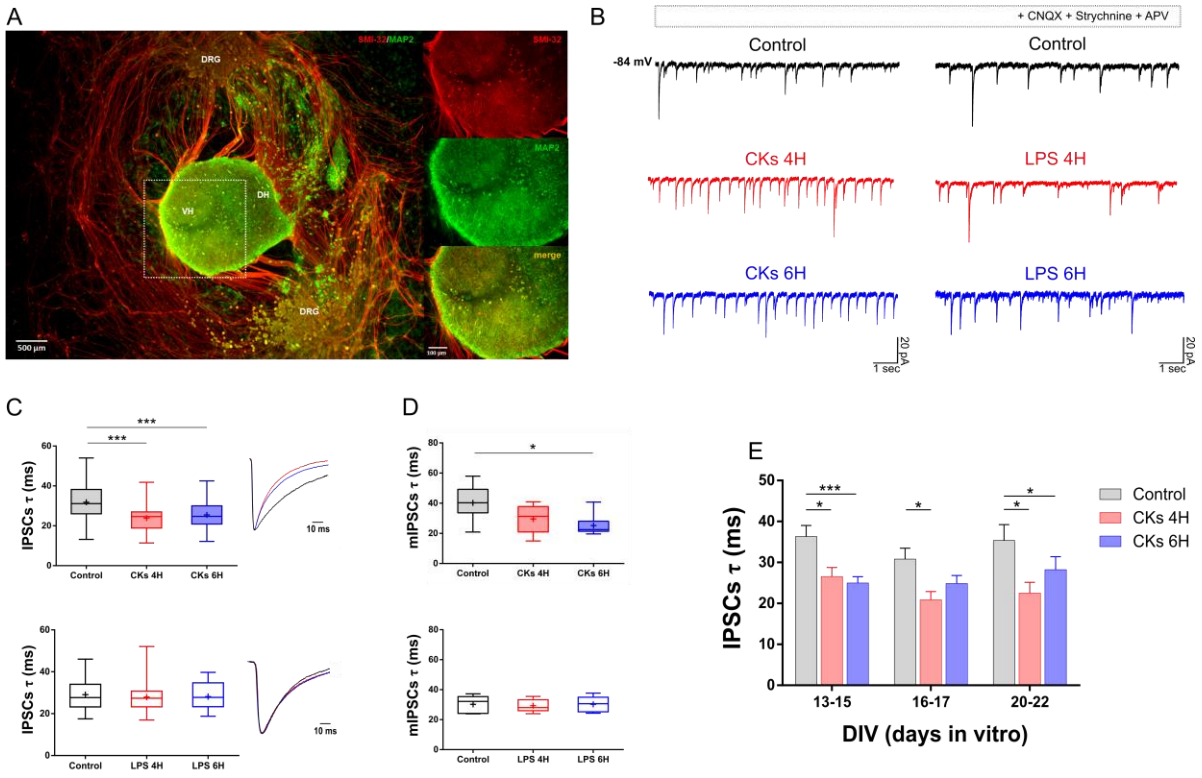

Figure 1. CKs and LPS differently affect $GABA_A$ receptor-mediated synaptic currents in organotypic spinal culture.

A, Immunofluorescence labelling of organotypic co-cultured DRG and spinal cord slice (2 WIV), mature neurons and neuronal processes are visualized by SMI-32 (in red) and MAP2 (in green) markers. The dashed area is shown at higher magnification in the right panels. VH = ventral fissure, DH = dorsal horn, DRG = dorsal root ganglia. **B**, Pharmacologically isolated IPSCs recorded from ventral interneurons at 2 WIV. CKs 4H (in red, left) and 6H (in blue, left) enhanced IPSC frequency, on the opposite LPS 4H (in red, right) and 6H (in blue, right) did not affect IPSCs occurrence. **C**, Box plots summarized τ values from pooled experiments in CKs (top) or LPS (bottom), insets show superimposed, averaged IPSCs (same cells as in B), note the changes in IPSCs duration in CKs **D**, Box plots summarized τ values from pooled experiments in CKs (top) or LPS (bottom), insets show superimposed, averaged mIPSCs, note the changes in IPSCs duration in CKs. Box plot are mean ± SD while column graph is mean ± SEM analyzed with one-way ANOVA: **P*<0.05, ** *P*<0.01, *** *P*<0.001.

Thus, in spinal explants, global network activity was similarly affected by the two danger signals, CKs and LPS. We next focused our attention on the fast Cl^- mediated neurotransmission due to $GABA_A$ receptor activation, a potential CKs target in spinal circuits (Kawasaki *et al.*, 2008; Zhou *et al.*, 2011; Zhang and Dougherty, 2011; Medelin *et al* 2018).
We recorded $GABA_A$ receptor-mediated synaptic events (IPSCs; Fig. 1 B) pharmacologically isolated in the presence of CNQX (10 μM), APV (25 μM) and strychnine (1μM). CKs treatments (4H and 6H; n = 30, 31; respectively) significantly increased IPSCs frequency (4.9 ± 1.9 Hz CKs 4H; 4.6 ± 2.2 Hz CKs 6H; box plots in Fig. S2 A) when compared to Control (3.1 ± 1.6 Hz, n = 35; ***P < 0.001 Control vs CKs 4H and **P = 0.006 vs CKs 6H, one-way ANOVA; box plots in Fig. S2 A). Conversely, in LPS treatments (LPS 4H, LPS 6H; n = 34, n = 28, respectively; Fig. 1 B, right tracings) IPSCs frequency was slightly, although not significantly affected by the inflammatory stimulus (3.0 ± 2.6 Hz LPS 4H; 3.3 ± 2.7 Hz LPS 6H) when compared to their relative Control (2.0 ± 1.5 Hz, n = 37; box plots in Fig. S2 A).
We next explored the kinetic properties of the IPSCs. Consistent with our previous findings (Medelin *et al.*, 2018), CKs treatments significantly accelerated the IPSCs decay time constant (τ) after both CKs 4H and CKs 6H exposures (23.9 ± 6.3 ms CKs 4H; 25.5 ± 6.4 ms CKs 6H; Fig. 1 C, top, box plot and inset) when compared to Control (31.8 ± 9.4 ms Control; ***P < 0.001 CTRL *vs* CKs4H, ***P < 0.001 Control *vs* CKs 6H, one-way ANOVA; Fig. 1 C). Differently, LPS (4H and 6H) did not modulate the τ of the IPSCs that remained unchanged (27.9 ± 7.1 ms LPS 4H; 28.1 ± 6.3 ms LPS 6H) in respect to Control (29.1 ± 7.4 ms Control; Fig. 1 C, bottom box plot and inset). The values of IPSCs amplitude (18.0 ± 10.1 pA Control; 19.1 ± 8.8 pA CKs 4H; 17.7 ± 11.2 pA CKs 6H; 15.7 ± 8.9 pA Control; 11.3 ± 4.5 pA LPS 4H; 13.1 ± 7.3 pA LPS 6H; Fig. S2 B) and rise time (2.5 ± 0.9 ms Control; 2.1 ± 0.8 ms CKs 4H; 2.4 ± 1.1 ms CKs 6H; 2.6 ± 1.0 ms Control; 2.5 ± 1.0 ms LPS 4H; 2.6 ± 0.9 ms LPS 6H; Fig. S2 C) were unaffected by all treatments. We extended our characterisation to the properties of miniature GABAergic currents (mPSCs; recorded in the presence of TTX). The results in this group of cells (Fig. 1 D) confirmed that Control and CKs 6H mPSCs differed significantly in their decay kinetics (mPSCs τ value: 40.9 ± 11.7 ms Control; 29.4 ± 11.6 ms CKs 4H; 24.3 ± 6.4 ms CKs 6H; n=9, 7, 9, respectively; *P = 0.024 Control vs CKs 6H, one-way ANOVA) in a manner similar to that of spontaneous IPSCs. mIPSCs decay time remained unchanged

upon LPS treatments (30.2 ± 5.9 ms Control; 29.3 ± 4.3 ms LPS 4H; 30.2 ± 5.3 ms LPS 6H; *n*=5, 5, 5, respectively; Fig. 1D, bottom) in accordance with the spontaneous IPSCs.

Since IPSCs decay time may be developmentally regulated (Liu and Wong-Riley, 2004), we plotted the τ values detected in Control and in CKs 4H and 6H against the time of growth *in vitro*. Bar plots in Fig. 1 E show that the effects of CKs on the GABAergic current duration were effective at any age of maturation *in vitro*, excluding a correlation between the modulation of IPSCs decay time and the developmental stage of spinal cord slices *in vitro* (13-15 DIV: 36.3 ± 2.7 ms Control; 26.5 ± 2.2 ms CKs 4H; 24.5 ± 1.6 ms CKs 6H; *n*=14, 10, 15, respectively; **P* = 0.011 Control *vs* CKs 4H; ****P* < 0.001 Control *vs* CKs 6H; 16-17 DIV: 30.8 ± 2.7 ms Control; 20.9 ± 2.0 ms CKs 4H; 26.3 ± 2.3 ms CKs 6H; *n*=17, 15, 12, respectively; **P* = 0.013 Control *vs* CKs 4H; 20-22 DIV: 37.6 ± 3.6 ms Control; 22.5 ± 2.6 ms CKs 4H; 26.2 ± 2.3 ms CKs 6H; *n*=8, 6, 6, respectively; **P* = 0.011 Control *vs* CKs 4H; **P* = 0.041 Control *vs* CKs 6H; one-way ANOVA).

Thus, both CKs and LPS treatments boosted PSCs frequency, but only CKs specifically affected the GABAergic synaptic transmission.

We next examined the presence and distribution of GABAergic neurons immunohistochemically targeting either isoforms of GABA-synthesizing enzyme (GAD), namely GAD65/67 (Pribiag *et al.*, 2013). We quantified and compared GAD65/67 labelling in all conditions (Fig. S3, A-D). Immunoreactivity for GAD65/67 was visible throughout the spinal explants where neurons were identified by a specific immunofluorescence marker (class III β-tubulin, Fig. S3 A and C). At lower magnification, scattered soma, extensive neural processes, and bouton-like structures appeared to be stained for both GAD isoforms and were not affected by CKs or LPS treatments, quantified in Fig. S3 B and D.

CKs and LPS promote diverse responses in the spinal explants glial resident-cells

In response to different microenvironment stimuli, microglia and astrocytes may switch to active states, highlighted by changes in cell number and morphology. Microglia and astrocytes were visualized in organotypic spinal explants by Iba1 and GFAP co-immunolabelling, shown in Fig. 2 A and B.

CKs 4H and 6H treatments promoted a significant increase in $Iba1^+$ cells (99.8 ± 5.5 cells/mm^2 Control; 155.3 ± 21.5 cells/mm^2 CKs 4H; 183.7 ± 15.7 cells/mm^2 CKs 6H; **P* = 0.032 Control

vs CKs 4H; ****P* < 0.001 Control *vs* CKs 6H; one-way ANOVA; Fig. 2 C, left). The same treatments promptly induced a significant increase in GFAP intensity (158.1 ± 35.7 % CKs 4H; 229.3 ± 37.3 % CKs 6H; **P* = 0.024 Control *vs* CKs 4H, ****P* < 0.001 *vs* CKs 6H; ****P* < 0.001 CKs 4H *vs* CKs 6H; one-way ANOVA; Fig. 2 C, middle) with no major changes in GFAP voxel (119.0 ± 22.4 % CKs 4H; 121.3 ± 37.1 % CKs 6H; Fig. 2 C, right). On the opposite, LPS, summarized in the plots in Fig. 2 D, provoked only mild increases in $Iba1^+$ cells (100.8 ± 8.2 cell/mm^2 Control; 112.8 ± 7.4 cell/mm^2 LPS 4H; 132.2 ± 11.7 cell/mm^2 LPS 6H), and in the GFAP intensity (110.4 ± 18.7 % LPS 4H; 141.1 ± 15.1 % LPS 6H), with no changes in GFAP voxel (102.5 ± 4.1% LPS 4H; 99.4 ± 3.3% LPS 6H). These observations suggest that CKs, differently from LPS, promoted a significant increase in microglia proliferation and astrogliosis in spinal cord cultures.

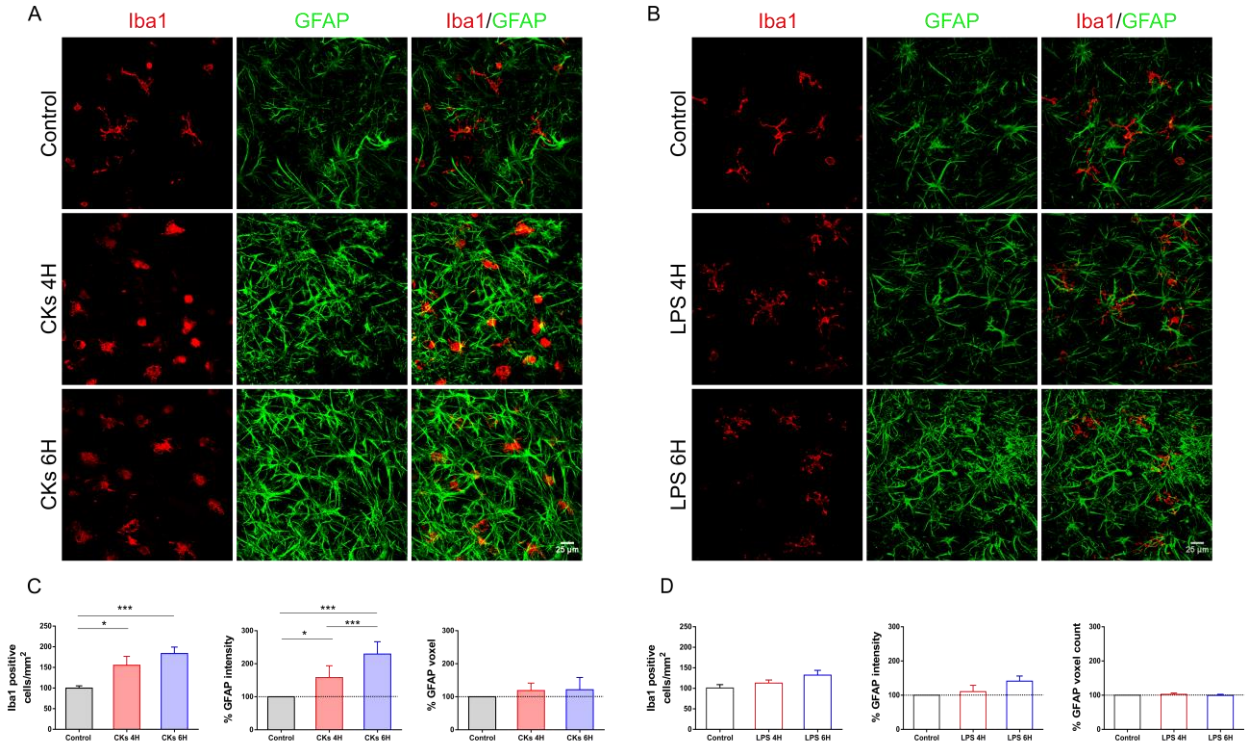

Figure 2. CKs and LPS induced different tissue reactivity in spinal organotypic slices. **A-B,** Representative confocal images of organotypic spinal slices immunolabelled for Iba1 (in red) and GFAP (in green), visualizing microglia and astrocytes, respectively, prior and after CKs or LPS treatments (4H and 6H) **C**, Bar plots summarize $Iba1^+$ cells/mm^2, GFAP intensity (express as % of control) and GFAP voxel (express as % of control) prior and after CKs treatments (4H and 6H). **D**, Bar plots summarize $Iba1^+$ cells/mm^2, GFAP intensity (express as % of control) and GFAP voxel (express as % of control) prior and after LPS treatments (4H

and 6H). Bar plots report mean values ± SEM analyzed with one-way ANOVA: *P<0.05, ** P<0.01, *** P<0.001.

CKs and LPS modulate microglia morphology with opposite effects on cell complexity

In this set of experiments, we assessed CKs and LPS ability to shape the morphology of Iba1$^+$ cells. To this aim, we quantified the total dendrites length, an accepted index to measure the cellular processes growth (Sidharth *et al.*, 2011), and the ratio between dendrite end- and attachment-points, a measure of the degree of ramification within each dendrite branching of Iba1$^+$ cell (Fig. 3 A and B). Upon CKs 4H and 6H treatments, microglia (Fig. 3 A) showed a significant decrease in both the total dendrite lengths (270.3 ± 144.8 µm Control; 99.7 ± 65.6 µm CKs 4H; 93.8 ± 81.2 µm CKs 6H; ***P < 0.001 Control *vs* CKs 4H; ***P < 0.001 Control *vs* CKs 6H; one-way ANOVA; Fig. 3 C, top) and end/attachment points ratio (2.4 ± 1.4 Control; 1.2 ± 0.4 CKs 4H; 1.2 ± 0.5 CKs 6H; ***P < 0.001 Control *vs* CKs 4H; ***P < 0.001 Control *vs* CKs 6H; one-way ANOVA; Fig. 3 C, bottom). These changes are indicative of a switch in microglia morphology from the ramified shape to the amoeboid one. In parallel, in slices stimulated by LPS, we observed opposite changes in cell morphology. In fact, Fig. 3 A and D show a significant increment of the Iba1$^+$ cell dendrites at LPS 6H (346.6 ± 194.9 µm Control; 306.1 ± 126.2 µm LPS 4H; 472.6 ± 255.9 µm LPS 6H; ***P < 0.001 Control *vs* LPS 6H; ***P < 0.001 LPS 4H vs LPS 6H; one-way ANOVA) with no reduction in the ramification of dendritic branching (2.6 ± 1.3 Control; 2.3 ± 1.1 LPS 4H; 2.7 ± 1.3 LPS 6H). Finally, we evaluated and compared the production of cytokines and chemokines by spinal slices in response to pro-inflammatory stress. The summarizing plots of Fig. 3 E show that the exposure to CKs (top) and LPS (bottom) significantly increased the release of pro-inflammatory cytokines, measured in the supernatant, such as TNF-α (in LPS), IL-6, INF-γ (in both LPS and CKs), as well as the release of chemokines including CXCL1 and CXCL2 necessary for the recruitment of innate immune cells (*0.01 < P < 0.05; **0.001 < P < 0.01; ***P < 0.001, n=14, one-way ANOVA). On the other hand, IL-4 and IL-10 are significantly raised upon CKs stimuli, while a reduction in IL-4 accompanied by no changes in IL-10 levels were detected after LPS treatments. The release of pro- and anti-inflammatory cytokines, in addition to the production of chemokines, suggests that the activation of inflammatory mechanisms, although

different, occurred in spinal slices stimulated by both CKs and LPS at any time point (4H and 6H).

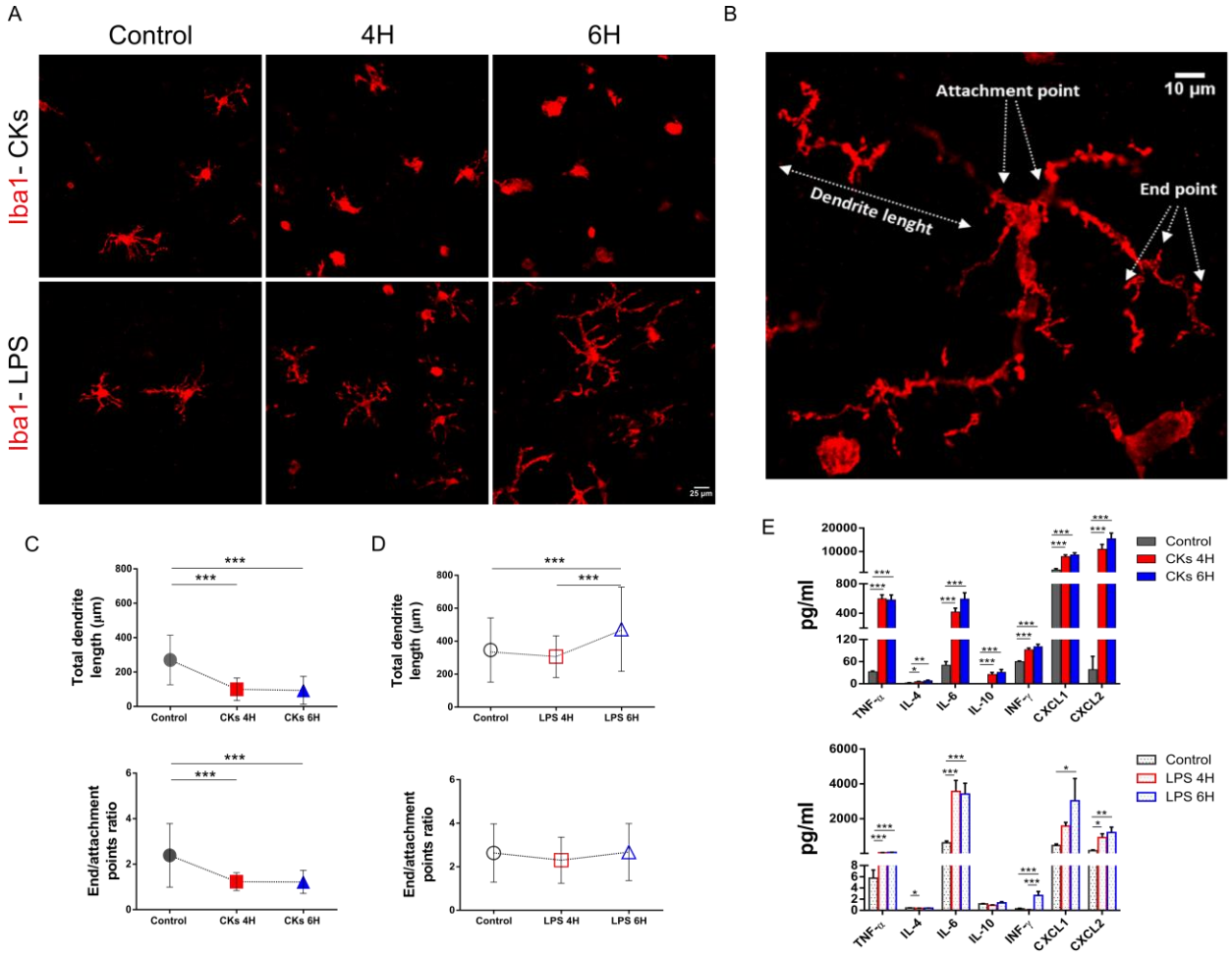

Figure 3. Microglia morphology is differentially modulated by CKs and LPS treatments in organotypic slices.

A, Representative confocal images comparing Iba1 immunolabelling in untreated (control), CKs and LPS treated cultures (4H and 6H). **B,** High magnification confocal micrograph illustrates the morphological analysis: dendrites length and their end/attachment points are indicated by arrows. **C-D,** Plots summarize the measured parameters in pooled experiments, note the significant decrease in total dendrites length and end/attachment points ratio upon CKs 4H and 6H (C), on the opposite, a significant increase in total dendrites length is reported at LPS 6H with no changes in end/attachment point ratio (D). **E**, Production of cytokines (TNF-α; IL-4; IL-6; IL-10; INF-γ) and chemokines (CXCL1; CXCL2) determined by Milliplex assay in organotypic culture supernatants after incubation with CKs (top) and LPS (bottom) for 4H or 6H. Column graphs report mean values ± SEM of 22 and 14 independent experiments respectively analyzed with one-way ANOVA: **P*<0.05, ** *P*<0.01, *** *P*<0.001.

Prolonged exposure to LPS does not change the spinal tissue response

In the central nervous system LPS binds to the Toll-like receptors (TLRs), especially TLR4, expressed on the microglia surface. This signal involves several proteins resulting in the production and release of cytokines, chemokines and other inflammatory factors (Rahimifard *et al.*, 2017). Since LPS, differently from CKs (Maria Schäfers and Linda Sorkin, 2008), does not act directly on neurons, we tested whether a longer (24H) exposure to LPS may ultimately lead to changes in GABAergic transmission and kinetic. Fig. 4 reports the effects of LPS 24H in terms of PSCs frequency (21.7 ± 6.7 Hz Control; 30.5 ± 5.0 Hz LPS 24H; n = 8 and 12, respectively; $^{**}P$ = 0.003 Control *vs* LPS 24H; Student's *t*-test; Fig. 4 A), IPSCs frequency (1.2 ± 0.8 Hz Control; 2.5 ± 0.9 Hz LPS 24H; $^{**}P$ = 0.007 Control *vs* LPS 24H; Student's *t*-test; Fig. 4 B) and IPSCs decay time constant (32.7 ± 10.2 ms Control; 29.7 ± 5.5 ms LPS 24H, Fig. 4 C, scaled averaged IPSCs are superimposed in the inset). In addition, $Iba1^+$ cells at LPS 24H (Fig. 4 D) displayed the characteristic morphology with longer branching in ramified cells (quantified in plots of Fig. 4 D, total dendrites length: 249.6 ± 96.0 µm Control; 393.4 ± 216.9 µm LPS 24H; $^{***}P < 0.001$ Control *vs* LPS 24H; Student's *t*-test; end/attachment points ratio: 1.2 ± 1.5 Control; 1.3 ± 1.5 LPS 24H) in the absence of changes in terms of $Iba1^+$ cells (53.1 ± 2.9 cells/mm^2 Control; 55.3 ± 2.9 cells/mm^2 LPS 24H). These results indicated that while the trend in increasing IPSCs frequency brought about by LPS turned into a significant change upon prolonged exposure (compare Fig. S2 A to Fig. 4 B), the kinetic of GABAergic currents was not modulated by longer danger signal, and the effects on microglia dendrite lengths stabilized after 6H.

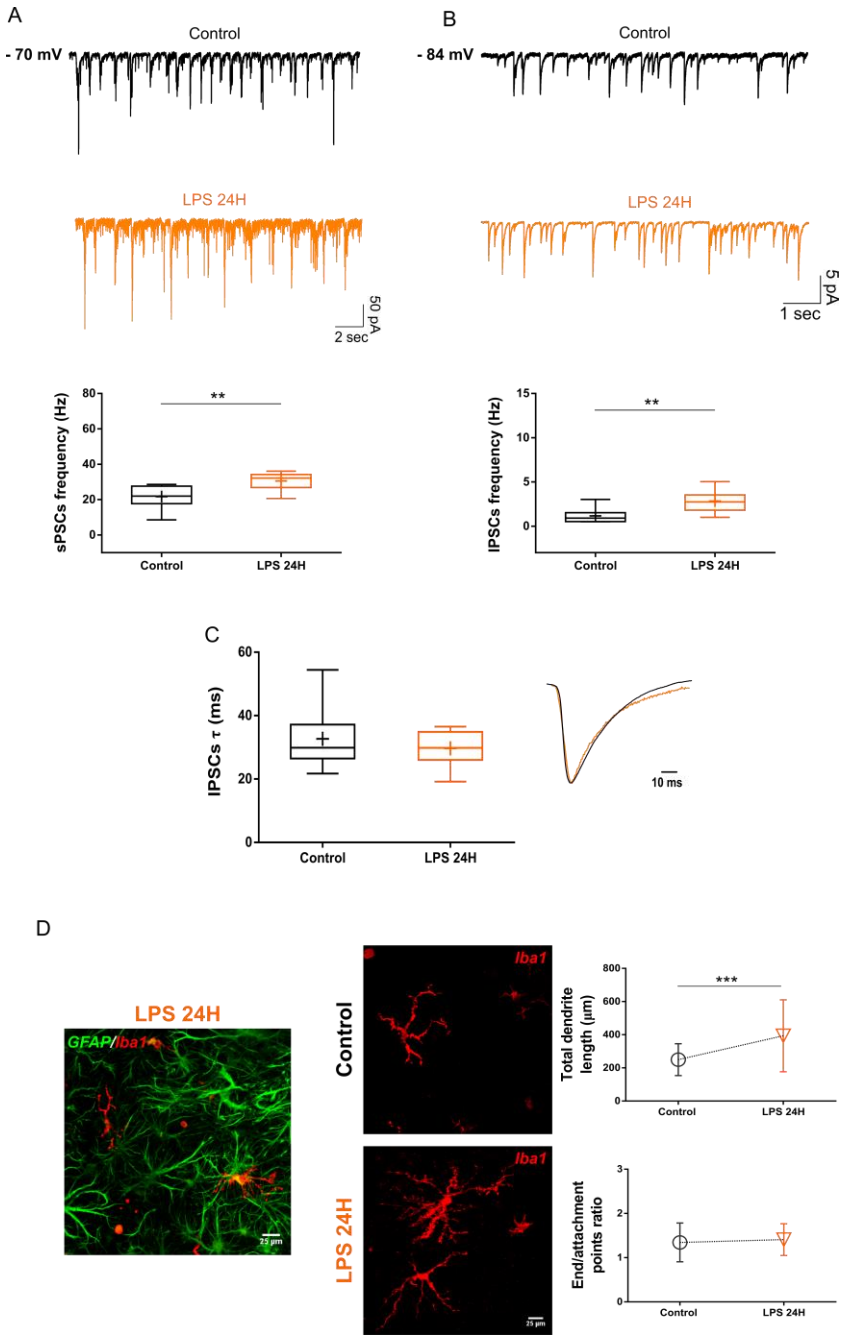

Figure 4. LPS-prolonged exposure in organotypic spinal slices does not alter IPSCs decay.

A, Representative traces of spontaneous PSCs recorded from control (in black) and LPS 24H (in orange) ventral interneurons. Polled data are summarized by the box plot showing a significant increase of PSCs frequency upon LPS 24H. **B**, Pharmacologically isolated IPSCs are recorded from control (in black) and LPS 24H (in orange) ventral interneuron (same cells as in A). The box plot summarizes the IPSCs frequency from pooled experiments and exhibits a significant increased frequency brought about by LPS 24H. **C**, The boxplot summarizes the values of τ for control and LPS, in the inset averaged, scaled, superimposed traces of the two conditions are shown. Note that no changes were detected in IPSCs decay time constant. **D**,

Left, representative image of the LPS 24H-treated organotypic culture labelled with GFAP (green) and Iba1 (red). High magnification Iba1 micrographs are shown (middle), and plots summarize the morphology changes of microglia at LPS 24H. Note the significant increase in total dendrites length (top).

CKs modulate GABAergic current duration by tuning $GABA_AR$ subunit composition

We found that $GABA_A$-PSCs from 4H and 6H CKs slices, but not from LPS ones, decayed faster than those from Controls (Medelin *et al.,* 2018). This tuning in inhibitory synaptic signals appears specifically exerted by CKs-induced neuroinflammation. We further investigated in the present work the mechanisms responsible for this effect on the kinetic properties of GABAergic receptors and therefore the $GABA_A$-PSC time course. Our results on mIPSCs excluded the involvement of presynaptic processes (such as GABA release synchronization) that may affect synaptic time course, in fact, the decay of IPSCs is also faster for unitary synaptic events (mPSCs).

We addressed whether differences in the intracellular chloride concentration $[Cl^-]_i$ might affect IPSC kinetics (Funk *et al.,* 2008; Moroni *et al.,* 2011).

We incubated the slices with Bumetanide (10 μM; 24H), a pharmacological agent that blocks the activity of NKCC1, the most abundant co-transporter membrane-protein determining intracellular chloride levels (Ben-Ari, 2017), to experimentally reduce $[Cl^-]_i$ prior to CKs 4H (see sketch of the experimental settings in Fig. 5 A).

Bumetanide *per se* induced an increase in PSCs and IPSCs frequencies that were not significantly improved by CKs 4H (Fig. 5 B and Fig. S4). More intriguingly, Bumetanide reduced significantly the duration of GABAergic currents that were not further shortened by CK 4H (33.1 ± 8.1 ms Control; 22.3 ± 6.2 ms BUM 24H; 22.3 ± 6.5 ms BUM 24H + CKs 4H; *n*=10, 11, 10, respectively; ***P* = 0.005 Control vs BUM 24H; **P* = 0.012 Control vs BUM 24H + CKs 4H; one-way ANOVA; Fig. 5 C).

Fig. 5 D shows the measurement of the reversal potential of IPSCs in Control, Bumetanide and Bumetanide plus CKs 4H. The E_{Cl} value in Control (–48.5 ± 3.7 mV; n = 7) was close to the approximate theoretical value expected for the Cl^- equilibrium potential for our intracellular and extracellular chloride concentrations (–50 mV; Medelin *et al.,* 2016). However, the reversal potential was significantly shifted to more negative values by blocking NKCC1 (–54.2 ± 4.3 mV BUM 24H, n = 8; **P* = 0.025 Control vs BUM 24H; one-way ANOVA), suggesting that local intracellular chloride concentrations are lower. It is important to note that in

organotypic cultures, upon Bumetanide treatments, the Cl^- reversal potential differed from the predicted theoretical value, suggesting a real shift in the internal chloride concentration as a result of improved extrusion (DeFazio *et al.,* 2000; Ostroumov *et al.,* 2011), regardless the 24 mM Cl^- intracellular pipette solution.

Pro-inflammatory CKs, in the presence of NKCC1 block, slightly increased such a shift (–56.2 ± 3.5 mV BUM 24H + CKs 4H; $n = 8$; $^{**}P = 0.003$ Control vs BUM 24H + CKs 4H; one-way ANOVA). The absence of significant changes in IPSCs decay time constant and reversal potential when CKs were incubated in the presence of Bumetanide might indicate an occluding mechanisms in regulating $[Cl^-]_i$.

To shed light in CKs potential regulation of intracellular chloride, and thus of IPSCs τ, we estimated and compared E_{Cl} in CKs and LPS treatments. Fig. 5 E and F show that the reversal potential of IPSCs was not altered by these treatments alone (–52.0 ± 7.5 mV Control; –51.5 ± 5.2 mV CKs 4H; –54.1 ± 6.0 mV CKs 6H; $n = 9, 10, 8$, respectively; –49.6 ± 7.8 mV Control; –49.7 ± 9.9 mV LPS 4H; –52.3 ± 6.0 mV LPS 6H; $n = 13, 8, 8$, respectively). Regardless the similar E_{Cl} extrapolated in all the recording conditions, only CKs 4H and 6H induced the expected changes in the IPSCs duration ($\tau = 31.8 \pm 5.1$ ms Control; 23.9 ± 8.1 ms CKs 4H; 20.7 ± 3.4 ms CKs 6H; $n=9, 10, 8$, respectively; $^{*}P = 0.031$ Control vs CKs 4H; $^{**}P = 0.003$ Control vs CKs 6H; one-way ANOVA; $\tau = 26.4 \pm 5.2$ ms Control; 26.2 ± 6.3 ms LPS 4H; 27.5 ± 6.9 ms LPS 6H; $n=13, 8, 8$, respectively). These results show that changes in E_{Cl} might indeed modulate IPSCs duration in the organotypic spinal interneurons, however, CKs apparently are not tuning the inhibitory current duration by shifts in the E_{Cl}.

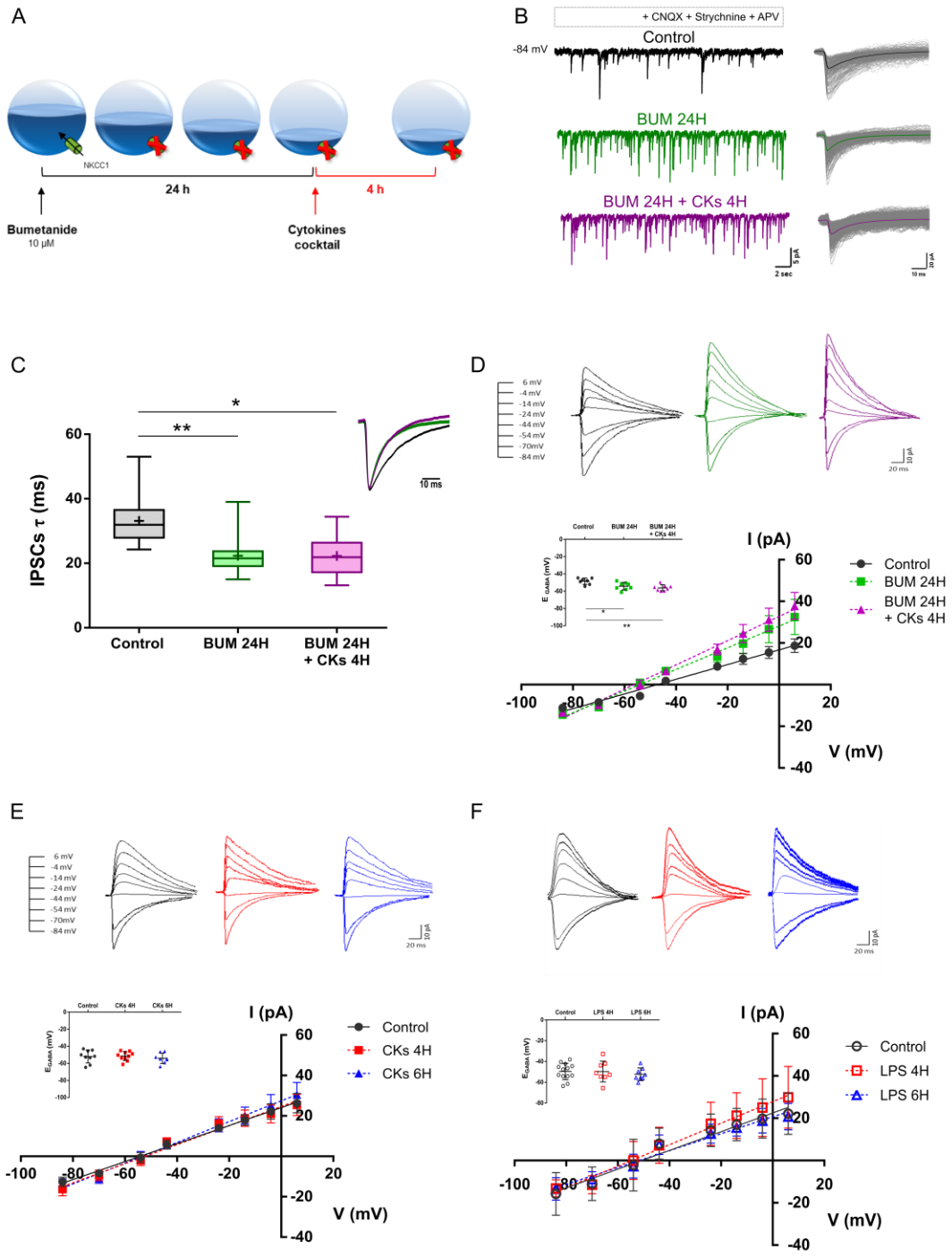

Figure 5. Bumetanide but not CKs and LPS affected the IPSCs reversal potential in organotypic slices

A, Sketch of the protocol used to treat slices with bumetanide for 24H (BUM 24H) followed by CKs 4H. **B**, Representative traces (left) and superimposed isolated events (right) of IPSCs in control, after BUM 24H (green), and BUM 24H + CKs 4H (magenta) ventral interneurons. **C**, The boxplot summarizes the τ values measured in the three conditions, note the similar and

significant reduction in τ at BUM 24H and BUM 24H + CKs 4H; in the inset superimposed averaged and scaled IPSCs in the three conditions. **D**, IPSCs averaged and superimposed traces (top) recorded at different V_h in control (black), BUM 24H (green) and BUM 24H + CKs 4H (magenta). I–V curves were obtained by plotting $GABA_A$-PSCs mean amplitude against Vh. Note the significant differences in the approximate calculated reversal potential at BUM 24H and BUM 24H + CKs 4H compared to control. **E**, IPSCs averaged and superimposed traces (top) recorded at different V_h in control (black), CKs 4H (red) and CKs 6H (blue). I–V curves were obtained by plotting $GABA_A$-PSCs mean amplitude against Vh. Note the similar approximate calculated reversal potential in all conditions. **F**, IPSCs averaged and superimposed traces (top) recorded at different V_h in control (black), LPS 4H (red) and LPS 6H (blue). I–V curves were obtained by plotting $GABA_A$-PSCs mean amplitude against Vh. Note the similar approximate calculated reversal potential in all conditions.

Another well-documented process that changes GABAergic inhibition is the switch in the α1-subunit expression that is traditionally associated with a modulation in IPSCs kinetics, which become faster (Vicini *et al.* 2001). To address the potential changes in the receptor subunit composition due to CKs treatment, we tested IPSCs kinetics in the presence of Zolpidem (100 nM; 15-20 min), an allosteric modulator of $GABA_AR$ subunits that at low concentration is highly selectively for the $GABA_AR$ α1 subunit (Perrais and Ropert et al., 1999). Fig. 6 A shows sample superimposed isolated IPSCs recorded from Control, CKs 4H, and CKs 6H, before and after Zolpidem applications. After CKs 4H and 6H, IPSCs τ was, as expected, significantly reduced (33.3 ± 4.5 ms Control; 25.4 ± 4.7 ms CKs 4H; 26.0 ± 4.0 ms CKs 6H; *n*=9, 10, 9, respectively; **P* = 0.019 Control vs CKs 4H; **P* = 0.045 Control vs CKs 6H). Subsequent applications of Zolpidem did not alter IPSCs τ in Control (36.3 ± 3.9 ms), while significantly prolonged τ values detected in CK 4H and 6H (34.5 ± 6.9 ms CKs 4H; 34.2 ± 6.0 ms CKs 6H; ***P* = 0.003 CKs 4H -Zolpidem vs CKs 4H +Zolpidem; **P* = 0.017 CKs 6H -Zolpidem vs CKs 6H +Zolpidem; two-way ANOVA) which did not differ anymore from Control IPSCs (summarized in plots of Fig. 6 B). These results strongly suggest that CKs treatments regulated the duration of GABAergic inhibition via postsynaptic changes of the α1 subunit.

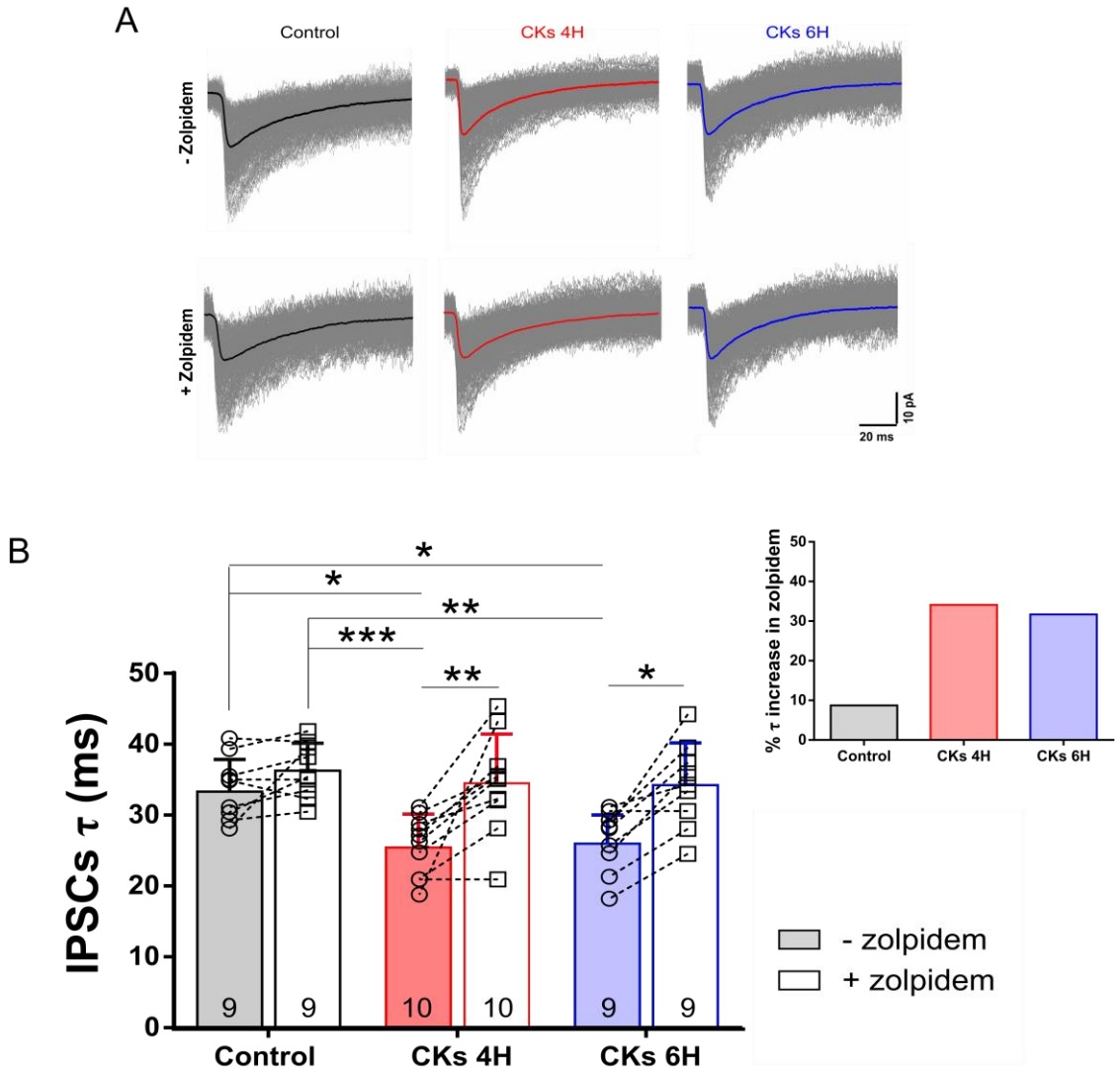

Figure 6. Block of $GABA_A$ receptor α1 subunit by Zolpidem prolonged IPSCs in CKs but not in control.

A, Superimposed IPSCs recorded in control and CKs (4H and 6H) in the presence or in the absence of zolpidem. Averaged IPSCs are shown in black (control, left), in red (CKs 4H, middle) and in blue (CKs 6H, right) **B**, Bar plot summarizes the values of τ in Control, CKs 4H, and CKs 6H IPSCs, before and after bath application of zolpidem. Note that the significant decrease in IPSCs τ upon CKs treatments (4H and 6H) was reversed by zolpidem. In the inset: the plot summarizes the % of τ increase in zolpidem, note the increase by 8.71% in control, by 34.09% in CKs 4H, and by 31.69% in CKs 6H.

Conclusions

Together, these results suggest that the CKs specifically regulate post-synaptically the efficacy of GABAergic inhibition in spinal ventral interneurons. Such a regulation of spinal pre-motor interneuron activity implies a modulation of $GABA_A$ subunit expression and may impair spinal network operation. Shortening of IPSCs together with microglia and astrocytes activation may represent a specific mechanism of certain CKs combinations, potentially a targetable pathway in spinal neuroinflammatory diseases.

Abbreviations

APV, (2*R*)-amino-5-phosphonovaleric acid

BSA, bovine serum albumin

BUM, bumetanide

CKs, cytokines

CNQX, 6-cyano-7-nitroquinoxaline-2,3-dione

DIV, days *in vitro*

DRG, dorsal root ganglia

FBS, fetal bovine serum

GAD65/67, Glutamate decarboxylase

GFAP, glial fibrillary acidic protein

GM-CSF, granulocyte-macrophage colony-stimulating factor

Iba1, ionized calcium-binding adapter molecule 1

IL-1β, interleukin-1beta

LPS, lipopolysaccharide

MAP2, microtubule-associated protein 2

mPSCs, miniature post-synaptic currents

PBS, Phosphate-buffered saline

PSCs, post-synaptic currents

RT, room temperature

SMI-32, neurofilament H non-phosphorylated

TNF-α, tumor-necrosis factor-alfa

TTX, tetrodotoxin

WIV, week *in vitro*

Supplementary Figures

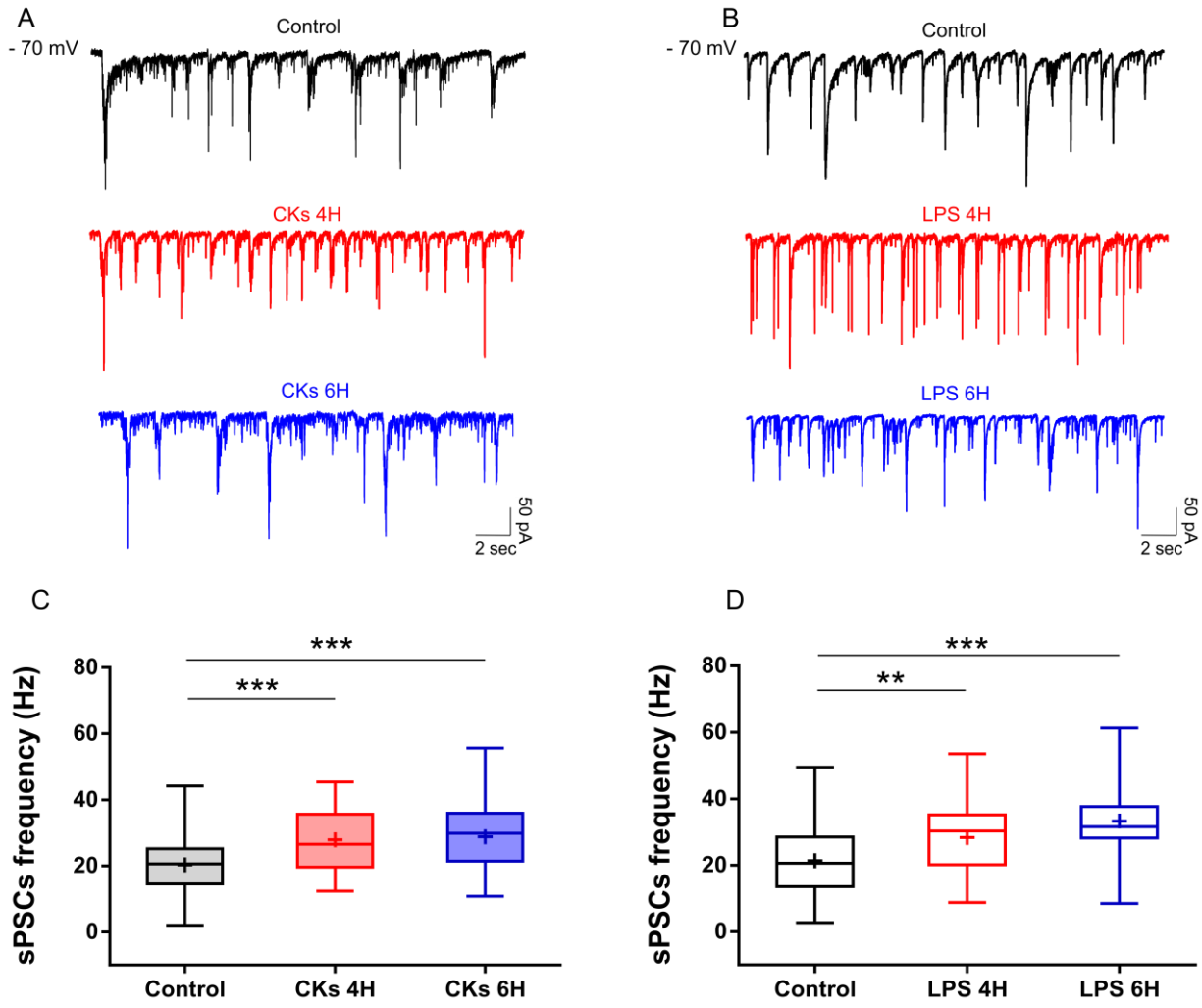

Supplementary Figure S1. CKs and LPS significantly increased spontaneous PSCs in organotypic slices.
A-B, Representative traces of PSCs in control (black), upon incubation in CKs (4H red and 6H blue; left) and in LPS (4H red and 6H blue; right). **C-D**, Box plots summarize the frequency values recorded in all conditions.

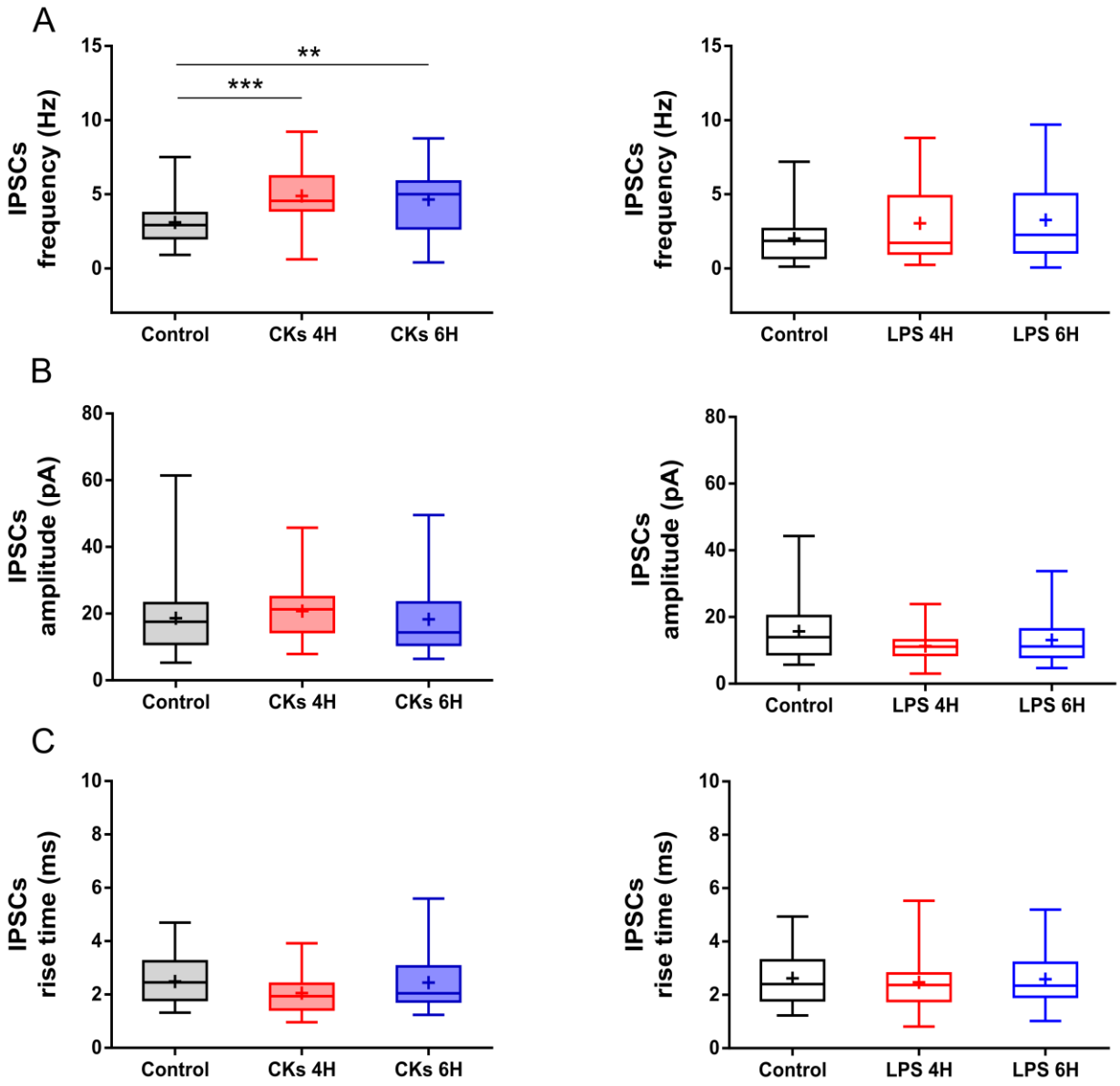

Supplementary Figure S2. CKs and LPS impact on pharmacologically isolated $GABA_A$ receptor-mediated IPSCs.

A-C, Box plots illustrate the mean value of IPSCs frequency, amplitude and rise time upon CKs and LPS treatments. A significant increase is observed only in the IPSCs frequency at CKs 4H and 6H compared to control.

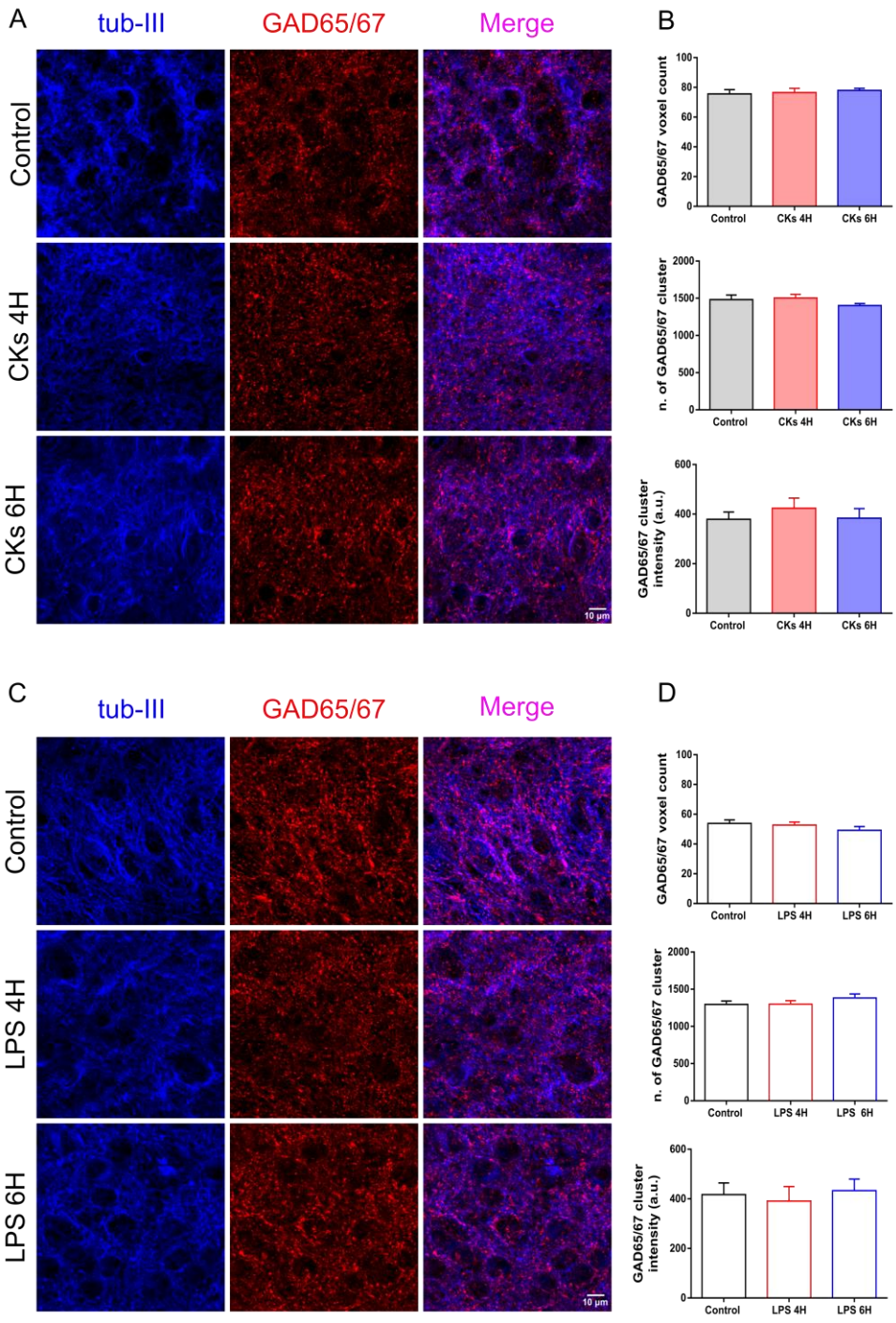

Supplementary Figure S3. GAD65/67 distribution in organotypic slices treated by CKs and LPS.

A, **C**, Representative images of spinal slices labelled for β-tubulin III (in blue) and GAD65/67 (in red) show GABAergic neurons and processes **B**, **D**, Bar plots summarize the number of GAD65/67 voxel, the number of cluster and the cluster intensity in all conditions. Note the absence of changes in any measured parameter.

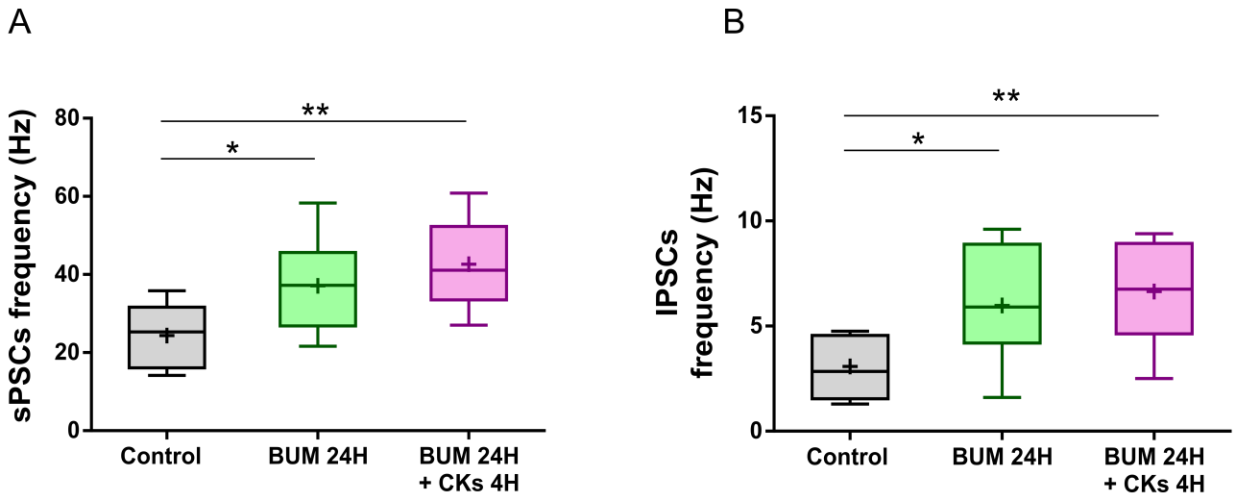

Supplementary Figure S4. Spontaneous PSCs and IPSCs frequency after bumetanide 24H and in bumetanide plus CKs.

A, Quantification of PSCs frequency recorded from control, bumetanide-treated slices prior and after CKs. Note the significant increase in PSCs frequency BUM 24H and BUM 24H + CKs 4H compared to control. **B**, Bar plots summarized a significant increase in IPSCs frequency upon BUM 24H and BUM 24H + CKs 4H compared to control.

References

Fabbro A, Villari A, Laishram J, Scaini D, Toma FM, Turca A, *et al.* Spinal cord explants use carbon nanotubes interfaces to enhance neurite outgrowth and to fortify synaptic inputs. ACS Nano. 2012;6:2041-2055.

Furlan F, Taccola G, Grandolfo M, Guasti L, Arcangeli A, Nistri A, *et al.* ERG conductance expression modulates the excitability of ventral horn GABAergic interneurons that control rhythmic oscillations in the developing mouse spinal cord. J Neurosci. 2007;27:919-928.

Galante M, Nistri A, Ballerini L. Opposite changes in synaptic activity of organotypic rat spinal cord cultures after chronic block of AMPA/kainate or glycine and $GABA_A$ receptors. J Physiol. 2000; 523 Pt 3:639-51.

Ho SY, Chao CY, Huang HL, Chiu TW, Charoenkwan P, Hwang E. NeurphologyJ: an automatic neuronal morphology quantification method and its application in pharmacological discovery. BMC Bioinformatics. 2011 Jun 8;12:230.

Medelin M, Giacco V, Aldinucci A, Castronovo G, Bonechi E, Sibilla A, *et al.* Neuro-immune crosstalk in organotypic spinal slices: investigating the protective role of an NGF-mimetic. Molecular Brain. 2018;11:3.

Medelin M, Rancic V, Cellot G, LaishramJ, Veeraraghavan P, Rossi C, *et al.* Altered development in GABA co-release shapes glycinergic synaptic currents in cultured spinal slices of the $SOD1^{G93A}$ mouse model of ALS. J Physiol. 2016;594:3827-3840.

Usmani S, Aurand ER, Medelin M, Fabbro A, Scaini D, Laishram J, *et al.* 3D meshes of carbon nanotubes guide functional reconnection of segregated spinal explants. Sci Adv. 2016;2:e1600087.

Vicini S, Ferguson C, Prybylowski K, Kralic J, Morrow AL, Homanics GE. GABA(A) receptor alpha1 subunit deletion prevents developmental changes of inhibitory synaptic currents in cerebellar neurons. J Neurosci. 2001 May 1;21(9):3009-16.

Conclusion

Neuroinflammation is a powerful mechanism used by the CNS as defence, which is typically activated in response to damage and infection. A non-resolution of the inflammatory processes lead to a chronic phase that represents a key event in several neurodegenerative diseases. In this work, we further confirmed organotypic spinal slices as a good model to test the spinal network synaptic activity during neuroinflammatory stress due to the easy access to pre-motor interneurons with electrophysiological techniques. Especially, these complex tissue maintains the basic spinal cord architecture as well as the neuronal and glial resident cells. This represents an essential feature to investigate the neuronal excitability and specific synaptic changes of a precise region of interest under physiological and pathological condition.

The principal findings of this work is that in CKs-treated slices, the interneuronal GABAergic transmission is affected, resulting in an impaired in the pre-motor spinal circuits. This effect was exclusively mediated by CKs, in contrast to LPS, which did not affect the $GABA_AR$ kinetic. Our data support the hypothesis that CKs act by post-synaptic modification resulting in the inhibitory transmission alteration.

A part from the intrinsic synaptic activity, environmental factors are surely able to trigger neuronal dysregulation and among them, we decided to focus, therefore, on glial cells. An essential contribution in neuroinflammatory disorders is mediated by microglia and astrocytes, which represents the principal mediators of the inflammatory response. In fact, depending on different stimuli (CKs or LPS) they show distinct behaviour that reflects the alteration exhibits by spinal interneurons in their synaptic activity.

Furthermore, we investigated the mechanisms by which pro-inflammatory cytokines induce modification on the inhibitory component, and in particular, we assessed two processes capable of modifying the $GABA_AR$ kinetic: changes in the intracellular chloride concentration ($[Cl^-]_i$) and receptor subunit composition. Despite CKs induce faster GABAergic synaptic currents, they do not affect the $[Cl^-]_i$ excluding the hypothesis of a possible action on the chloride homeostasis. Moreover, using Zolpidem a selective modulator of the α1 subunit we restored the regular $GABA_AR$ kinetic. These results clarify the path by which CKs are able to modulate mechanisms such as synthesis, trafficking, or assembling associated with the $GABA_AR$ subunits.

In conclusion, expanded our knowledge about the communication between neuroinflammation, glial cells and neuronal spinal networks. Furthermore, understanding the molecular pathways that promote the dysregulation of inhibitory spinal synaptic represents a future perspective to produce new therapies that could be essential for the spinal neurodegeneration disorders.

References

Accardi, M., Daniels, B., Brown, P., Fritschy, J., Tyagarajan, S. & Bowie, D. (2014). Mitochondrial reactive oxygen species regulate the strength of inhibitory GABA-mediated synaptic transmission. Nat. Commun., 5, 3168.

Achilles K, Okabe A, Ikeda M, Shimizu-Okabe C, Yamada J, Fukuda A, Luhmann HJ, Kilb W. (2007). Kinetic properties of Cl^- uptake mediated by Na^+-dependent K^+-$2Cl^-$ cotransport in immature rat neocortical neurons. J Neurosci. 27(32):8616-27.

Akiyama, H., Ikeda, K., Katoh, M., McGeer, E.G., and McGeer, P.L. (1994). Expression of MRP14, 27E10, interferon-alpha and leukocyte common antigen by reactive microglia in postmortem human brain tissue. J. Neuroimmunol. 50:195–201.

Alaynick, W. A., Jessell, T. M. and Pfaff, S. L. (2011) SnapShot: spinal cord development. Cell 146,178-178 e1.

Ali, N. J., & Olsen, R. W. (2001). Chronic benzodiazepine treatment of cells expressing recombinant $GABA_A$ receptors uncouples allosteric binding: studies on possible mechanisms. J Neurochem 79, 1100– 1108.

Allain, A.E., Baïri, A., Meyrand, P., Branchereau, P. (2004). Ontogenetic changes of the GABAergic system in the embryonic mouse spinal cord. Brain Res. 1000, 134– 147.

Allain, A.E., Baïri, A., Meyrand, P., Branchereau, P. (2006). Expression of the glycinergic system during the course of embryonic development in the mouse spinal cord and its co-localization with GABA immunoreactivity. J. Comp. Neurol. 496, 832-46.

Allan, S.M. and Rothwell, N.J. (2001). Cytokines and acute neurodegeneration. Nat. Rev. Neurosci. 2:734–744.

Aloisi, F. (2001). Immune function of microglia. Glia 36:165–179.

Alvarez, F.J., Jonas, P.C., Sapir, T., Hartley, R., Berrocal, M.C., Geiman, E.J., Todd, A.J., Goulding, M. (2005). Postnatal phenotype and localization of spinal cord V1 derived interneurons. J. Comp. Neurol. 493, 177-92.

Andriezen WL. (1893). The neuroglia elements of the brain. BMJ; 2:227–230.

Antonucci F, Turola E, Riganti L, Caleo M, Gabrielli M, Perrotta C, Novellino L, Clementi E, Giussani P, Viani P, Matteoli M, Verderio C. (2012). Microvesicles released from microglia stimulate synaptic activity via enhanced sphingolipid metabolism. EMBO J. 31(5):1231-40.

Arosio, D., Ricci, F., Marchetti, L., Gualdani, R., Albertazzi, L., and Beltram, F. (2010). Simultaneous intracellular chloride and pH measurements using a GFP-based sensor. Nat. Methods 7, 516–518.

Avossa D, Rosato-Siri MD, Mazzarol F, Ballerini L. (2003). Spinal circuits formation: a study of developmentally regulated markers in organotypic cultures of embryonic mouse spinal cord. Neuroscience. 122(2):391-405.

Ballerini L, Galante M, Grandolfo M, Nistri A. (1999). Generation of rhythmic patterns of activity by ventral interneurons in rat organotypic spinal slice culture. J Physiol. 517 (Pt 2):459-75.

Ballerini L, Galante M. (1998). Network bursting by organotypic spinal slice cultures in the presence of bicuculline and/or strychnine is developmentally regulated. Eur J Neurosci. 10(9):2871-9.

Barbeau H, Ladouceur M, Norman KE, Pépin A, Leroux A. (1999). Walking after spinal cord injury: evaluation, treatment, and functional recovery. Arch Phys Med Rehabil. 80(2):225-35.

Barnard, E. A., Skolnick, P., Olsen, R.W., Mohler, H., Sieghart,W., Biggio, G., Braestrup, C., Bateson, A. N., & Langer, S. Z. (1998). International Union of Pharmacology. XV. Subtypes of g-aminobutyric acid$_A$ receptors: classification on the basis of subunit structure and function. Pharmacol Rev 50, 291–313.

Barnes, E. M. (2001). Assembly and intracellular trafficking of GABA$_A$ receptors. Int Rev Neurobiol 48, 1– 29.

Bavelier, D., Levi, D., Li, R., Dan, Y. & Hensch, T. (2010). Removing brakes on adult brain plasticity: from molecular to behavioral interventions. J. Neurosci., 30, 14964–14971.

Beattie EC, Stellwagen D, Morishita W, Bresnahan JC, Ha BK, Von Zastrow M, Beattie MS, Malenka RC (2002). Control of synaptic strength by glial TNFalpha. Science 295:2282–2285.

Becher B, Spath S, Goverman J. (2017). Cytokine networks in neuroinflammation. Nat Rev Immunol. 17(1):49-59.

Beckervordersandforth R, Tripathi P, Ninkovic J, Bayam E, Lepier A, Stempfhuber B, Kirchhoff F, Hirrlinger J, Haslinger A, Lie DC, Beckers J, Yoder B, Irmler M, Gotz M. (2010). In vivo fate mapping and expression analysis reveals molecular hallmarks of prospectively isolated adult neural stem cells. Cell Stem Cell. 7:744–758.

Belelli, D., Harrison, N., Maguire, J., Macdonald, R., Walker, M. & Cope, D. (2009) Extrasynaptic GABA$_A$ receptors: form, pharmacology, and function. J. Neurosci. 29, 12757–12763.

Ben-Ari Y, Khalilov I, Kahle KT, Cherubini E. (2012). The GABA excitatory/inhibitory shift in brain maturation and neurological disorders. Neuroscientist. 18(5):467-86.

Ben-Ari Y. (2017). NKCC1 Chloride Importer Antagonists Attenuate Many Neurological and Psychiatric Disorders. Trends Neurosci. 40(9):536-554.

Ben-Ari, Y. (2002). Excitatory actions of GABA during development: the nature of the nurture. Nat. Rev. Neurosci., 3, 728–739.

Bennett, V., Lambert, S., Davis, J.Q., and Zhang, X. (1997) Molecular architecture of the specialized axonal membrane at the node of Ranvier. Soc. Gen. Physiol. Series 52:107–120.

Benson, J. A., Low, K., Keist, R., Mohler, H., & Rudolph, U. (1998). Pharmacology of recombinant γ-aminobutyric acid$_A$ receptors rendered diazepam-insensitive by point-mutated α-subunits. FEBS Lett 431, 400–404.

Benveniste, E.N. (1998). Cytokine actions in the central nervous system. Cytok. Growth Factor Rev. 9:259–275.

Blaesse, P., Airaksinen, M.S., Rivera, C. & Kaila, K. (2009) Cation–chloride cotransporters and neuronal function. Neuron, 61, 820–838.

Blum, B. P., and Mann, J. J. (2002). The GABAergic system in schizophrenia. Int J Neuropsychopharm 5, 159– 179.

Boulanger, L. M. (2009). Immune proteins in brain development and synaptic plasticity. Neuron 64, 93–109.

Bouthour, W., Leroy, F., Emmanuelli, C., Carnaud, M., Dahan, M., Poncer, J. & L_evi, S. (2012). A human mutation in Gabrg2 associated with generalized epilepsy alters the membrane dynamics of GABAA receptors. Cereb. Cortex, 22, 1542–1553.

Bowery, N. G., Bettler, B., Froestl, W., Gllagher, J. P., Marshall, F., Raiteri, M., Bonner, T. I., & Enna, S. J. (2002). International Union of Pharmacology. XXXIII. Mammalian g-aminobutyric acid$_B$ receptors: structure and function. Pharmacol Rev 54, 247– 264.

Branchereau, P., Chapron, J., Meyrand, P., 2002. Descending 5-hydroxy-tryptamine raphe inputs repress the expression of serotonergic neurons and slow the maturation of inhibitory systems in mouse embryonic spinal cord. J. Neurosci. 22, 2598–2606.

Brickley, S.G. & Mody, I. (2012) Extrasynaptic GABA$_A$ receptors: their function in the CNS and implications for disease. Neuron, 12, 23–34.

Briscoe, J., Pierani, A., Jessell, T.M., Ericson, J. (2000). A homeodomain protein code specifies progenitos cell identity and neuronal fate in the ventral neural tube. Cell 101, 435-445.

Brussaard, A. B., Kits, K. S., Baker, R. E., Willems, W. P. A., Leyting- Vermeulen, J. W., Voorn, P., Smit, A. B., Bicknell, R. J., & Herbison, A. E. (1997). Plasticity in fast synaptic inhibition of adult oxytocin neurons caused by switch in GABA$_A$ receptor subunit expression. Neuron 19, 1103– 1114.

Burm SM, Peferoen LA, Zuiderwijk-Sick EA, Haanstra KG, 't Hart BA, van der Valk P, Amor S, Bauer J, Bajramovic JJ. (2016). Expression of IL-1β in rhesus EAE and MS lesions is mainly induced in the CNS itself. J Neuroinflammation. 13(1):138.

Butt, A.M. and Berry, M. (2000). Oligodendrocytes and the control of myelination in vivo: new insights from the rat anterior medullary velum. J. Neurosci. Res. 59:477–488.

Butt, A.M., Ibrahim, M., and Berry, M. (1997). The relationship between developing oligodendrocyte units and maturing axons during myelinogenesis in the anterior medullary velum of neonatal rats. J. Neurocytol. 26:327–338.

Centonze D, Muzio L, Rossi S, Cavasinni F, De Chiara V, Bergami A, Musella A, D'Amelio M, Cavallucci V, Martorana A, Bergamaschi A, Cencioni MT, Diamantini A, Butti E, Comi G, Bernardi G, Cecconi F, Battistini L, Furlan R, Martino G. (2009). Inflammation triggers synaptic alteration and degeneration in experimental autoimmune encephalomyelitis. J Neurosci. 18; 29(11):3442-52.

Chao, C.C., Molitor, T.W., and Hu, S. (1993). Neuroprotective role of IL-4 against activated microglia. J. Immunol. 151:1473–1481.

Chari DM (2007). Remyelination in multiple sclerosis. Int. Rev. Neurobiol. 79: 589–620.

Chen WW, Zhang X, Huang WJ. (2016). Role of neuroinflammation in neurodegenerative diseases (Review). Mol Med Rep. 13(4):3391-6.

Cherubini E, Gaiarsa JL, Ben-Ari Y. (1991). GABA: an excitatory transmitter in early postnatal life. Trends Neurosci. 14(12):515-9.

Christenson, J., Cullheim, S., Grillner, S., Hökfelt, T. (1990). 5-hydroxytryptamine immunoreactive varicosities in the lamprey spinal cord have no synaptic specializations - an ultrastructural study. Brain Res. 512, 201–209.

Christian, C., Herbert, A., Holt, R., Peng, K., Sherwood, K., Pangratz-Fuehrer, S., Rudolph, U. & Huguenard, J. (2013) Endogenous positive allosteric modulation of GABAA receptors by diazepam binding inhibitor. Neuron, 78, 1063–1074.

Colton C. A. (2009). Heterogeneity of microglial activation in the innate immune response in the brain. J. Neuroimmune Pharmacol. 4 399–418

Compston A, Coles A (2002). Multiple sclerosis. Lancet. 359 (9313): 1221–31.

Coulter, D. A. (2001). Epilepsy-associated plasticity in g-aminobutyric acid receptor expression, function, and inhibitory synaptic properties. Int Rev Neurobiol 45, 237–252.

Cowley KC, Schmidt BJ. (1997). Regional distribution of the locomotor pattern-generating network in the neonatal rat spinal cord. J Neurophysiol. 77(1):247-59.

Craig, A.D. (2003). Pain mechanisms: labelled lines versus convergence in central processing. Annu. Rev. Neurosci. *26,* 1–30.

Cua, D.J., Sherlock, J., Chen, Y., Murphy, C.A., Joyce, B., Seymour, B., Lucian, L., To, W., Kwan, S., Churakova, T., Zurawski S, Wiekowski M, Lira SA, Gorman D, Kastelein RA, Sedgwick JD. (2003). Interleukin-23 rather than interleukin-12 is the critical cytokine for autoimmune inflammation of the brain. Nature 421, 744–748.

Cumano A, Godin I. (2007). Ontogeny of the hematopoietic system. Annu Rev Immunol 25: 745–785.

Czubowicz K, Głowacki M, Fersten E, Kozłowska E, Strosznajder RP, Czernicki Z. (2017). Levels of selected pro- and anti-inflammatory cytokines in cerebrospinal fluid in patients with hydrocephalus. Folia Neuropathol. 55(4):301-307.

Dasen JS, De Camilli A, Wang B, Tucker PW, Jessell TM. (2008). Hox repertoires for motor neuron diversity and connectivity gated by a single accessory factor, FoxP1. Cell. 134(2):304-16.

Davis-Dusenbery BN, Williams LA, Klim JR, Eggan K. (2014). How to make spinal motor neurons. Development. 141(3):491-501.

Dawson, R.L., Levien, J.M., and Reynolds, R. (2000). NG2-expressing cells in the central nervous system: are they oligodendrocyte progenitors? J. Neurosci. Res. 61:471–479.

Deczkowska A, Baruch K, Schwartz M. (2016). Type I/II Interferon Balance in the Regulation of Brain Physiology and Pathology. Trends Immunol. 37(3):181-192.

Delpy, A., Allain, A.E., Meyrand, P., Branchereau, P., 2008. NKCC1 cotransporter inactivation underlies embryonic development of chloride-mediated inhibition in mouse spinal motoneuron. J. Physiol. 586, 1059–1075.

Dieni, C., Chancey, J. & Overstreet-Wadiche, L. (2013) Dynamic functions of GABA signaling during granule cell maturation. Front. Neural Circuits, 6, 113.

Dong, Z., Sinanan, A., Parkinson, D., Parmantier, E., Mirsky, R., and Jessen, K.R. (1999). Schwann cell development in embryonic mouse nerves. *J*. Neurosci. Res. 56:334–348.

Dougherty, K.D., Dreyfus, C.F., and Black, I.B. (2000). Brain-derived neurotrophic factor in astrocytes, oligodendrocytes, and microglia/macrophages after spinal cord injury. *Neurobiol. Dis.* 7:574–585.

Doyon N, Vinay L, Prescott SA, De Koninck Y. (2016). Chloride Regulation: A Dynamic Equilibrium Crucial for Synaptic Inhibition. Neuron. 16;89(6):1157-1172.

Doyon, N., Ferrini, F., Gagnon, M., and De Koninck, Y. (2013). Treating pathological pain: is KCC2 the key to the gate? Expert Rev. Neurother. 13, 469–471.

Doyon, N., Prescott, S.A., Castonguay, A., Godin, A.G., Kröger, H., and De Koninck, Y. (2011). Efficacy of synaptic inhibition depends on multiple, dynamically interacting mechanisms implicated in chloride homeostasis. PLoS Comput. Biol. 7, e1002149.

Duong, T. T., Finkelman, F. D., Singh, B., Strejan, G. H. (1994) Effect of anti-interferon-γ monoclonal antibody treatment on the development of experimental allergic encephalomyelitis in resistant mouse strains. J. Neuroimmunol. 53, 101–107.

Dzhala, V.I., Talos, D.M., Sdrulla, D.A., Brumback, A.C., Mathews, G.C., Benke, T.A., Delpire, E., Jensen, F.E., and Staley, K.J. (2005). NKCC1 transporter facilitates seizures in the developing brain. Nat. Med. 11, 1205–1213.

Eng LF. (1985). Glial fibrillary acidic protein (GFAP): the major protein of glial intermediate filaments indifferentiated astrocytes. J Neuroimmunol. 8:203–214.

Ericson, J., Rashbass, P., Schedl, A., Brenner-Morton, S., Kawakami, A., van Heyningen, V., Jessell, T.M., Briscoe, J. (1997a). Pax6 controls progenitor cell identity and neuronal fate in response to graded Shh signaling. Cell 90, 169-80.

Esiri MM, Izzi al MS, Reading MC. (1991). Macrophages, microglial cells, and HLA-DR antigens in fetal and infant brain. J Clin Pathol 44: 102–106.

Farrant, M. & Nusser, Z. (2005) Variations on an inhibitory theme: phasic and tonic activation of $GABA_A$ receptors. Nat. Rev. Neurosci., 6, 215–229.

Ferber, I. A., Brocke, S., Taylor-Edwards, C., Ridgway, W., Dinisco, C., Steinman, L., Dalton, D., Fathman, C. G. (1996) Mice with a disrupted IFN-γ gene are susceptible to the induction of experimental autoimmune encephalomyelitis (EAE). J. Immunol. 156, 5–7.

Ferguson, A.R., Christensen, R.N., Gensel, J.C., Miller, B.A., Sun, F., Beattie, E.C., Bresnahan, J.C., Beattie, M.S. (2008). Cell death after spinal cord injury is exacerbated by rapid TNF alpha-induced trafficking of GluR2-lacking AMPARs to the plasma membrane. J. Neurosci. 28, 11391e11400.

Ferrini, F., and De Koninck, Y. (2013). Microglia control neuronal network excitability via BDNF signalling. Neural Plast. 2013, 429815.

Fiumelli H, Woodin MA. (2007). Role of activity-dependent regulation of neuronal chloride homeostasis in development. Curr Opin Neurobiol. 17(1):81-6.

Fritschy, J.M., Panzanelli, P. & Tyagarajan, S.K. (2012) Molecular and functional heterogeneity of GABAergic synapses. Cell. Mol. Life Sci., 69, 2485–2499.

Frohman, E.M., Racke, M.K., and Raine, C.S. (2006). Multiple sclerosis–the plaque and its pathogenesis. N. Engl. J. Med. 354, 942–955.

Furlan F, Guasti L, Avossa D, Becchetti A, Cilia E, Ballerini L, Arcangeli A. (2005). Interneurons transiently express the ERG K^+ channels during development of mouse spinal networks in vitro. Neuroscience. 135(4):1179-92.

Furlan F, Taccola G, Grandolfo M, Guasti L, Arcangeli A, Nistri A, Ballerini L. (2007). ERG conductance expression modulates the excitability of ventral horn GABAergic interneurons that control rhythmic oscillations in the developing mouse spinal cord. J Neurosci. 27:919-928.

Gähwiler BH, Capogna M, Debanne D, McKinney RA, Thompson SM. (1997). Organotypic slice cultures: a technique has come of age. Trends Neurosci. 20(10):471-7.

Gao, B.X., Stricker, C., Ziskind-Conhaim, L. (2001). Transition from GABAergic to glycinergic synaptic transmission in newly formed spinal networks. J. Neurophysiol. 86, 492-502.

Gardoni, F., Boraso, M., Zianni, E., Corsini, E., Galli, C.L., Cattabeni, F., Marinovich, M., Di Luca, M., Viviani, B. (2011). Distribution of interleukin-1 receptor complex at the synaptic membrane driven by interleukin-1beta and NMDA stimulation. J. Neuroinflammation 8, 14.

Gebicke-Haerter, P.J., Spleiss, O., Ren, L.Q., Li, H., Dichmann, S., Norgauer, J., and Boddeke, H.W. (2001). Microglial chemokines and chemokine receptors. Prog. Brain Res. 132:525–532.

Ginhoux F, Lim S, Hoeffel G, Low D and Huber T. (2013). Origin and differentiation of microglia. Front. Cell. Neurosci. 10.3389/fncel.2013.00045.

Giulian, D. and Ingeman, J.E. (1988). Colony-stimulating factors as promoter of ameboid microglia. J. Neurosci. 8:4707–4717.

Giulian, D., Johnson, B., Krebs, J.F., George, J.K., and Tapscott, M. (1991). Microglial mitogens are produced in the developing and injured mammalian brain. J. Cell Biol. 112:323–333.

Glass CK, Saijo K, Winner B, Marchetto MC, Gage FH. (2010). Mechanisms underlying inflammation in neurodegeneration. Cell.140:918–34.

Goldman JE. (1995). Lineage, migration, and fate determination of postnatal subventricular zone cells in the mammalian CNS. J Neurooncol. 24:61–64.

Gosgnach, S., Lanuza, G.M., Butt, S.J., Saueressig, H., Zhang, Y., Velasquez, T., Riethmacher, D., Callaway, E.M., Kiehn, O., Goulding, M. (2006).V1 spinal neurons regulate the speed of vertebrate locomotor outputs. Nature 440, 215-9.

Goulding, M., Lanuza, G., Sapir, T., Narayan, S. (2002). The formation of sensorimotor circuits. Curr. Opin. Neurobiol. 12, 508-15.

Graeber, M.B. (2010).Changing face of microglia. Science 330, 783–788.

Grillner S. (2003). The motor infrastructure: from ion channels to neuronal networks. Nat. Rev. Neurosci. 4:573–86.

Grillner, S., Cangiano, L., Hu, G., Thompson, R., Hill, R., Wallén, P. (2000). The intrinsic function of a motor system–from ion channels to networks and behavior. Brain Res. 886, 224–236.

Grillner, S., Deliagina, T., Ekeberg, O., el Manira, A., Hill, R.H., Lansner, A., Orlovsky, G.N., Wallén, P. (1995). Neural networks that co-ordinate locomotion and body orientation in lamprey. Trends Neurosci. 18, 270–279.

Grillner, S., Ekeberg, El Manira, A., Lansner, A., Parker, D., Tegnér, J., Wallén, P. (1998). Intrinsic function of a neuronal network - a vertebrate central pattern generator. Brain Res. Brain Res. Rev. 26, 184-97.

Hanisch UK, Kettenmann H. (2007). Microglia: active sensor and versatile effector cells in the normal and pathologic brain. Nat Neurosci. 10(11):1387-94. 10.1038/nn1997.

Hanisch UK. (2013). Functional diversity of microglia – how heterogeneous are they to begin with? Front Cell Neurosci. 7: 65.

Hanson MG, Landmesser LT. (2003). Characterization of the circuits that generate spontaneous episodes of activity in the early embryonic mouse spinal cord. J Neurosci. 23(2):587-600.

Hartman, B.K., Agrawal, C.H., Agrawal, D., and Kalmbach, S. (1982). Development and maturation of central nervous system myelin: comparison of immunohistochemical localisation of proteolipid protein and basic protein in myelin and oligodendrocytes. Proc. Natl. Acad. Sci. USA 79:4217–4220.

Henneberger, C., Juttner, R., Rothe, T., & Grantyn, R. (2002). Postsynaptic action of BDNF on GABAergic synaptic transmission in the superficial layers of the mouse superior colliculus. J Neurophysiol 88, 595–603.

Hildebrand, C., Remahl, S., Persson, H. and Bjartmar, C. (1993). Myelinated nerve fibres in the CNS. Prog. Neurobiol. 40:319–384.

Hinckley, C.A., Hartley, R., Wu, L., Todd, A., Ziskind-Conhaim, L. (2005). Locomotor-like rhythms in a genetically distinct cluster of interneurons in the mammalian spinal cord. J. Neurophysiol. 93, 1439-49.

Hochman S. (2007). Spinal cord. Curr Biol. 17(22):R950-5.

Hochstim C, Deneen B, Lukaszewicz A, Zhou Q, Anderson DJ. (2008). Identification of positionally distinct astrocyte subtypes whose identities are specified by a homeodomain code. Cell. 133:510–522.

Hosie, A.M., Wilkins, M.E., da Silva, H.M. & Smart, T.G. (2006) Endogenous neurosteroids regulate GABAA receptors through two discrete transmembrane sites. Nature, 444, 486–489.

Houston CM, Bright DP, Sivilotti LG, Beato M, Smart TG. (2009a). Intracellular chloride ions regulate the time course of GABA-mediated inhibitory synaptic transmission. J Neurosci. 29(33):10416-23.

Houston, C.M., He, Q. & Smart, T.G. (2009b). CaMKII phosphorylation of the $GABA_A$ receptor: receptor subtype- and synapse-specific modulation. J. Physiol., 587, 2115–2125.

https://www.studyblue.com/notes/note/n/lecture-18-structure-layout-of-the-spinal-cord-white-grey-matter-spinal-nerves/deck/17260645

Hübner, C.A., Lorke, D.E., and Hermans-Borgmeyer, I. (2001). Expression of the Na-K-2Cl-cotransporter NKCC1duringmousedevelopment. Mech. Dev. 102, 267–269.

Hughes, V. (2012). Microglia: the constant gardeners. Nature 485, 570–572.

Hutcheon, B., Morley, P., & Poulter, M. O. (2000). Developmental change in $GABA_A$ receptor desensitization kinetics and its role in synapse function in rat cortical neurons. J Physiol. 522, 3 – 17.

Hutchins KD, Dickson DW, Rashbaum WK, Lyman WD. (1990). Localization of morphologically distinct microglial populations in the developing human fetal brain: Implications for ontogeny. Brain Res Dev Brain Res 55: 95–102.

Ikeda, O., Murakami, M., Ito, H., Yamazaki, M., Nemoto, T., Koda, M., Nakayama, C., and Moriya, H. (2001). Acute up-regulation of brain-derived neurotrophic factor expression resulting from experimentally induced injury in the rat spinal cord. Acta Neuropathol. 102:239–245.

Jacob, T.C., Moss, S.J. & Jurd, R. (2008). $GABA_A$ receptor trafficking and its role in the dynamic modulation of neuronal inhibition. Nat. Rev. Neurosci., 9, 331–343.

Jankowska E. (2001). Spinal interneuronal systems: identification, multifunctional character and reconfigurations in mammals. J Physiol, 533, pp. 31-40.

Jankowska, E. (1992). Interneuronal relay in spinal pathways from proprioceptors. Prog. Neurobiol. *38*, 335–378.

Jessell, T. M. (2000). Neuronal specification in the spinal cord: inductive signals and transcriptional codes. Nat.Rev.Genet. 1, 20–29.

Jha MK, Lee WH, Suk K. (2016). Functional polarization of neuroglia: implications in neuroinflammation and neurological disorders. Biochem Pharmacol. 103:1 16.10.1016/j.bcp.2015.11.003.

Jovanovic, J. N., Thomas, P., Brandon, N. J., Sieghart, W., Smart, T. G., & Moss, S. J. (2001). Acute modulation of $GABA_A$ receptor phosphorylation and function by neurotrophins. Soc Neurosci Abstr 27, 503.07.

Jüttner, R., Meier, J., & Grantyn, R. (2001). Slow IPSC kinetics, low levels of α1 subunit expression and paired-pulse depression are distinct properties of neonatal inhibitory GABAergic synaptic connections in the mouse superior colliculus. Eur J Neurosci 13, 2088–2098.

Kaila, K., Price, T.J., Payne, J.A., Puskarjov, M., and Voipio, J. (2014). Cationchloride cotransporters in neuronal development, plasticity and disease. Nat. Rev. Neurosci. 15, 637–654.

Kawasaki Y, Zhang L, Cheng JK, Ji RR. (2008). Cytokine mechanisms of central sensitization: distinct and overlapping role of interleukin-1beta, interleukin-6, and tumor necrosis factor-alpha in regulating synaptic and neuronal activity in the superficial spinal cord. J Neurosci. 28(20):5189-94.

Kettenmann H, Verkhratsky A. (2008). Neuroglia: the 150 years after. Trends Neurosci. 31:653–659.

Kiefer, R., Schweitzer, T., Jung, S., Toyka, K.V., and Hartung, H.P. (1998). Sequential expression of transforming growth factor-β1 by T-cells, macrophages, and microglia in rat spinal cord during autoimmune inflammation. J. Neuropathol. Exp. Neurol. 57:385–395.

Kiehn O, Hounsgaard J, Sillar KT. 1997 Basic building blocks of vertebrate spinal central pattern generators. In Neurons, networks and motor behaviour (Eds. PSG Stein et al.). The MIT Press, Cambridge, Massachusetts, pp. 47–59.

Kiehn O, Kjaerulff O. (1996). Spatiotemporal characteristics of 5-HT and dopamine-induced rhythmic hindlimb activity in the in vitro neonatal rat. J Neurophysiol. 75(4):1472-82.

Kittler, J. T., & Moss, S. J. (2001). Neurotransmitter receptor trafficking and the regulation of synaptic strength. Traffic 2, 437– 448.

Kittler, J. T., Delmas, D., Jovanovic, J. N., Brown, I. R., Smart, T. G., and Moss, S. J. (2000). Constitutive endocytosis of $GABA_A$ receptors by an association with the adaptin AP2 complex modulates inhibitory synaptic currents in hippocampal neurons. J Neurosci 20, 7972– 7977.

Knabl, J., Witschi, R., Hösl, K., Reinold, H., Zeilhofer, U.B., Ahmadi, S., Brockhaus, J., Sergejeva, M.,Hess, A., Brune, K., et al. (2008).Reversal of pathological pain through specific spinal GABAA receptor subtypes. Nature 451, 330–334.

Kneussel, M. (2002). Dynamic regulation of $GABA_A$ receptors at synaptic sites. Brain Res Rev 39, 74– 83. (1889). Handbuch der gewebelehre des menschen. p. 6umgearb. aufl. ed., n.p.

Korn, T., Bettelli, E., Oukka, M., and Kuchroo, V.K. (2009). IL-17 and Th17 cells. Annu. Rev. Immunol. 27, 485–517.

Kowalczyk, S., Winkelmann, A., Smolinsky, B., Förstera, B., Neundorf, I., Schwarz, G. & Meier, J.C. (2013). Direct binding of $GABA_A$ receptor β2 and β3 subunits to gephyrin. Eur. J. Neurosci., 37, 544–554.

Kremer E, Lev-Tov A. (1997). Localization of the spinal network associated with generation of hindlimb locomotion in the neonatal rat and organization of its transverse coupling system. J Neurophysiol. 77(3):1155-70.

Krishnan, G.P., and Bazhenov, M. (2011). Ionic dynamics mediate spontaneous termination of seizures and postictal depression state. J. Neurosci. 31, 8870–8882.

Kruglov AA, Lampropoulou V, Fillatreau S, Nedospasov SA. (2011). Pathogenic and protective functions of TNF in neuroinflammation are defined by its expression in T lymphocytes and myeloid cells. J Immunol. 187(11):5660-70.

Kulkarni OP, Lichtnekert J, Anders HJ, Mulay SR. (2016). The Immune system in tissue environments regaining homeostasis after injury: Is "inflammation" always inflammation? Mediators Inflamm. 2856213.

Kumar, H., Kawai, T., and Akira, S. (2011). Pathogen recognition by the innate immune system. Int. Rev. Immunol. 30, 16–34.

Lambert, J. J., Belelli, D., Harney, S. C., Peters, J. A., & Frenguelli, B. G. (2001). Modulation of native and recombinant $GABA_A$ receptors by endogenous and synthetic neuroactive steroids. Brain Res Rev 37, 68– 80.

Lanuza, G.M., Gosgnach, S., Pierani, A., Jessell, T.M., Goulding, M. (2004). Genetic identification of spinal interneurons that coordinate left-right locomotor activity necessary for walking movements. Neuron 42, 375-86.

Lassmann, H., Bruck, W., and Lucchinetti, C. (2001). Heterogeneity of multiple sclerosis pathogenesis: implications for diagnosis and therapy. Trends Mol. Med. 7, 115–121.

Lawson, L.J., Perry, V.H., Dri, P., and Gordon, S. (1990) Heterogeneity in the distribution and morphology of microglia in the normal adult mouse brain. Neuroscience 39:151–170.

Lee HY, Kléber M, Hari L, Brault V, Suter U, Taketo MM, Kemler R, Sommer L. (2004). Instructive role of Wnt/beta-catenin in sensory fate specification in neural crest stem cells. Science. 303(5660):1020-3.

Lee, T.H., Kato, H., Chen, S.T., Kogure, K., and Itoyama, Y. (2002). Expression disparity of brain-derived neurotrophic factor immunoreactivity and mRNA in ischemic hippocampal neurons. NeuroReport 13:2271–2275.

Lemonnier, E., Degrez, C., Phelep, M., Tyzio, R., Josse, F., Grandgeorge, M., Hadjikhani, N., and Ben-Ari, Y. (2012). A randomised controlled trial of bumetanide in the treatment of autism in children. Transl. Psychiatry 2, e202.

Leong, S.K. and Ling, E.A. (1992) Amoeboid and ramified microglia: their interrelationship and response to brain injury. Glia 6:39–47.

Levison SW, Young GM, Goldman JE. (1999). Cycling cells in the adult rat neocortex preferentially generate oligodendroglia. J Neurosci Res. 57:435–446.

Lewis, D.A., Hashimoto, T. & Volk, D.W. (2005). Cortical inhibitory neurons and schizophrenia. Nat. Rev. Neurosci., 6, 312–324.

Li, H., Tornberg, J., Kaila, K., Airaksinen, M.S., and Rivera, C. (2002). Patterns of cation-chloride cotransporter expression during embryonic rodent CNS development. Eur. J. Neurosci. 16, 2358–2370.

Libbey JE, Fujinami RS. (2010). Experimental autoimmune encephalomyelitis as a testing paradigm for adjuvants and vaccines. Vaccine. DOI: 10.1016/j.vaccine.2010.08.103.

Lin, J., Ju, W., Foster, K., Lee, S., Ahmadian, G., Wyszynski, M., Wang, Y., and Sheng, M. (2000). Distinct molecular mechanisms and divergent endocytotic pathways of AMPA receptor internalization. Nat Neurosci 3, 1282– 1290.

Liu, J., Marino, M.W., Wong, G., Grail, D., Dunn, A., Bettadapura, J., Slavin, A.J., Old, L., and Bernard, C.C. (1998). TNF is a potent anti-inflammatory cytokine in autoimmune-mediated demyelination. Nat. Med. 4:78–83.

Lloyd AF, Davies CL, Miron VE. (2017). Microglia: origins, homeostasis, and roles in myelin repair. Curr Opin Neurobiol. 47:113-120.

Lobsiger, C.S., Taylor, V., and Suter, U. (2002). The early life of a Schwann cell. Biol. Chem. 383:245–253.

Luscher, B., Fuchs, T. & Kilpatrick, C.L. (2011) GABAA receptor trafficking- mediated plasticity of inhibitory synapses. Neuron, 70, 385–409.

Ma, W., Behar, T., Barker, J.L. (1992). Transient expression of GABA immunoreactivity in the developing rat spinal cord. J. Comp. Neurol. 325, 271–290.

Malatesta P, Hack MA, Hartfuss E, Kettenmann H, Klinkert W, Kirchhoff F, Gotz M. (2003). Neuronal or glial progeny: regional differences in radial glia fate. Neuron. 37:751–764.

Malizia, A. L. (1999). What do brain imaging studies tell us about anxiety disorders? JPsychopharmacol 13, 372–378.

Mandolesi G, Gentile A, Musella A, Centonze D. (2015). IL-1β dependent cerebellar synaptopathy in a mouse model of multiple sclerosis. Cerebellum. 14(1):19-22.

Marshall CA, Goldman JE. (2002). Subpallial dlx2-expressing cells give rise to astrocytes and oligodendrocytes in the cerebral cortex and white matter. J Neurosci. 22:9821–9830.

Masahira N, Takebayashi H, Ono K, Watanabe K, Ding L, Furusho M, Ogawa Y, Nabeshima Y, Alvarez-Buylla A, Shimizu K, Ikenaka K. (2006). Olig2-positive progenitors in the embryonic spinal cord give rise not only to motoneurons and oligodendrocytes, but also to a subset of astrocytes and ependymal cells. Dev Biol. 293:358–369.

McLean DL, Merrywest SD, Sillar KT. (2000). The development of neuromodulatory systems and the maturation of motor patterns in amphibian tadpoles. Brain Res. Bull. 53:595–603.

Medelin M, Giacco V, Aldinucci A, Castronovo G, Bonechi E, Sibilla A, Tanturli M, Torcia M, Ballerini L, Cozzolino F, Ballerini C. (2018). Neuro-immune crosstalk in organotypic spinal slices: investigating the protective role of an NGF-mimetic. Molecular Brain. 11:3.

Medelin M, Rancic V, Cellot G, Laishram J, Veeraraghavan P, Rossi C, Muzio L, Sivilotti L, Ballerini L. (2016). Altered development in GABA co-release shapes glycinergic synaptic currents in cultured spinal slices of the $SOD1^{G93A}$ mouse model of ALS. J Physiol. 594:3827-3840.

Meyer S.J., and Quenzer L.F., (2013). Psychopharmacology: Drugs, the Brain, and Behavior, Second Edition. Sinauer Associates.

Millan, M.J. (2002). Descending control of pain. Prog. Neurobiol. 66, 355–474.

Miller, D.H., Khan, O.A., Sheremata, W.A., Blumhardt, L.D., Rice, G.P., Libonati, M.A., Willmer-Hulme, A.J., Dalton, C.M., Miszkiel, K.A., and O'Connor, P.W. (2003) A controlled trial of natalizumab for relapsing multiple sclerosis. N. Engl. J Med. 348:15–23.

Miranda-Contreras, L., Benítez-Díaz, P., Peña-Contreras, Z., Mendoza-Briceño, R.V., Palacios-Prü, E. (2002). Levels of amino acid neurotransmitters during neurogenesis and in histotypic cultures of mouse spinal cord. Dev. Neurosci. 24, 59–70.

Mohler, H., Fritschy, J. M., Luscher, B., Rudolph, U., Benson, J., & Benke, D. (1996). The $GABA_A$-receptors: from subunits to diverse functions. In T. Narahashi (Ed.), Ion Channels, Vol. 4 (pp. 89–113). New York: Plenum Press.

Moody WJ, Bosma MM. (2005). Ion channel development, spontaneous activity, and activity-dependent development in nerve and muscle cells. Physiol Rev. 85(3):883-941

Morrow, A. L., Van Doren, M. J., Penland, S. N., & Matthews, D. B. (2001). The role of GABAergic neuroactive steroids in ethanol action, tolerance and dependence. Brain Res Rev 37, 98– 109.

Mou, L., Dias, B., Gosnell, H. & Ressler, K. (2013). Gephyrin plays a key role in BDNF-dependent regulation of amygdala surface $GABA_A$Rs. Neuroscience, 255, 33–44.

Mukherjee, J., Kretschmannova, K., Gouzer, G., Maric, H.M., Ramsden, S.L., Tretter, V., Harvey, K., Davies, P.A., Triller, A., Schindelin, H. & Moss, S.J. (2011). The residence time of $GABA_A$Rs at inhibitory synapses is determined by direct binding of the receptor α1 subunit to gephyrin. J. Neurosci., 31, 14677–14687.

Nakayama K, Nishimaru H, Kudo N. (2002). Basis of changes in left-right coordination of rhythmic motor activity during development in the rat spinal cord. J Neurosci. 22(23):10388-98.

Nissen, U.V., Mochida, H., Glover, J.C. (2005). Development of projection specific interneurons and projection neurons in the embryonic mouse and rat spinal cord. J. Comp. Neurol. 483, 30-47.

O'Donovan MJ, Chub N, Wenner P. (1998). Mechanisms of spontaneous activity in developing spinal networks. J Neurobiol. 37(1):131-45.

Owens, T., Wekerle, H., and Antel, J. (2001). Genetic models for CNS inflammation. Nat. Med. 7:161–166.

Pascual O, Ben Achour S, Rostaing P, Triller A, Bessis A. (2012). Microglia activation triggers astrocyte-mediated modulation of excitatory neurotransmission. Proc Natl Acad Sci U S A. 109(4):E197-205.

Paul, J., Yevenes, G.E., Benke, D., Lio, A., Ralvenius, W.T., Witschi, R., Scheurer, L., Cook, J.M., Rudolph, U., Fritschy, J.M. & Zeilhofer, H.U. (2013). Antihyperalgesia by α2-$GABA_A$ receptors occurs via a genuine spinal action and does not involve supraspinal sites. Neuropsychopharmacology, 39, 477–487.

Payne, J.A., Rivera, C., Voipio, J., and Kaila, K. (2003). Cation-chloride co-transporters in neuronal communication, development and trauma. Trends Neurosci. 26, 199–206.

Pekny M, Nilsson M. (2005). Astrocyte activation and reactive gliosis. Glia. 50:427–434.

Phelps, P.E., Alijani, A., Tran, T.S. (1999). Ventrally located commissural neurons express the GABAergic phenotype in developing rat spinal cord. J. Comp. Neurol. 409, 285–298.

Pierani, A., Brenner-Morton, S., Chiang, C., Jessell, T.M. (1999). A sonic hedgehog-independent, retinoid-activated pathway of neurogenesis in the ventral spinal cord. Cell 97, 903-15.

Pierani, A., Moran-Rivard, L., Sunshine, M.J., Littman, D.R., Goulding, M., Jessell, T.M. (2001). Control of interneuron fate in the developing spinal cord by the progenitor homeodomain protein Dbx1. Neuron 29, 367-84.

Platel, J.C., Lacar, B. & Bordey, A. (2007) GABA and glutamate signaling: homeostatic control of adult forebrain neurogenesis. J. Mol. Histol., 38, 602–610.

Prescott, S.A. (2015). Synaptic inhibition and disinhibition in the spinal dorsal horn. Prog. Mol. Biol. Transl. Sci. 131, 359–383.

Raivich, G., Jones, L.L., Werner, A., Bluthmann, H., Dötschmann, T., and Kreutzberg, G.W. (1999). Molecular signals for glial activation: pro- and anti-inflammatory cytokines in the injured brain. Acta Neurochir. Suppl. 73:21–30.

Ransohoff RM. (2016). How neuroinflammation contributes to neurodegeneration. Science. 353: 777-783.

Ravikumar M, Jain S, Miller RH, Capadona JR, Selkirk SM. (2012) An organotypic spinal cord slice culture model to quantify neurodegeneration. J Neurosci Methods;211(2):280-8.

Re, F., Belyanskaia, S.L., Riese, R.J., Cipriani, B., Fischer, F.R., Granucci, F., Ricciardi-Castagnoli, P., Brosnan, C., Stern, L.J., Strominger, J.L., and Santambrogio, L. (2002). Granulocyte-macrophage colony-stimulating factor induces an expression program in neonatal microglia that primes them for antigen presentation. J. Immunol. 169:2264–2273.

Reichling, D.B., Kyrozis, A., Wang, J., MacDermott, A.B., (1994). Mechanisms of GABA and glycine depolarization-induced calcium transients in rat dorsal horn neurons. J. Physiol. 476, 411-21.

Rezaie P, Dean A, Male D, Ulfig N. (2005). Microglia in the cerebral wall of the human telencephalon at second trimester. Cereb Cortex 15: 938–949.

Rezaie P, Male D. (1999). Colonisation of the developing human brain and spinal cord by microglia: A review. Microsc Res Tech 45: 359–382.

Rezaie P, Male D. (2002). Mesoglia & microglia—A historical review of the concept of mononuclear phagocytes within the central nervous system. J Hist Neurosci 11: 325–374.

Rho, M.B., Wesselingh, S., Glass, J.D., McArthur, J.C., Choi, S., Griffin, J., and Tyor, W.R. (1995). A potential role for interferon-alpha in the pathogenesis of HIV-associated dementia. Brain Behav. Immun. 9:366–377.

Roberts A, Soffe SR, Wolf ES, Yoshida M, Zhao FY. (1998). Central circuits controlling locomotion in young frog tadpoles. Ann. N. Y. Acad. Sci. 860:19–34.

Rosato-Siri M, Grandolfo M, Ballerini L. (2002). Activity-dependent modulation of GABAergic synapses in developing rat spinal networks in vitro. Eur J Neurosci. 16(11):2123-35.

Rudolph, U. and Antkowiak, B. (2004) Molecular and neuronal substrates for general anaesthetics. Nat. Rev. Neurosci., 5, 709–720.

Saiepour, L., Fuchs, C., Patrizi, A., Sasso_e-Pognetto, M., Harvey, R.J. & Harvey, K. (2010) Complex role of collybistin and gephyrin in GABAA receptor clustering. J. Biol. Chem., 285, 29623–29631.

Salie R, Niederkofler V, Arber S. (2005). Patterning molecules; multitasking in the nervous system. Neuron. 45(2):189-92.

Sankowski R, Mader S, and Valdés-Ferrer SI. (2015) Systemic Inflammation and the Brain: Novel Roles of Genetic, Molecular, and Environmental Cues as Drivers of Neurodegeneration. Front Cell Neurosci. 9: 28.

Sapir, T., Geiman, E.J., Wang, Z., Velasquez, T., Mitsui, S., Yoshihara, Y., Frank, E., Alvarez, F.J., Goulding, M. (2004). Pax6 and engrailed 1 regulate two distinct aspects of Renshaw cell development. J. Neurosci. 24, 1255-64.

Sassoè-Pognetto, M., Panzanelli, P., Sieghart, W. & Fritschy, J.M. (2000) Co-localization of multiple GABAA receptor subtypes with gephyrin at postsynaptic sites. J. Comp. Neurol., 420, 481–498.

Saueressig, H., Burrill, J., Goulding, M. (1999). Engrailed-1 and netrin-1 regulate axon pathfinding by association interneurons that project to motor neurons. Development 126, 4201-12.

Schäfers M, Sorkin L. (2008). Effect of cytokines on neuronal excitability. Neurosci Lett. 437(3):188-93.

Schwartz M, Deczkowska A. (2016). Neurological disease as a failure of brain-immune crosstalk: The multiple faces of neuroinflammation. Trends Immunol. 37: 668-679.

Shabab T, Khanabdali R, Moghadamtousi SZ, Kadir HA, Mohan G. (2017). Neuroinflammation pathways: a general review. Int J Neurosci. 127(7): 624-633.

Sibilla S, Ballerini L. (2009). GABAergic and glycinergic interneuron expression during spinal cord development: dynamic interplay between inhibition and excitation in the control of ventral network outputs. Prog Neurobiol. 89(1):46-60.

Simons M, Nave KA. (2015). Oligodendrocytes: Myelination and Axonal Support. Cold Spring Harb Perspect Biol. 8(1):a020479.

Spicarova D, Nerandzic V, and Palecek J. (2011). Modulation of spinal cord synaptic activity by tumor necrosis factor a in a model of peripheral neuropathy. J Neuroinflammation. 8:177

Steardo L, Jr., Bronzuoli MR, Iacomino A, Esposito G, Steardo L, Scuderi C. (2015). Does neuroinflammation turn on the flame in Alzheimer's disease? Focus on astrocytes. Front Neurosci. 9:259. 10.3389/fnins.2015.00259.

Stein, V., Hermans-Borgmeyer, I., Jentsch, T.J., and Hübner, C.A. (2004). Expression of the KCl cotransporter KCC2 parallels neuronal maturation and the emergence of low intracellular chloride. J. Comp. Neurol. 468, 57–64.

Stellwagen D, Beattie EC, Seo JY, MalenkaRC (2005). Differential regulation of AMPA receptor and GABA receptor trafficking by tumor necrosis factor-α. J Neurosci 25:3219 –3228.

Stödberg, T., McTague, A., Ruiz, A.J., Hirata, H., Zhen, J., Long, P., Farabella, I., Meyer, E., Kawahara, A., Vassallo, G., et al. (2015). Mutations in SLC12A5 in epilepsy of infancy with migrating focal seizures. Nat. Commun. 6, 8038.

Streit J, Spenger C, Lüscher HR. (1991). An Organotypic Spinal Cord - Dorsal Root Ganglion - Skeletal Muscle Coculture of Embryonic Rat. II. Functional Evidence for the Formation of Spinal Reflex Arcs In Vitro. Eur J Neurosci. 3(11):1054-1068.

Tabarean IV, Korn H, Bartfai T. (2006). Interleukin-1beta induces hyperpolarization and modulates synaptic inhibition in preoptic and anterior hypothalamic neurons. Neuroscience. 141(4):1685-95.

Takeuchi, H., Jin, S., Wang, J., Zhang, G., Kawanokuchi, J., Kuno, R., Sonobe, Y., Mizuno, T., Suzumura, A. (2006). Tumor necrosis factor-alpha induces neurotoxicity via glutamate release from hemichannels of activated microglia in an autocrine manner. J. Biol. Chem. 281, 21362e21368.

Tancredi V, D'Arcangelo G, Grassi F, Tarroni P, Palmieri G, Santoni A, Eusebi F. (1992). Tumor necrosis factor alters synaptic transmission in rat hippocampal slices. Neurosci Lett. 146(2):176-8.

Tran, T.S., Alijani, A., Phelps, P.E. (2003). Unique developmental patterns of GABAergic neurons in rat spinal cord. J. Comp. Neurol. 456, 112–126.

Tran, T.S., Phelps, P.E. (2000). Axons crossing in the ventral commissure express L1 and GAD65 in the developing rat spinal cord. Dev. Neurosci. 22, 228–236.

Tremblay, ME., Lowery, RL., and Majewska, AK. (2010). Microglial interactions with synapses are modulated by visual experience. *PLoS Biol.* 8:e1000527. doi:10.1371/journal.pbio.1000527.

Tretter, V., Jacob, T.C., Mukherjee, J., Fritschy, J.M., Pangalos, M.N. & Moss, S.J. (2008). The clustering of GABAA receptor subtypes at inhibitory synapses is facilitated via the direct binding of receptor a2 subunits to gephyrin. J. Neurosci., 28, 1356–1365.

Verney C, Monier A, Fallet-Bianco C, Gressens P. (2010). Early microglial colonization of the human forebrain and possible involvement in periventricular white-matter injury of preterm infants. J Anat 217: 436–448.

Vicini, S., Ferguson, C., Prybylowski, K., Kralic, J., Morrow, A. L., & Homanics, G. E. (2001). $GABA_A$ receptor α1 subunit deletion prevents developmental changes of inhibitory synaptic currents in cerebellar neurons. J Neurosci 21, 3009– 3016.

Virchow, R. (1978) Cellular Pathology, 2nd ed. Chance, F., trans. Birmingham, AL: Gryphon Editors.

Vithlani, M., Hines, R., Zhong, P., Terunuma, M., Hines, D., Revilla-Sanchez, R., Jurd, R., Haydon, P., Rios, M., Brandon, N., Yan, Z. & Moss, S. (2013). The ability of BDNF to modify neurogenesis and depressive-like behaviours is dependent upon phosphorylation of tyrosine residues 365/367 in the $GABA_A$-receptor γ2 subunit. J. Neurosci., 33, 15567– 15577.

Vithlani, M., Terunuma, M. & Moss, S. (2011). The dynamic modulation of $GABA_A$ receptor trafficking and its role in regulating the plasticity of inhibitory synapses. Physiol. Rev., 91, 1009–1022.

Vitkovic, L., Bockaert, J., Jacque, C. (2000). "Inflammatory" cytokines: neuromodulators in normal brain? J. Neurochem. 74, 457e471.

Viviani, B., Bartesaghi, S., Gardoni, F., Vezzani, A., Behrens, M.M., Bartfai, T., Binaglia, M., Corsini, E., Di Luca, M., Galli, C.L., Marinovich, M. (2003). Interleukin- 1beta enhances NMDA receptor-mediated intracellular calcium increase through activation of the Src family of kinases. J. Neurosci. 23, 8692e8700.

Viviani, B., Gardoni, F., Marinovich, M. (2007). Cytokines and neuronal ion channels in health and disease. Int. Rev. Neurobiol. 82, 247e263.

Wang, C., Shimizu-Okabe, C., Watanabe, K., Okabe, A., Matsuzaki, H., Ogawa, T., Mori N, Fukuda A, Sato K. (2002b). Developmental changes in KCC1, KCC2 and NKCC1 mRNAs in the rat brain. Dev. Brain Res. 139, 59–66.

Wang, J. and Campbell, I.L. (2002a). Cytokine signaling in the brain: putting a SOCS in it? *J. Neurosci. Res.* 67:423–427.

Wheeler D, Knapp E, Bandaru VV, Wang Y, Knorr D, Poirier C, Mattson MP, Geiger JD, Haughey NJ. (2009). Tumor necrosis factor-alpha-induced neutral sphingomyelinase-2 modulates synaptic plasticity by controlling the membrane insertion of NMDA receptors. J Neurochem. 109(5):1237-49.

Whiting, P. J. (1999). The $GABA_A$ receptor gene family: new targets for therapeutic intervention. Neurochem Int 34, 387– 390.

Willenborg, D. O., Fordham, S., Bernard, C. C. A., Cowden, W. B., Ramshaw, I. A. (1996) IFN-γ plays a critical down-regulatory role in the induction and effector phase of myelin oligodendrocyte glycoprotein-induced autoimmune encephalomyelitis. J. Immunol. 157, 3223–3227.

Wilson, J.M., Hartley, R., Maxwell, D.J., Todd, A.J., Lieberam, I., Kaltschmidt, J.A., Yoshida, Y., Jessell, T.M., Brownstone, R.M. (2005). Conditional rhythmicity of ventral spinal interneurons defined by expression of the Hb9 homeodomain protein. J. Neurosci. 25, 5710-9.

Wingrove, P. B., Safo, P., Wheat, L., Thompson, S. A., Wafford, K. A., & Whiting, P. J. (2002). Mechanism of α-subunit selectivity of benzodiazepine pharmacology at γ-aminobutyric acid type A receptors. Eur J Neurosci 437, 31– 39.

Wohlfarth, K. M., Bianchi, M. T., & Macdonald, R. L. (2002). Enhanced neurosteroid potentiation of ternary $GABA_A$ receptors containing the δ subunit. J Neurosci 22, 1541– 1549.

Yan, X., Weng, H.R., 2013. Endogenous interleukin-1beta in neuropathic rats enhances glutamate release from the primary afferents in the spinal dorsal horn through coupling with presynaptic N-methyl-D-aspartic acid receptors. J. Biol. Chem. 288, 30544e30557.

Zhang H, Nei H, Dougherty PM. (2010). A p38 mitogen-activated protein kinase-dependent mechanism of disinhibition in spinal synaptic transmission induced by tumor necrosis factor-alpha. J Neurosci. 30(38):12844-55.

Zhang Y, Narayan S, Geiman E, Lanuza GM, Velasquez T, Shanks B, Akay T, Dyck J, Pearson K, Gosgnach S, Fan CM, Goulding M (2008). V3 spinal neurons establish a robust and balanced locomotor rhythm during walking. Neuron 60:84 –96.

Zhang, R., Lao, L., Ren, K., Berman, B.M. (2014). Mechanisms of acupuncture-electroacupuncture on persistent pain. Anesthesiology 120, 482e503.

Ziskind-Conhaim, L. (1998). Physiological functions of GABA-induced depolarizations in the developing rat spinal cord. Perspect. Dev. Neurobiol. 5, 279–287.

Zou, J.Y., Crews, F.T. (2005). TNF alpha potentiates glutamate neurotoxicity by inhibiting glutamate uptake in organotypic brain slice cultures: neuroprotection by NF kappa B inhibition. Brain Res. 1034, 11e24.